# Contribution of Lipid Kinase Vps34 to the Development and Function of Antigen Presenting Cells

By
J. Luke Postoak

Dissertation
Submitted to the Faculty of the
Graduate School of Vanderbilt University
in partial fulfillment of the requirements
for the degree of

DOCTOR OF PHILOSOPHY
in

Molecular Pathology and Immunology
December 17, 2022
Nashville, Tennessee

Approved:

Luc Van Kaer, Ph.D.
Sebastian Joyce, Ph.D.
Ray Stokes Peebles, Jr., M.D.
Carlos Henrique Serezani, Ph.D.
Daniel Moore, M.D., Ph.D.

## ACKNOWLEDGEMENTS

I would like to thank Dr. Luc Van Kaer for his guidance and support as my thesis advisor. I thank Drs. Mark Boothby, Sebastian Joyce, Mark Anderson, Paul Allen, Akiko Iwasaki, Maria-Luisa Alegre, and Marcel van den Brink for sharing valuable reagents. I thank Dr. Nancy Manley for providing the Foxn1-Cre mouse strain and for valuable contributions to the design and interpretation of many experiments. Finally, I would like to thank Drs. Lan Wu, Wenqiang Song, and Guan Yang for their critical technical contributions. This work was supported by grants from the NIH (R01DK104817 and R01AI139046) and predoctoral NIH training grants (T32HL069765 and T32AR059039). Work in this dissertation used the following core resources at Vanderbilt University Medical Center: Cell Imaging Shared Resource (supported by NIH grants P30CA068485, P30DK058404 and P30DK020593), Digital Histology Shared Resource, Translational Pathology Shared Resource (supported by NIH grant P30CA068485), and Flow Cytometry Shared Resource (supported by NIH grants P30CA068485, P30DK058404, and P30DK020593).

## TABLE OF CONTENTS

## LIST OF FIGURES

## LIST OF TABLES

# Chapter 1

# INTRODUCTION

## 1.1 Introduction to the immune system

The immune system is a network of barriers, cells, and molecules that protect the body from infectious agents and malignant cells. Most cells with specialized immune functions arise from the bone marrow. While some immune cells develop and mature in the bone marrow, others undergo critical steps in development at other anatomical sites soon after they egress the bone marrow. Once mature, immune cells either reside within peripheral tissues or circulate among the bloodstream, secondary lymphoid organs, and lymphatic system (Murphy and Weaver, 2016).

Cells of the immune system can be most broadly categorized into innate and adaptive immune cells. Innate immune cells respond quickly to signals through germline-encoded pattern recognition receptors which sense conserved pathogen- or danger-associated molecular patterns. Classically, the dynamics and amplitude of the innate immune response are constant from one pathogenic event to a subsequent one. Nevertheless, it is becoming increasingly appreciated that innate immune cells can undergo long-term functional reprogramming or “training” which is evoked by exogenous or endogenous stimuli and leads to an altered response towards a second non-specific challenge after the return to a non-activated state (Netea et al., 2020).

The adaptive immune system responds relatively slowly but has the capacity to recognize an enormous range of molecular determinants with remarkable specificity and fidelity. The adaptive immune response is also capable of developing immunological

memory to infection by a microbial pathogen which increases the speed by which it responds upon subsequent challenges. The adaptive immune system is comprised of T cells and B cells (collectively called adaptive lymphocytes) which sense cognate antigen (Ag) by means of clonally expressed Ag-specific B cell receptors (and their secreted form, antibodies) and T cell receptors (TCRs), respectively. The clonal expression of Ag receptors means that each lymphocyte is unique among the millions of adaptive lymphocytes that each organism possesses. Because of the exquisite specificity of Ag receptors, an organism must generate a peripheral repertoire of Ag receptors with a diversity capable of responding to an enormous variety of potential pathogens and transformed cells. Repertoire diversity is achieved by somatic recombination of gene segments encoding these highly variable proteins (Murphy and Weaver, 2016). The process by which receptor diversity is generated is intrinsically error prone and is at risk of producing Ag receptors that react against self-tissues. Therefore, developing lymphocytes must undergo testing to enforce the production of a diverse and functional yet self-tolerant Ag receptor repertoire in a process collectively known as central tolerance (Cheng and Anderson, 2018; Nemazee, 2017).

Although the innate and adaptive arms of the immune system are functionally distinct, an optimal immune response requires coordinated interactions between cells of both categories. B cell responses are augmented by innate immune cells called follicular dendritic cells that present native Ag to B cells in specialized lymphoid tissues (Kranich and Krautler, 2016). T cell activation is dependent on an intermediate cell to process and present peptide Ag in the context of major histocompatibility complex (MHC) molecules. Cells with a strong capacity for MHC-restricted Ag presentation are called professional

Ag presenting cells (APCs), including dendritic cells and macrophages of the innate immune system. These interactions go both ways as adaptive lymphocytes also have the capacity to recruit and influence the function of innate immune cells by secretion of chemical mediators called cytokines.

In addition to innate immune cells and conventional, adaptive lymphocytes, the immune system also contains a collection of in-between cells that do not fit neatly into the innate versus adaptive paradigm. These cells are called innate-like lymphocytes and may or may not express Ag-specific receptors of the adaptive immune system, yet they are poised to respond with innate-like speed to pathogenic insults but lack the capacity to develop classical immunological memory. These lymphocyte subsets share a similar developmental trajectory as conventional lymphocytes and display a number of common properties that permit them to integrate danger and stress signals dispatched by innate sensor cells to facilitate the generation of specialized effector immune responses tailored toward specific pathogens or other insults (Joyce, 2022; Van Kaer et al., 2022). Figure 1.1 summarizes the defining features of each arm of the immune system and includes prominent cell types in each.

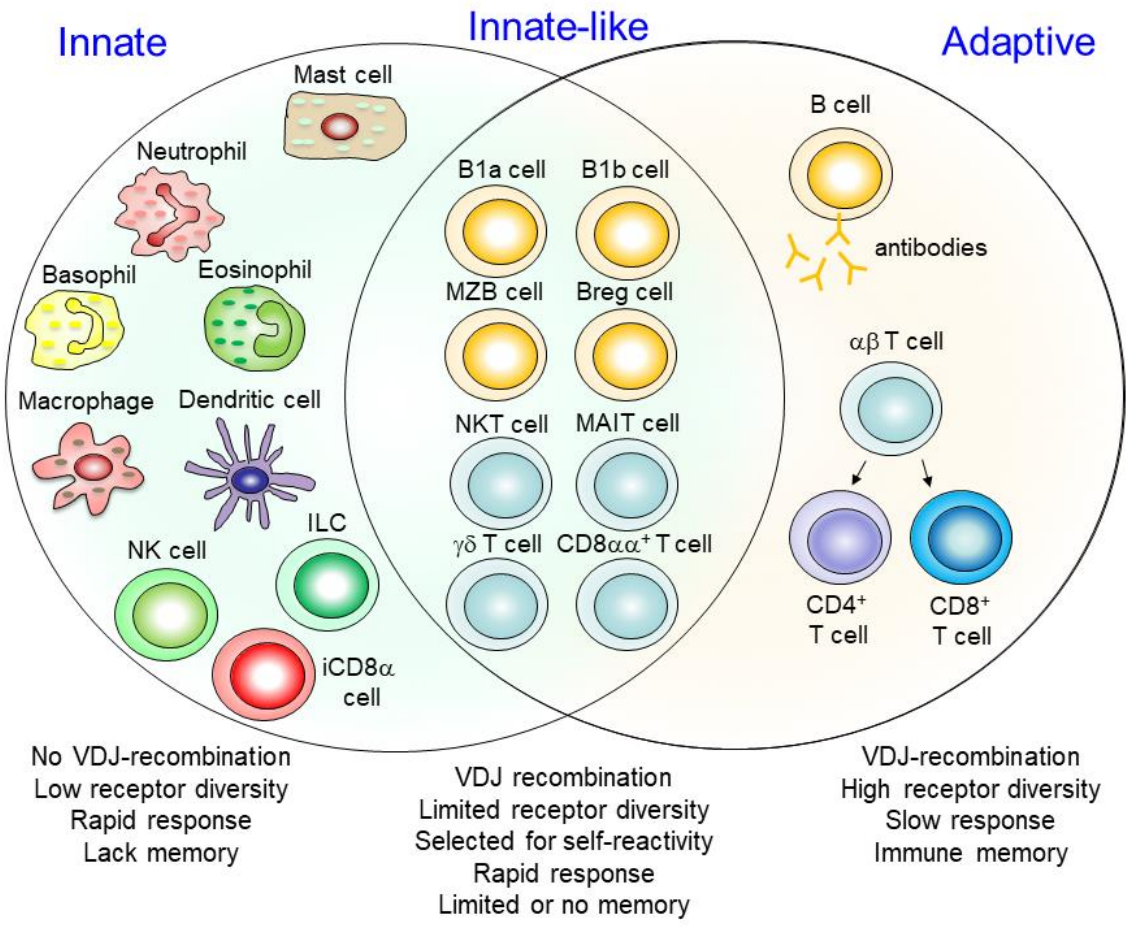


**Figure 1.1. The innate and adaptive arms of the immune system**. Immune cells are grouped according to their innate, innate-like or adaptive characteristics, which are listed at the bottom of the graph. Abbreviations: Breg, regulatory B; iCD8α, innate CD8α, ILC, innate lymphoid cell; MAIT, mucosal-associated invariant T; MZB, marginal zone B, NK, natural killer; NKT, natural killer T; VDJ, variable-diversity-joining.

### 1.2 Cellular and organismal role of Vps34

Vacuolar protein sorting 34 (Vps34, also known as Pik3C3) is the sole class III phosphoinositide 3-kinase (PI3K) member and is highly conserved from yeast to mammals. Vps34 associates with specific protein complexes to phosphorylate phosphatidylinositol at the 3' position on the inositol ring to produce the second messenger phosphatidylinositol 3-phosphate (PI3P) in specific subcellular compartments

(Backer, 2016). Scott Emr's group initially identified and characterized Vps34 in yeast screens for mutant strains defective in sorting hydrolytic enzymes to vacuoles, the yeast structural and functional analog of the animal cell lysosome (Herman and Emr, 1990; Robinson et al., 1988). Since then, Vps34 has been shown to play critical roles in a wide range of cellular processes, including macroautophagy, endocytosis, and phagocytosis, which contribute to immune cell functions such as lymphocyte development and antigen processing and presentation (Galluzzi and Green, 2019; Pishesha et al., 2022).

Vps34 consists of the minimal PI3K catalytic core and forms at least two distinct complexes, known as complex I and complex II, which mediate distinct cellular functions. The two complexes share the molecules Vps34, Beclin 1 (also called Atg6 in yeast) and the protein kinase-like Vps15 (also known as PIK3R4). Complex I uniquely contains Atg14 whereas complex II contains UVRAG. Additional regulatory subunits can associate with these complexes, including AMBRA in complex I and Rubicon in complex II (Stjepanovic et al., 2017). Furthermore, a recent study has proposed that additional subcomplexes of Vps34 potentially exist (Russell et al., 2013). In addition to functions that are dependent on its catalytic activity, Vps34 also functions as a scaffolding protein in the assembly of the different Vps34 complexes (Bilanges et al., 2019). In the following sections I discuss cellular and organismal roles of Vps34 (Figure 1.2).

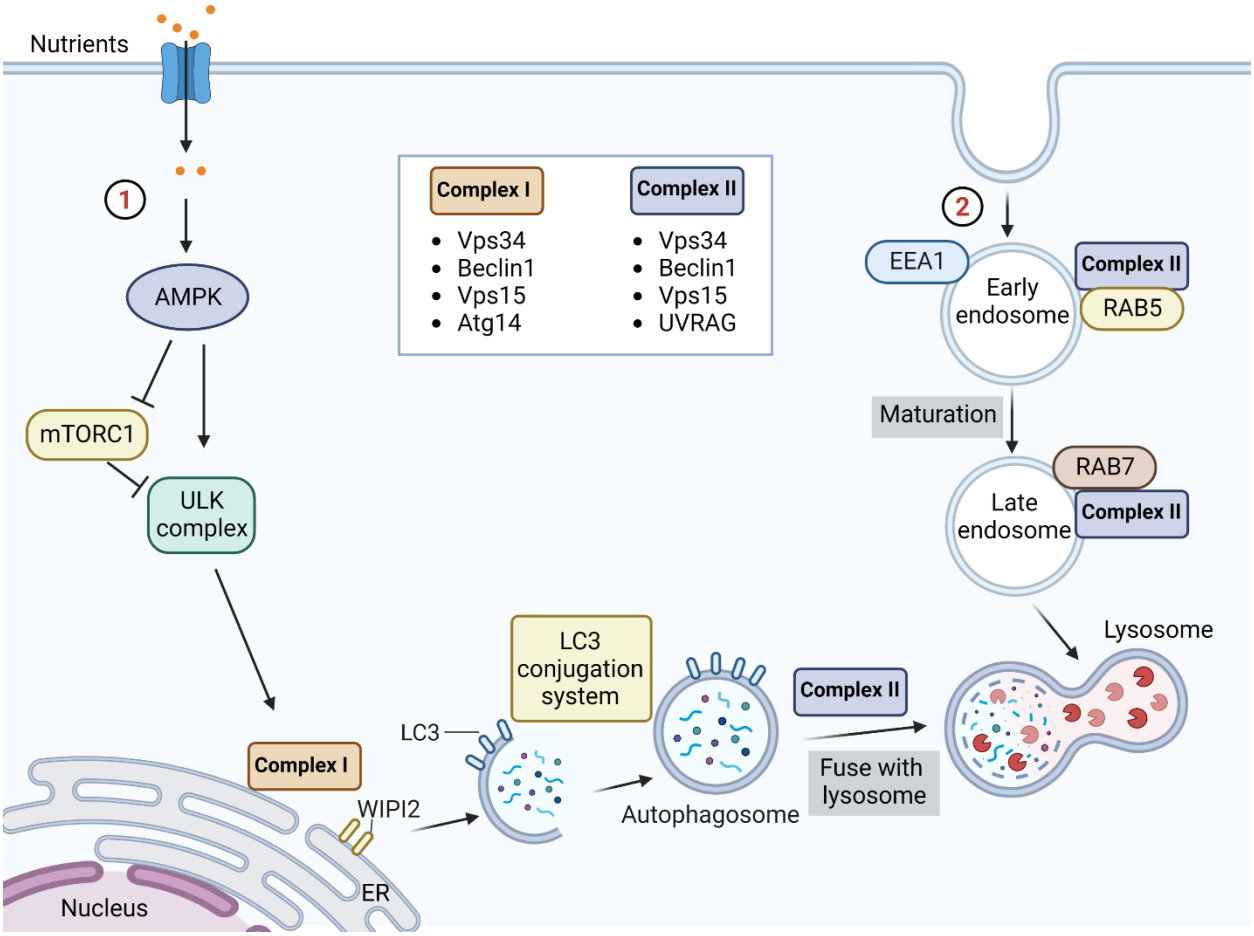


**Figure 1.2. Vps34 in autophagy and endosomal trafficking.** Upon nutrient deprivation mTORC1 is inhibited, leading to ULK complex derepression and translocation to the ER. The ULK complex activates Vps34 complex I to initiate autophagosome nucleation. Local PI3P production by Vps34 recruits WIPI2, which subsequently recruits the LC3 conjugation system that mediates autophagosome elongation. Vps34 complex II then promotes the fusion of the autophagosome to the lysosome for cargo degradation and recycling. **2.** During endocytosis, Vps15 binds RAB5–GTP, which recruits complex II to early endosomes to generate PI3P. PI3P then interacts with FYVE domain-containing effectors such as EEA1 that drive endosomal fusion. Additionally, complex II controls the maturation of RAB5-positive early endosomes into RAB7-positive late endosomes, which involves recruitment of effector proteins that inhibit and dissociate RAB5, thus initiating the so-called RAB switch. Finally, the complex II subunit UVRAG promotes late endosome/lysosome fusion by interacting with the homotypic fusion and vacuole protein sorting (HOPS) complex (not shown here), which plays a critical role in late endosomal trafficking and lysosome biogenesis (Liang et al., 2008). This figure was made with BioRender.com and adapted from (Bilanges *et al.*, 2019).

## Vps34 in macroautophagy

Autophagy is a catabolic cell process that delivers cytoplasmic cargo to the lysosome for degradation. There are at least three distinct forms of autophagy – chaperone-mediated autophagy, microautophagy, and macroautophagy – that differ in the mode of delivery of cargo to the lysosome. Macroautophagy, referred to hereafter simply as autophagy, is the major catabolic mechanism used by eukaryotic cells to maintain nutrient homeostasis and organellar quality control (Levine and Kroemer, 2019). It is mediated by a collection of over 30 evolutionarily conserved genes that, similar to Vps34, were discovered by genetic screens in yeast (Mizushima, 2018). Nutrient deprivation and other stresses initiate autophagy by inducing the dissociation of the mammalian/mechanistic target of rapamycin complex 1 (mTORC1) from the Atg1/ULK complex. After release from mTORC1, the Atg1/ULK complex translocates to the endoplasmic reticulum (ER) where it phosphorylates Atg14 and Vps34, leading to the recruitment and activation of Vps34 complex I. Local PI3P production by Vps34 leads to the formation of an isolation membrane emerging from an omega-shaped subdomain membrane from the ER (omegasome). This local pool of PI3P also leads to recruitment of the proteins WIPI2 and DFCP1 which are required to recruit two ubiquitin-like proteins, Atg12 and Atg8 (the latter is called microtubule-associated protein 1A/1B-light chain 3 [LC3] in mammals) and their associated conjugation systems, the E1-like conjugation system Atg7, and the E2-like conjugation system Atg10. Activation of these conjugation systems results in the covalent binding of Atg12 with Atg5, which together bind Atg16L1 to form pre-autophagosome structures from the isolation membrane. In a second ubiquitin conjugation reaction, Atg4 cleaves LC3 to LC3-I, which is then lipidated by Atg7 and Atg3 to generate LC3-

phosphatidylethanolamine (LC3-II). LC3-II associates with newly formed autophagosome membranes until they fuse with lysosomes. The generation and degradation of LC3-II is often employed to monitor autophagy (Klionsky et al., 2016). Following fusion with lysosomes the contents of autophagosomes are degraded and the resulting products are released into the cytosol by lysosomal permeases and recycled to generate new cellular constituents and energy. Although this maturation–fusion process involves Vps34 complex II, the precise mechanism remains poorly understood (Van Kaer et al., 2019; Yu et al., 2018).

**Vps34 in the endocytic system**

Endocytosis is a process by which eukaryotic cells take up macromolecules and particulate substances from extracellular space. In this process, the material to be ingested is progressively enclosed by a small portion of the plasma membrane, which first invaginates and then pinches off to form an endocytic vesicle containing the ingested substance or particle. Endocytosed cargo can be recycled to the cell surface, trafficked to the trans-Golgi network (TGN) through the retrograde system, or sorted to multivesicular bodies (MVBs)/late endosomes for lysosomal degradation (Alberts, 2002). Multiple lipid phosphatases and kinases and their products, including PI3P and Vps34, contribute to endocytic trafficking (Wallroth and Haucke, 2018). Vps34 complex II is targeted to early endosomes by the binding of the WD40 domain of Vps15 to activated Rab5 (Christoforidis et al., 1999). PI3P generated by Vps34 at the early endosome recruits effector proteins that contain FYVE or phox homology (PX) domains such as EEA1, Hrs, and rabenosyn-5. These effectors regulate the docking and fusion of cargo

containing vesicles from the plasma membrane as well as sorting of the enclosed cargo which can either be recycled back to the plasma membrane or delivered to the lysosome for degradation (Li et al., 2013). In addition to its role in regulating the early stages of endocytosis, Vps34 complex II has also been implicated in the late stages of endosomal trafficking via Vps15 and Rab7 binding (Jaber et al., 2016; Stein et al., 2003; Vieira et al., 2003). Finally, several reports have identified endosomal sorting dependent upon Vps34 catalytic activity as necessary for the maturation of the protease cathepsin D in lysosomes (Jaber *et al.*, 2016; Reifler et al., 2014; Ronan et al., 2014; Row et al., 2001).

**Organismal role of Vps34**

Vps34 deficiency has been studied in several yeast, invertebrate, and murine model organisms. In *Saccharomyces cerevisiae*, mutations in the *Vps34* gene results in mis-sorting of several vacuolar hydrolases, as described earlier. It also results in temperature-sensitive growth defects, vacuole segregation defects during mitosis, as well as a disruption of autophagy (Herman and Emr, 1990; Kihara et al., 2001; Schu et al., 1993). In *Caenorhabditis elegans*, LET-512/VPS34, the homologue of yeast Vps34, was found to be ubiquitously expressed in all tissues and developmental stages. Mutations in *let-512/Vps34* caused an arrest in worm development at or shortly after the molts from L3 to L4 or from L4 to adult and was associated with defective membrane transport (Roggo et al., 2002). In *Drosophila melanogaster*, deletion of the *Vps34* gene causes hemizygous larval lethality, failure in autophagosome formation and defective endocytosis in fat body cells (Juhasz et al., 2008). In mice, homozygous mutations in *Vps34* causes embryonic death between days 7.5 and 8.5 of embryogenesis (Zhou et al., 2011). *Vps34* null mice

display severe defects in cell proliferation during development that was associated with significantly reduced mTORC1 signaling. Vps34 has a complex relationship with mTORC1 signaling. AMPK directed suppression of mTORC1 is necessary for activating Vps34-dependent autophagy, yet Vps34 has been implicated in mammalian cells as being necessary for lysosomal positioning and activation of mTORC1 in response to acute stimulation with amino acids (Byfield et al., 2005; Gulati et al., 2008; Hong et al., 2017; Nobukuni et al., 2005; Yoon et al., 2011). Of note, deletion of autophagy-essential genes downstream of Vps34 in the autophagy pathway (e.g., ATG3, ATG5, ATG7, ATG12 or ATG16L1) results in perinatal death that coincides with the massive induction of autophagy after birth (Kuma et al., 2017). This highlights the non-autophagic functions of Vps34 that are necessary for development. Furthermore, mice with homozygous *Vps34*-kinase-dead knock-in mutations perished at a similar time during development as Vps34 null mutants, indicating that catalytic activity of Vps34 was required for development (Bilanges et al., 2017). Heterozygous adult *Vps34*-kinase-dead knock-in mice displayed increased insulin sensitivity and glucose tolerance. Heterozygous mutants also displayed partial protection against high-fat diet-induced liver steatosis, which was associated with increased AMPK activation. Collectively these studies highlight that, while Vps34 is not a direct signal transducer, it can indirectly regulate signaling of protein kinases through its function in endosomal trafficking. Finally, tissue-specific ablation of Vps34 in mice has revealed an indispensable role for Vps34 in organ function and cell survival, including cells of the immune system.

### 1.3 Thymic APCs direct T cell development and repertoire selection

The thymus is a primary lymphoid organ located directly above the heart that supports the differentiation and selection of T cells (Miller, 2020). After recruitment to the thymus, developing T cells rearrange their TCR α and β genes to collectively generate an Ag receptor repertoire with the breadth to react to an expanse of potential antigens derived from pathogens and transformed cells. However, many Ag receptor rearrangements will not produce functional TCRs. Furthermore, of the productively rearranged TCRs, many will be unable to bind their cognate antigen when presented by the host's limited set of MHC molecules. Therefore, a positive selection step during T cell development ensures that a functional TCR is generated with the capacity to recognize antigens in the context of the host's own MHC molecules (Breed et al., 2018). Those immature T cells that fail to interact with any of the self-MHC molecules expressed in the host will undergo apoptosis, in a process commonly referred to as "death by neglect". The quasi-random rearrangement of TCRs will also produce clones that react strongly to self-peptide/MHC complexes. Therefore, a negative selection step culls autoreactive T cells from the repertoire or diverts them into a regulatory lineage.

T cell progenitors are recruited to the thymus and guided through development and selection steps by discrete populations of thymic APCs. After commitment to the T cell lineage, the fate of a developing thymocyte is mainly directed by the strength of the interaction of the TCR with self-peptide/MHC complexes displayed by thymic APCs. This is known as the affinity/avidity model of thymocyte selection (Figure 1.3) (Moran and Hogquist, 2012). Weak interactions are required to protect thymocytes from death by neglect and to promote the positive selection of naïve T cells. Strong interactions enforce

tolerance through negative selection by apoptosis or differentiation into Foxp3$^{+}$ regulatory T cells (Tregs) (Klein et al., 2014). Positive selection and tolerance induction mainly occur within discrete thymic microenvironments, the cortex and the medulla, respectively. Both compartments contain selection niches that are composed of different types of APCs that are specialized for their unique roles in promoting thymocyte development and selection. Thus, the thymus is composed of microenvironments that coordinate a spatial and temporal segregation of thymocyte selection (Klein *et al.*, 2014). In this section I will discuss the diverse thymic APCs and how they promote the selection of a TCR repertoire with the capacity to respond to various antigens yet is tolerant to self-tissue (Figure 1.4).

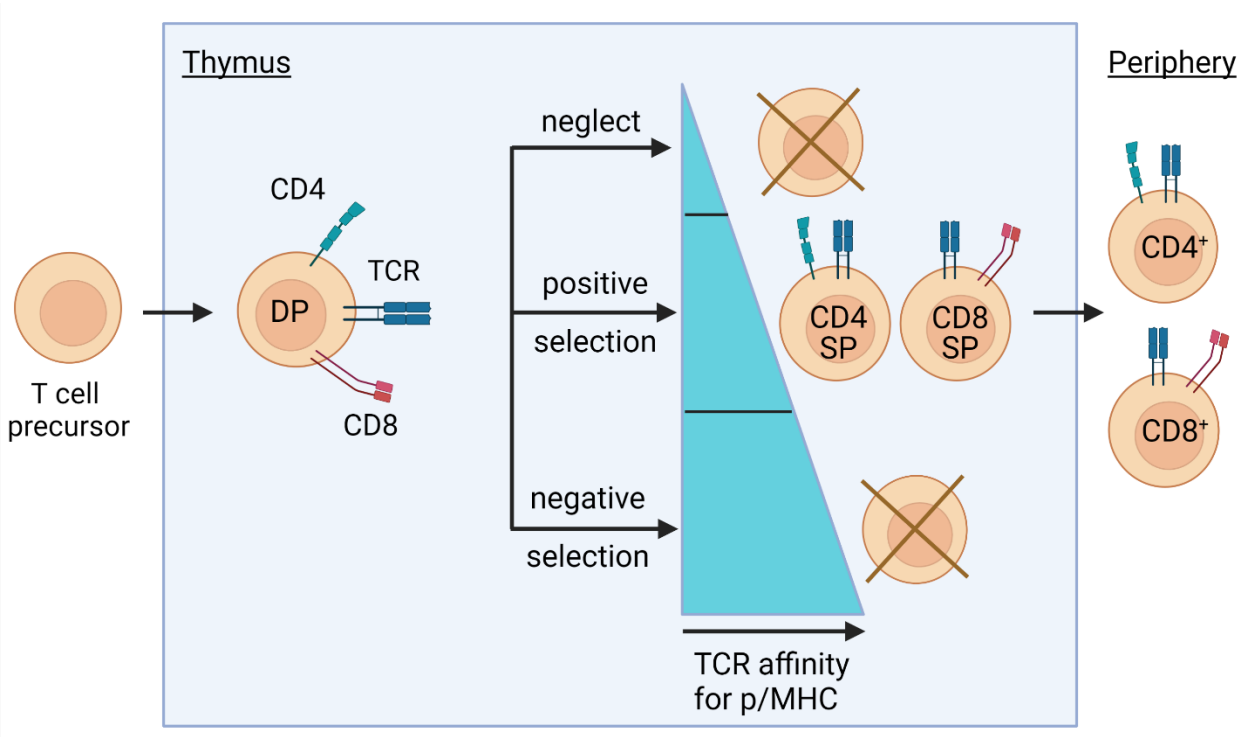


**Figure 1.3. Affinity model of T cell selection.** DP thymocytes expressing a newly rearranged TCR audition in the thymus to become mature SP T cells. Here, the affinity of the TCR for self-peptide/MHC presented by thymic APCs drives the outcome. TCRs with intermediate levels of affinity are promoted for positive selection. TCRs with very weak or

very strong affinities fail positive selection by neglect or negative selection, respectively, and die. This figure was made with BioRender.com.

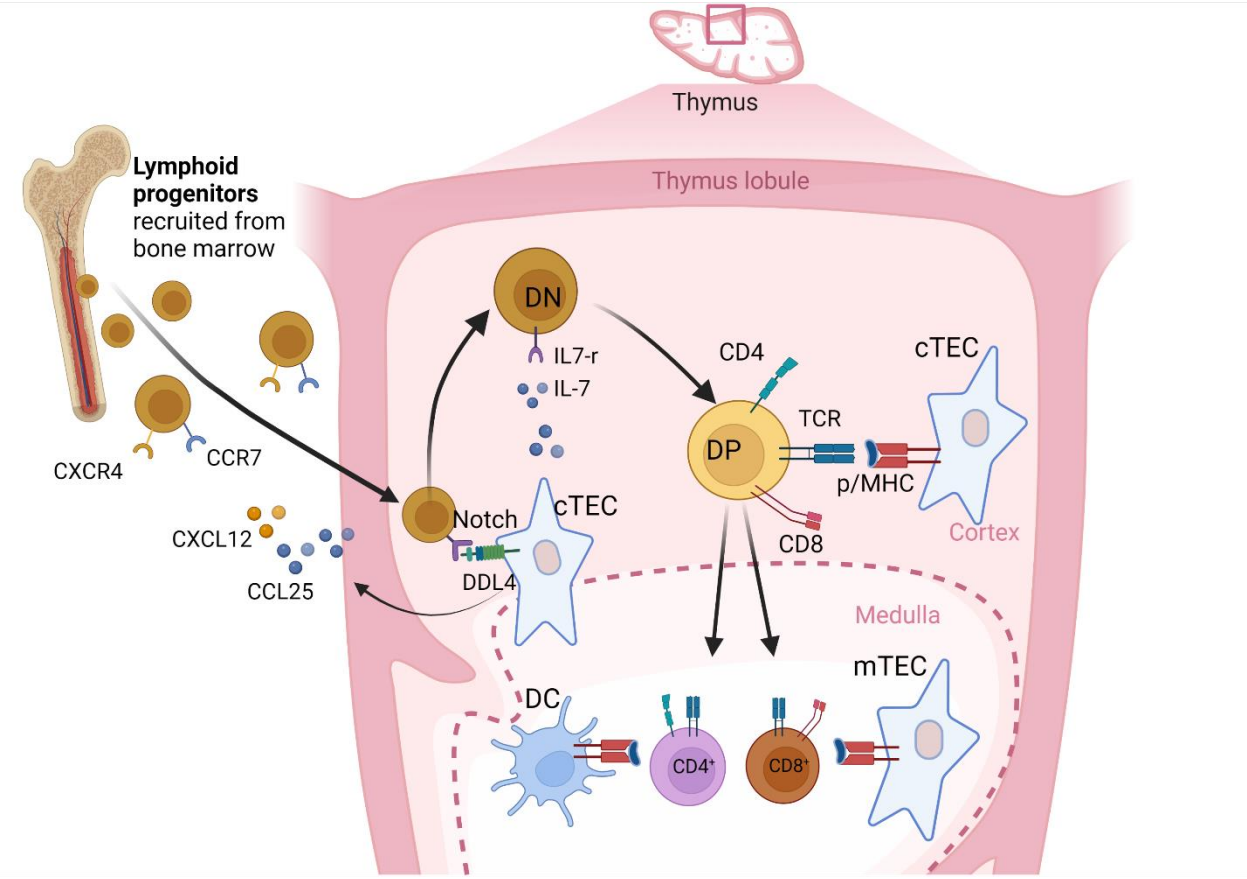


**Figure 1.4. Thymic stromal cells guide T cell development.** T cell precursors are recruited to the thymus and commit to the T cell lineage via cortical thymic epithelial cell (cTEC)-dependent NOTCH signaling. After successive stages of double-negative (DN) development, thymocytes express a T cell receptor (TCR) and both CD4 and CD8 coreceptors (DP). cTECs undergo positive selection on self-peptide/MHC complexes displayed by cTECs. After positive selection, CD4 and CD8 single positive thymocytes traffic to the medulla to scan medullary TECs (mTECs) and dendritic cells (DCs) for strong TCR-self-peptide/MHC interactions leading to tolerance induction. This figure was made with BioRender.com.

## Cortical thymic epithelial cells

### *The role of cortical thymic epithelial cells in initiating T cell development.*

Before thymic selection can occur, lymphoid progenitors must traffic from the bone marrow to the thymus and commit to the T cell developmental program. Cortical thymic epithelial cells (cTECs) express several key molecules that are crucial for initial T cell development (Kadouri et al., 2020; Takahama et al., 2017). cTECs secrete high levels of two key cytokines, CXC-chemokine ligand 12 (CXCL12) and CC-chemokine ligand 25 (CCL25), which promote the homing of lymphoid progenitor cells into the thymus via CXC-chemokine receptor 4 (CXCR4) and CC-chemokine receptor 7 (CCR7) signaling (Gossens et al., 2009; Jenkinson et al., 2007; Plotkin et al., 2003). Progenitor cells arrive at the junction of the cortex and medulla and then traffic outward to the subscapular region of the thymic cortex (Takahama, 2006). cTECs express high levels of the Notch ligand delta-like ligand 4 (DLL4), which instructs the recruited lymphoid progenitors to commit to the T cell lineage (Hozumi et al., 2008; Koch et al., 2008). Thymocytes progress through a developmental pathway before positive selection that is commonly identified by the expression of cell surface markers CD44 and CD25 and divided into so-called double-negative (DN) stages 1-4 (DN1-DN4), which represent $CD44^{+}CD25^{-}$, $CD44^{+}CD25^{+}$, $CD44^{-}CD25^{+}$, $CD44^{-}CD25^{-}$ subsets, respectively. During this developmental progression, cTECs express various cytokines, such as IL-7 and stem cell factor (SCF), that promote the proliferation and survival of the developing thymocytes (Alves et al., 2009). Upon expressing a rearranged TCR, thymocytes start to express both CD4 and CD8 (DP) coreceptors and are then tested for positive selection on cTECs. cTECs are the sole stromal cell type necessary for positive selection, and accumulating evidence suggests

that the crucial role of cTECs is, at least in part, a result of the unique machineries that these cells use to process and present antigen. It is likely that these proteolytic pathways cause cTECs to present a largely unique peptide/MHC ligandome (also referred to as immunopeptidome) that is distinct from other thymic or peripheral APCs and is optimized for positive selection (Klein *et al.*, 2014).

***Generation of self-peptide/MHC complexes for positive selection.***

The peptide cargo of MHC class I molecules is predominantly derived from newly synthesized cytosolic protein antigens and defective ribosomal products (DRiPs) (Van Kaer, 2002; Wearsch and Cresswell, 2008; Yewdell, 2011). Such antigens are degraded by the proteasome to peptides, which are subsequently transported to the lumen of the ER by the heterodimeric transporter associated with antigen processing (TAP) and then bind with peptide-receptive MHC class I proteins before trafficking through the Golgi apparatus to the cell surface (Figure 1.5). The core proteasome complex is composed of four heptameric rings – two outer α rings and two inner β rings (Groll et al., 1997; Unno et al., 2002). Three forms of proteasomes with different catalytic activities have been identified based on the composition of the β subunits. While other cell types express either the constitutive proteasome (β1, β2, and β5) or the immunoproteasome (β1i, β2i, and β5i), cTECs uniquely express the thymoproteasome (β1i, β2i, and β5t [encoded by *Psmb11*]) (Takada et al., 2017). The specific expression of the thymoproteasome suggests that cTECs display a unique set of self-peptides bound to MHC class I molecules that are crucial for positive selection. Indeed, *Psmb11* knockout (thymoproteasome deficient) mice display severe defects in the positive selection of CD8SP but not CD4SP T cells resulting in 20–30% of normal peripheral $CD8^+$ T cell

cellularity (Murata et al., 2007). Strikingly, the pool of $CD8^+$ T cells selected in thymoproteasome-deficient mice was significantly less responsive to infection. This suggests that positive selection on thymoproteasome-dependent peptides conditions mature $CD8^+$ T cell reactivity (Takada et al., 2015). Based on these studies it was unclear whether positive selection required TCR interaction with unique peptides not displayed on other thymic APCs (i.e., during negative selection) or if the thymoproteasome generated peptides specialized for positive selection. This question was directly tested by examining mice in which the β5t-encoding locus was disrupted with a β5i-encoding gene knock-in mutation. These mice were further crossed to β5i-knockout mice. This resulted in a mouse strain in which cTECs expressed β5i-containing immunoproteasomes instead of β5t-containing thymoproteasomes, and all other cells in the body (including APCs responsible for negative selection) expressed constitutive proteasomes (Xing et al., 2013). CD8SP selection was still greatly diminished in these mice indicating that the role of the thymoproteasome in thymic selection is not merely to generate peptides distinct from other thymic APCs but to generate unique peptides that are specialized to promote positive selection.

For the MHC class II pathway, MHC II molecules are synthesized in the ER followed by functional maturation in endosomal compartments that contain abundant antigenic peptides (Figure 1.5). In the ER, newly synthesized MHC II α and β subunits form a complex together with a non-polymorphic chaperone called invariant chain or CD74 (Blum et al., 2013). The invariant chain serves to protect the MHC II peptide binding groove and contains an N-terminal targeting motif that directs the MHC II molecule to endosomal-lysosomal antigen-processing compartments (Roche and Furuta, 2015).

Invariant chain also promotes the stability of MHC molecules. Without invariant chain expression, MHC II molecules aggregate, are retained in the ER, and do not reach the cell surface. Because of this, mice lacking invariant chain are deficient in $CD4^+$ T cell lymphopoiesis (Viville et al., 1993). Furthermore, by associating with MHC II molecules, the invariant chain prevents antigenic peptide binding and safeguards against peptide loading too early in the MHC II biosynthetic pathway. After assembly in the ER, MHC II-invariant chain complexes are directed to the endocytic pathway via direct targeting from the TGN or by endocytosis from the plasma membrane. In acidic endosomes/lysosomes, the invariant chain is progressively degraded by proteases resulting in a peptide that is embedded in the ligand binding groove that is roughly 20 residues in length and called class II-associated invariant chain peptide (CLIP) (Pishesha *et al.*, 2022). Studies analyzing protease-deficient mice revealed that a number of enzymes including cathepsins (S, L, F) and asparaginyl endopeptidase (AEP) mediate invariant chain degradation in a cell type-specific manner (Watts, 2004). In cTECs, cathepsin L plays a key role in invariant chain processing (Nakagawa et al., 1998). MHC II alleles with a low affinity for CLIP are genetically associated with the development of autoimmunity (Busch et al., 2005). This may reflect a role for MHC II-CLIP complexes in TECs for promoting the development of a self-tolerant TCR repertoire. CLIP release from MHC II molecules in late endosomes is promoted by the heterodimeric peptide exchange factor DM (H2-DM in mice). DM induces a conformational change in MHC II molecules which liberates CLIP and promotes its replacement with a higher affinity peptide. DM can remove any low affinity peptides from MHC II, therefore iterative interactions with DM controls the production of MHC II complexes bound with high affinity peptides. DM-mediated removal

of CLIP in TECs plays a critical role in thymic selection. DM knockout mice have a defect in positive selection of $CD4^+$ T cells resulting in mild T cell lymphopenia (Fung-Leung et al., 1996; Martin et al., 1996; Miyazaki et al., 1996). Subsequent studies revealed that DM in TECs was required for the generation of specific TCR clones (Pacholczyk et al., 2006; Wong et al., 2007). The activity of DM is negatively regulated by another heterodimeric MHC II accessory molecule called DO which is mainly expressed in mTECs and B cells and has been implicated in shaping the $CD4^+$ TCR repertoire and susceptibility to autoimmune disease (Welsh et al., 2020).

In addition to expressing a unique proteasomal catalytic subunit important for MHC class I binding peptides, cTECs also express a distinct spectrum of lysosomal and endosomal proteases, including cathepsin L and thymus-specific serine protease (TSSP), that are necessary for optimal positive selection of an immunoreactive pool of $CD4^+$ T cells. (Kondo et al., 2017). While cathepsin L is important for invariant chain degradation in cTECs, it is also implicated in the generation of positively selecting ligands. Cathepsin L-deficient mice show significant defects in the positive selection of a polyclonal repertoire of $CD4^+$ T cells as well as a complete block in the development of several MHC class II-restricted transgenic TCRs (Honey et al., 2002). Cathepsin L may play a role in conditioning the peripheral repertoire as cathepsin L knockout mice display less severe autoimmune disease in some models (Maehr et al., 2005; Schurigt et al., 2012), although the contribution of repertoire skewing to disease progression cannot be discounted. TSSP-deficient mice display a more subtle thymic selection phenotype with normal polyclonal $CD4^+$ T cell numbers but defective positive selection of certain MHC class II-restricted transgenic TCRs and altered Ag-specific immune responses (Gommeaux et al.,

2009; Viret et al., 2011a). TSSP deficiency also results in resistance of non-obese diabetic (NOD) mice to diabetes (Serre et al., 2015; Viret et al., 2011b; Viret et al., 2015) and spontaneous colorectal cancer (Brisson and Carrier, 2015). In addition to the expression of unique proteolytic machinery, TECs (and particularly cTECs) display high rates of constitutively active autophagy (Mizushima et al., 2004; Nedjic et al., 2008). Autophagy has been demonstrated to contribute to antigen processing by delivering autophagosome cargo for lysosomal proteolysis and thus contributing to the pool of antigens loaded on MHC II molecules (Munz, 2021). Consistent with the idea that autophagy shapes the cTEC immunopeptidome, positive selection of several MHC class II-restricted but not class I-restricted transgenic TCRs was altered upon interference with macroautophagy in the thymic epithelium (Nedjic *et al.*, 2008). Finally, the stability and rate of surface turnover of MHC II molecules is tightly regulated in cTECs and optimized for positive selection. cTECs constitutively express the transmembrane protein CD83 which interferes with the March 8-mediated ubiquitination and lysosomal degradation of MHC II molecules. Therefore, CD83 promotes the surface stability of MHC class II molecules expressed by cTECs. CD83-deficient mice exhibit significant defects in the positive selection of $CD4^+$ but not $CD8^+$ T cells (Liu et al., 2016; von Rohrscheidt et al., 2016). This latter finding lends support to the kinetic signaling model of T cell lineage commitment, which proposes that relatively longer durations of TCR interaction with positively selecting p/MHC II complexes promotes CD4 SP selection (Singer et al., 2008).

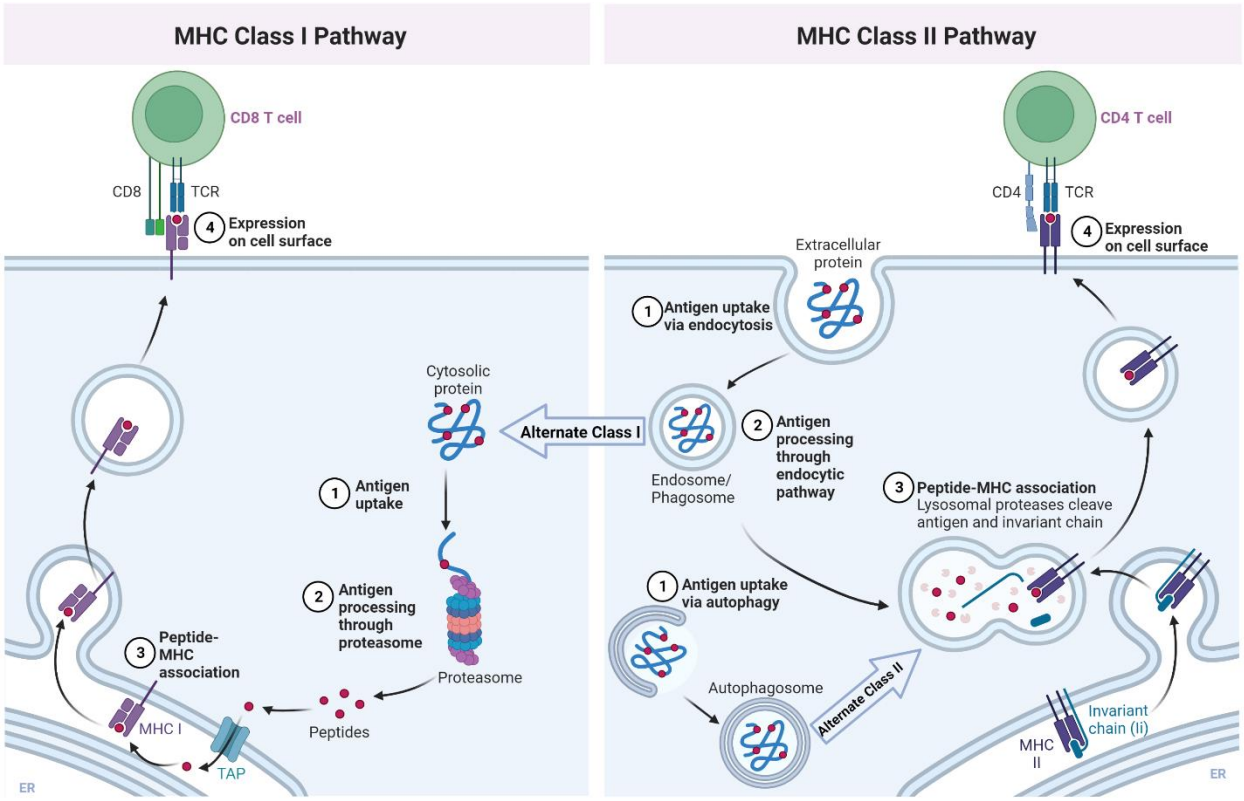


**Figure 1.5. The pathways of antigen presentation.** MHC class I ligands originate from cytosolic proteins that are processed by the proteasome and transported into the ER for loading onto newly synthesized MHC I molecules. MHC II molecules are generated in the ER and bound to the nonpolymorphic chaperone invariant chain (Ii). MHC II-Ii complexes are trafficked through the Golgi apparatus to endosomal/lysosomal compartments that are rich in antigenic peptides derived from endocytosis or autophagy. Ii is degraded by cathepsin proteases to a peptide called class II-associated invariant chain peptide (CLIP). The peptide editor DM promotes the exchange of CLIP for peptides that bind MHC II with higher affinity before egressing to the cell membrane. This figure was made with BioRender.com.

### Medullary thymic epithelial cells

After DP thymocytes pass positive selection in the cortex they upregulate the chemokine receptor CCR7 and are attracted to the thymic medulla where medullary TECs (mTECs) express the CCR7 ligands CCL19 and CCL21 (Nitta et al., 2009; Ueno et al., 2004). mTECs are dispensable for the development of αβT cells and serve only to enforce tolerance through clonal deletion or inducing Foxp3-expressing $CD4^+$ thymus-derived

Tregs (tTregs). Mice that lack mTECs or do not express MHC II molecules specifically on mTECs develop severe spontaneous autoimmunity (Irla et al., 2010; Laufer et al., 1996). Mature mTECs express high levels of MHC molecules as well as the costimulatory molecule CD80 which make them potent APCs necessary to induce strong TCR signaling in autoreactive thymocytes (Abramson and Anderson, 2017). In order to enforce central tolerance, mTECs must express and present to developing thymocytes the complete array of self-peptides that they might encounter once they mature and circulate in the periphery. To this end, mTECs express up to 90% of the entire coding genome in a phenomenon called “promiscuous gene expression” (Sansom et al., 2014). Promiscuous gene expression critically depends on the transcriptional regulator called autoimmune regulator (AIRE) which promotes the ectopic expression of otherwise tissue-restricted antigens. Mice deficient in AIRE or with ablation of AIRE-expressing cells contain severe autoimmune manifestations characterized by robust lymphocyte infiltration into endocrine organs (Anderson et al., 2002; Metzger et al., 2013). In humans, mutations in *AIRE* causes a disease called autoimmune polyendocrinopathy candidiasis ectodermal dystrophy (APECED), which is a life-threatening autoimmune disease that attacks multiple organs and has its onset in childhood (Besnard et al., 2021). More recently, a zinc finger transcription factor Fezf2 has been identified as an additional regulator of promiscuous gene expression in mTECs. Interestingly, the spectrum of genes regulated by Fezf2 and AIRE appear distinct, but Fezf2 knockout mice similarly develop autoimmune disease (Takaba et al., 2015). The loading of intracellular peptide on MHC II molecules has been proposed, like cTECs, to involve the autophagy pathway. A study found that when a model antigen was targeted to the autophagy pathway in mTECs it

more efficiently induced the negative selection of corresponding Ag-specific $CD4^+$ T cells than did the control antigen that was located to the cytosol but not targeted to autophagosomes (Aichinger et al., 2013). Furthermore, the same study also showed that a mitochondrial version of a model antigen required autophagy for tolerogenic presentation by mTECs, whereas the direct presentation of a membrane-bound form of the same antigen was autophagy-independent (Aichinger *et al.*, 2013; Klein *et al.*, 2014). Therefore, it is possible that autophagy contributes antigen from specific intracellular compartments to the MHC class II pathway for tolerance.

**Dendritic cells and B cells**

The thymic medulla also contains haematopoietically derived APCs that contribute to central tolerance. There are three thymic DCs populations: $CD8^+$ conventional DCs, $Sirp\alpha^+$ conventional DCs, and plasmacytoid DCs (Oh and Shin, 2015). Thymic DCs contribute to both negative selection and Treg induction via direct antigen presentation and antigen acquired from the blood and mTECs (Waisman et al., 2017). Furthermore, migratory $Sirp\alpha^+$ conventional DCs can present peripheral self-antigens (Audiger et al., 2017). B cells are also present in the medulla of the thymus and thought to play a non-redundant role in negative selection and Treg induction (Castaneda et al., 2021). While thymic DCs present tissue-restricted antigens derived from mTECs, accumulating evidence suggests that a subset of thymic B cells express AIRE to drive clonal deletion of autoreactive $CD4^+$ clones (Cepeda et al., 2018; Gies et al., 2017; Yamano et al., 2015).

### 1.4 Contribution of autophagy to B cell development and humoral immunity

B cell development produces three distinct classes of naïve B cells: the B-1 lineage and 2 B-2 lineages, follicular (FO), and marginal zone (MZ) B cells. These B cell subsets vary in location, capacity for self-renewal, and functional specialization (Allman and Pillai, 2008). Activation and differentiation of peripheral B cells are antigen driven and augmented by second signals including toll-like receptor (TLR) ligands and T cell help to generate antibody-producing cells. A subset of B cells collaborate with T cells in MHC-TCR-dependent interactions to undergo further differentiation in the germinal center (GC) to produce recirculating memory B cells or plasmablasts that can become long-lived plasma cells in the bone marrow (BM) (Victora and Nussenzweig, 2022). The metabolic demands differ for various B cell subsets and fluctuate over the lifespan of a B cell, from development to maintenance of a memory cell. Furthermore, mature B cells can occupy various niches that differ greatly in the nutrients that are available. Therefore, B cells must tightly regulate a metabolic program to generate sufficient energy while balancing anabolism, catabolism, and a pool of essential molecules to serve as metabolic intermediates (Boothby and Rickert, 2017). Autophagy is the primary catabolic mechanism used by cells to maintain nutrient homeostasis and organellar quality control (Levine and Kroemer, 2019). In B cells, autophagy plays critical roles in maintaining organelle function, especially mitochondria and ER, to promote an optimal B cell response (Metur and Klionsky, 2021). In this section I will discuss the role that B cell autophagy plays in B cell development and humoral immunity.

## B cell development and maturation

In postnatal mice, self-renewing multipotent hematopoietic stem cells (HSCs) in the bone marrow give rise to blood cells, including B cells, with progressively more limited differentiation potential. The specialized microenvironment of the bone marrow provides signals both for the development of lymphocyte progenitors and for the subsequent differentiation of B cells. The HSCs first differentiate into multipotent progenitor cells (MPPs) which can produce both lymphoid and myeloid cells but are no longer self-renewing stem cells. MPPs express a cell-surface receptor known as FLT3 that binds the membrane-bound FLT3 ligand on stromal cells which promotes their differentiation into common lymphoid progenitors (CLPs). The differentiation of MPPs into CLPs induces the expression of the receptor for interleukin-7 (IL-7). The progenitors establish contact with mesenchymal and epithelial microenvironments that produce factors essential for B-cell development including IL-7 and stem-cell factor (SCF) which interacts with the receptor Kit on the precursor B cells. At this stage, commitment to the B cell lineage (pro-B cell) is specified by induction of the transcription factor E2A and expression of the V(D)J-rearrangement machinery RAG1 and RAG2. Each pro-B cell undergoes independent rearrangement of the heavy-chain locus. A successful rearrangement leads to the production of intact μ heavy chains, and the cells progress to the pre-B cell stage. Sensing this maturation step, the cells then proliferate, exit the cell cycle, and start to rearrange Ig light-chain gene segments. The light-chain pairs with the previously rearranged heavy-chain and is expressed as IgM molecules at the cell surface, and these cells can then be classified as immature B cells. At this stage, the surface IgM can bind antigens. The immature B cells are tested for reactivity to self-antigen present in the bone marrow

microenvironment. Self-reactivity at this point promotes signaling that triggers its elimination via negative selection. Immature B cells that pass this step emigrate the bone marrow and complete maturation in the spleen. Immature B cells in the spleen proceed through two distinct transitional stages. Maturation through the transitional stages requires weak signaling through the BCR and a prosurvival cytokine called B-cell activating factor (BAFF) which is abundantly produced by follicular DCs. Mature splenic B cells are mainly FO B cells with MZ B cells comprising a smaller percentage that are, as the name suggests, enriched at the marginal zones of the white pulp/red pulp junctions. Homeostatic maintenance of mature B-2 B cells requires tonic BCR signaling and BAFF signaling (Allman and Pillai, 2008; Khan, 2009; Melchers, 2015; Murphy and Weaver, 2016; Nemazee, 2017).

Several studies have analyzed the role of autophagy in B cell development and mature homeostasis with conflicting results. In radiation bone marrow chimeras transplanted with *Atg5*$^{-/-}$ fetal hematopoietic cells, B cell development was negatively affected at the transition from the pro- to pre-B cell stage in the bone marrow (Miller et al., 2008). However, subsequent studies that analyzed B cell development in mice with conditional deletion of *Atg5* (Arnold et al., 2016) or *Atg16l* (Martinez-Martin et al., 2017) driven by Cre recombinase controlled under the *CD79a* promoter, or *Atg7* (Chen et al., 2014) or *Atg16l* (Martinez-Martin *et al.*, 2017) under the *CD19* promoter revealed no alterations in B cell development. It is also unclear whether autophagy is required for maintenance of mature naïve B cells as conditional deletion of *Atg5* via *CD79a*- or *CD21*-driven Cre recombinase resulted in decreased numbers FO B cells (Arnold *et al.*, 2016).

However, CD19-Cre mediated deletion of *Atg7* did not result in alterations to peripheral B-2 B cell numbers (Chen *et al.*, 2014).

**B-1 B cells**

B-1 B cells, which can further be divided into B-1a and B-1b B cells, are enriched in peritoneal and pleural cavities and are thought to be the predominant sources of circulating immunoglobulins (Igs) termed natural IgM antibodies (Baumgarth, 2016). B-1 B cells constitutively produce natural IgM which fulfills many functions in tissue homeostasis and pathogen exposure. While the role of autophagy in maintaining mature B-2 B cell homeostasis remains unclear, genetic ablation of Atg5, Atg7, or Atg16l consistently resulted in defects in B-1a B cells (Arnold *et al.*, 2016; Chen *et al.*, 2014; Clarke et al., 2018; Martinez-Martin *et al.*, 2017). A recent study reported that B-1 B cells display unique metabolic requirements and depend on autophagy to maintain the capacity for self-renewal (Clarke *et al.*, 2018).

**B cell activation**

Naïve B cells in the spleen follicles are activated in response to Ag recognition by the BCR (Phan et al., 2009). Ag binding initiates a downstream BCR signaling cascade and the internalization, processing, and presentation of BCR-bound antigen on MHC class II molecules. The response to antigen alone is insufficient for the complete activation of B cells and often results in death. Full B cell activation requires a second, temporally distinct signal from antigen-specific helper T cells, typically through CD40 ligand interaction, or through TLR agonists in the absence of helper T cells (Kwak et al., 2019). The activation

of B cells triggers cell proliferation accompanied by metabolic rewiring including induction of autophagy (Raza and Clarke, 2021). Upon activation, naïve B cells can adopt one of three fates following interactions with helper T cells. Naïve B cells can differentiate into short-lived plasma cells that produce pathogen-specific antibodies. Naïve B cells can differentiate into GC B cells to generate class switched antibodies and then subsequently differentiate into long-lived plasma cells and memory cells. And finally, naïve B cells may also give rise to memory B cells in the follicle independently of GCs (Akkaya et al., 2020).

Although autophagy increases during plasmablast differentiation induced by TLR4 agonists, studies analyzing Atg5-deficient B cells indicated that it is dispensable for B cell differentiation. However, autophagy promotes plasma cell maintenance and sustained antibody production by ameliorating ER stress and preventing the accumulation of damaged mitochondria (Arnold *et al.*, 2016; Pengo et al., 2013).

The GC reaction is also characterized by a strong induction of B cell autophagy. Interestingly, WIPI2-mediated noncanonical autophagy appears to promote GC responses while canonical autophagy (e.g., Atg16l-dependent) has no significant impact on the primary GC response (Martinez-Martin *et al.*, 2017). Additional studies analyzing the primary GC-derived Ab response in Atg5- and Atg7-deficient mice appear to confirm this observation (Chen *et al.*, 2014; Pengo *et al.*, 2013). Following a GC reaction, a subset of B cells survive and exit the GC and ultimately differentiate into memory B cells and long-lived plasma cells. B cells are able to differentiate into memory populations in the absence of autophagy but, unlike naïve B cells, require autophagy for homeostasis (Chen *et al.*, 2014; Chen et al., 2015).

### 1.5 Rationale for dissertation research

The overarching goal of this dissertation is to elucidate the contribution that the lipid kinase Vps34 makes to the development, homeostasis, and function of two important APCs, namely TECs and B cells. Vps34 is the sole class III PI3K and is significantly understudied relative to class I and II PI3Ks, especially in the context of immune cell function. Vps34 contributes to diverse cellular processes including endocytosis, vesicular trafficking, and autophagy – processes that contribute to MHC class II antigen processing and presentation. Furthermore, autophagy is a central mechanism by which cells respond to stress and maintain cellular homeostasis by delivering cytoplasmic constituents to the lysosome for recycling. **The central hypothesis for this thesis project is that Vps34-mediated cellular processes maintain organellar quality control to promote the homeostasis of mature TECs and B cells and uniquely control their capacity for MHC class II-restricted antigen presentation.** This hypothesis was tested in two research chapters. In chapter 2, we interrogated the intrathymic development and repertoire selection of $CD4^+$ T cells in mice with a TEC-specific deletion of Vps34. In chapter 3, we examined the capacity of Vps34-deficient B cells to maintain mature homeostasis and participate in MHC class II-restricted T cell dependent humoral responses.

This work represents the first comprehensive examination of the role Vps34 plays in TECs and B cells. The results of this thesis will provide novel insights into the mechanisms governing the generation and maintenance of cells of the adaptive immune system with practical implications for the development of therapeutics that leverage adaptive immunity such as vaccines.

# Chapter 2

# THYMIC EPITHELIAL CELLS REQUIRE VPS34 TO MAINTAIN CELLULAR HOMEOSTASIS AND CD4 T CELL SELECTION

## 2.1 Introduction

The thymus is a specialized primary lymphoid organ that functions to generate a pool of immunologically competent T cells that can recognize and eliminate foreign antigens while tolerating the body's own tissues (Kadouri *et al.*, 2020). T cells sense cognate peptide antigens bound to major histocompatibility complex (MHC) molecules through their diverse T cell receptors (TCRs) that are highly specific for a particular peptide-MHC complex. The generation of a broad and tolerant TCR repertoire is mainly directed by self-peptide/MHC complexes displayed by thymic epithelial cells (TECs) during thymocyte development in a process called thymic selection (Han and Zuniga-Pflucker, 2021; Takaba and Takayanagi, 2017). Cortical TECs (cTECs) present self-peptides bound to MHC class I or class II molecules to immature $CD4^+CD8^+$ (double-positive [DP]) thymocytes for positive selection of $CD8^+$ or $CD4^+$ (single-positive [SP]) T cells, respectively. Here, TCR engagement with low avidity or antagonistic peptide-MHC complexes provides prosurvival signals (Klein *et al.*, 2014).

MHC class II-mediated antigen presentation in cTECs relies on cellular processes and machinery that are unique among antigen-presenting cells (APCs) (Kondo *et al.*, 2017). While most APCs depend on extracellular sources to supply peptides for MHC class II binding, cTECs predominantly rely on intracellular sources for this process (Klein *et al.*, 2014). In addition to utilizing a unique spectrum of endosomal and lysosomal

proteases and relying on distinct machinery for trafficking of membrane proteins, a high frequency of cTECs is constitutively active in macroautophagy (Mizushima *et al.*, 2004; Nedjic *et al.*, 2008; Schuster et al., 2015). Autophagy is a catabolic cellular process that targets components of the cytosol to the lysosome for degradation and recycling (Levine and Kroemer, 2019). A previous study provided evidence that autophagosomal vesicles constantly fuse with the MHC class II peptide-loading compartment to facilitate antigen presentation (Schmid et al., 2007), raising the possibility that the autophagy pathway contributes to the repertoire of self-peptides that binds MHC class II molecules and is optimized for positive selection of $CD4^+$ T cells. Autophagy has common features with endocytosis and vesicle trafficking with which it shares effector molecules, including several of the autophagy-related (Atg) factors (Galluzzi and Green, 2019). However, how these processes and their shared machinery regulate antigen presentation remains incompletely understood.

Vacuolar protein sorting 34 (Vps34, also called Pik3c3) is a class III phosphoinositide 3-kinase (PI3K) that plays a role in endocytosis, intracellular vesicular trafficking, and autophagosome formation during autophagy (Backer, 2016). Vps34-deficient dendritic cells (DCs) display defective autophagic flux leading to the accumulation of aggregated cellular proteins and organelles (Parekh et al., 2017). Loss of Vps34 also significantly attenuated the $CD4^+$ T cell stimulatory capacity of DCs in response to a central nervous system-derived autoantigen that relies on the extracellular route of antigen processing (Yang et al., 2021). However, whether Vps34-mediated cellular processes regulate the intracellular route for MHC class II-mediated antigen processing that TECs rely on to generate a broad $CD4^+$ TCR repertoire is unknown.

In the present study, we analyzed mice with a TEC-specific deletion of *Vps34* to determine its effects on the antigen-presenting function of TECs. Our findings revealed a critical role for Vps34 in the capacity of TECs to facilitate the positive selection of $CD4^+$ but not $CD8^+$ T cells in a manner independent of the canonical, Atg5-dependent autophagy pathway.

## 2.2 Results

### TEC-specific Vps34 deficiency causes progressive thymic hypoplasia, blunted thymopoiesis, and T cell lymphopenia

To determine the function of Vps34 in TECs we employed mice expressing Cre recombinase from the endogenous *Foxn1* locus, with high Cre activity within TECs and their precursors (Gordon et al., 2007). To confirm Cre activity, we crossed Foxn1-Cre transgenic mice to Ai14 mice which contain a floxed-stop-tdTomato reporter cassette knocked into the *Rosa26* locus (Madisen et al., 2010) (Figure 2.1A). Flow cytometric analysis confirmed Cre reporter activity in TECs of $Cre^+$ $Ai14^+$ mice but not $Cre^-$ controls or in $CD45^+$ cells from either group (Figure 2.1B).

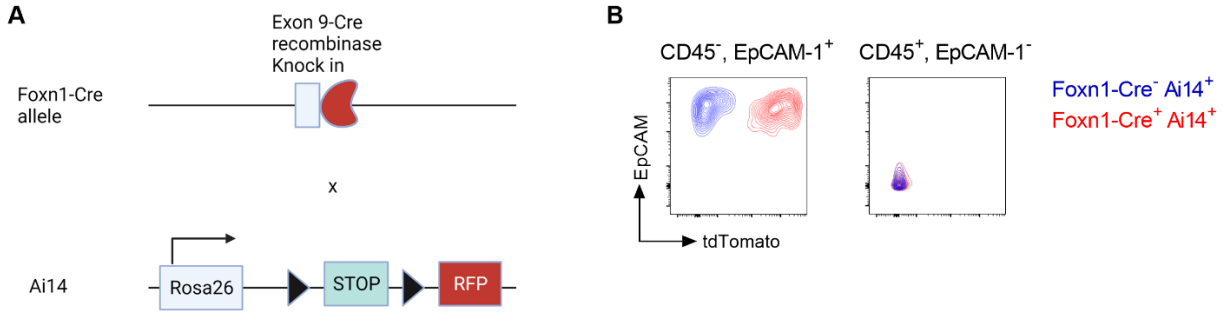


**Figure 2.1. TEC-specific Cre expression in Foxn1-Cre mice. (A)** Schematic of Cre reporter system where Cre activity excises the stop codon to allow constitutive RFP (TdTomato) expression. **(B)** Flow cytometric analysis of TECs ($CD45^-EpCAM^+$) and

$CD45^+$, $EpCAM^-$ thymocytes for tdTomato expression from Foxn1-$Cre^-$ $Ai14^+$ or Foxn1-$Cre^+$ $Ai14^+$ mice. The flow plot is representative of at least two independent experiments with two mice per group.

Next, we crossed Foxn1-Cre mice with mice carrying a floxed allele of the *Vps34* gene (Jaber et al., 2012) to generate mice with a TEC-specific loss of Vps34 (hereafter referred to as $Vps34^{TEC}$ mice). These animals were born at the expected Mendelian ratios and, apart from altered thymic development described below, did not show any obvious anatomical abnormalities, including the skin where Foxn1 is expressed by keratinocytes (Gordon *et al.*, 2007). Gross examination of the thoracic cavity revealed similar thymic size at one week of age but severely hypoplastic thymi by four weeks of age in $Vps34^{TEC}$ mice (Figure 2.2A). Coincident with thymic atrophy, $Vps34^{TEC}$ mice displayed a progressive loss in thymic cellularity (Figure 2.2B). Additionally, $Vps34^{TEC}$ mice had a progressive loss in $CD4^+CD8^+$ DP thymocytes, indicating a severe loss in thymic function by three weeks of age (Figure 2.2C). This loss of thymic function was associated with significant T cell lymphopenia in adult $Vps34^{TEC}$ mice, with a relatively stronger effect on the $CD4^+$ than the $CD8^+$ T cell compartment (Figure 2.3A). Consistent with the observed T cell lymphopenia, mature T cells in the periphery of $Vps34^{TEC}$ mice displayed a more activated phenotype as revealed by a decrease in the frequency of naïve $CD44^{lo}CD62L^{hi}$ T cells, likely resulting from increased homeostatic proliferation (Figure 2.3B). These data indicate that $Vps34^{TEC}$ mice exhibit rapid thymic involution, with profound loss of thymic function as the animals become juveniles, an age when thymic function normally peaks (Baran-Gale et al., 2020; Manley et al., 2011).

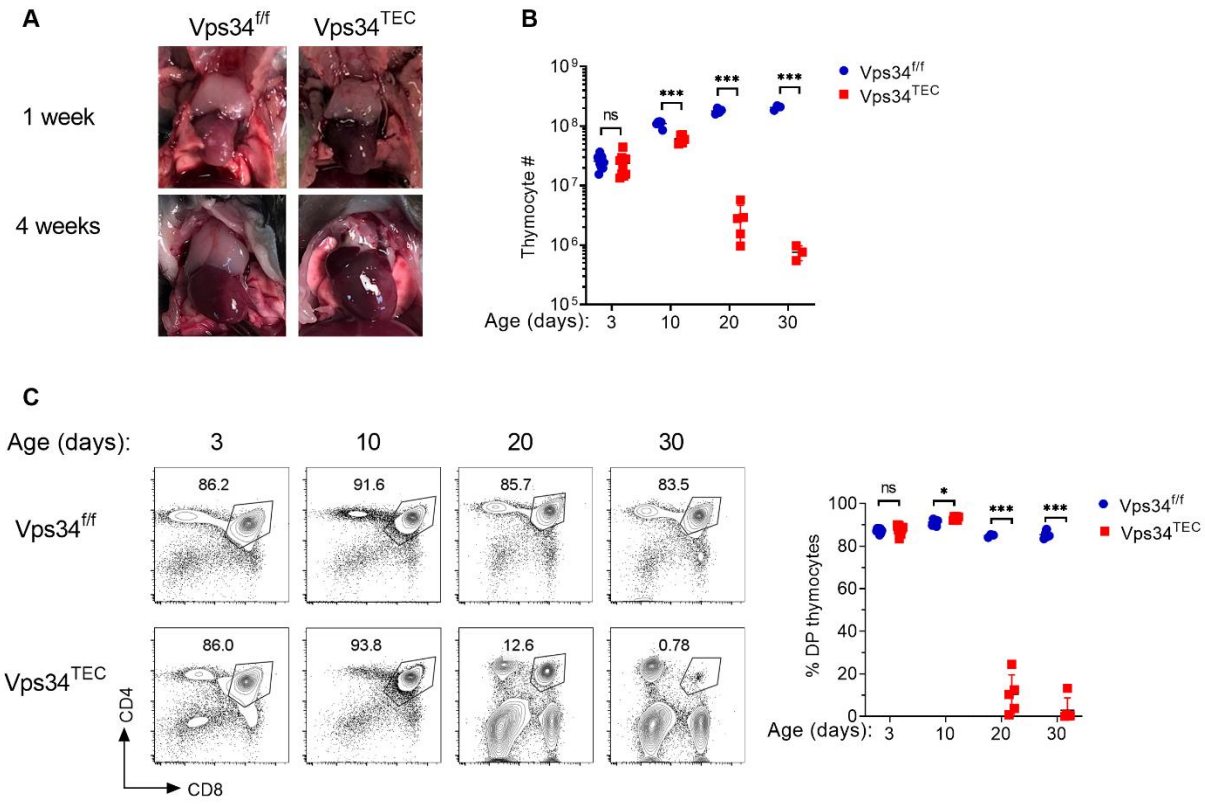


**Figure 2.2. Progressive loss of thymopoiesis in Vps34$^{TEC}$ mice. (A)** Thoracic cavity at 1 week (top) and 4 weeks (bottom) of age in Vps34$^{f/f}$ or Vps34$^{TEC}$ mice. **(B)** Total thymocyte cellularity at the indicated ages in Vps34$^{f/f}$ or Vps34$^{TEC}$ mice. **(C)** Flow cytometric analysis of CD4 and CD8 DP thymocytes at the indicated ages in Vps34$^{f/f}$ or Vps34$^{TEC}$ mice. The graph represents the frequency of DP thymocytes among all thymocytes. Data signify the mean ± SD. Data are representative of at least two independent experiments for each time point where each data point represents a biological replicate. *$p < 0.05$, ***$p < 0.001$; ns, not significant.

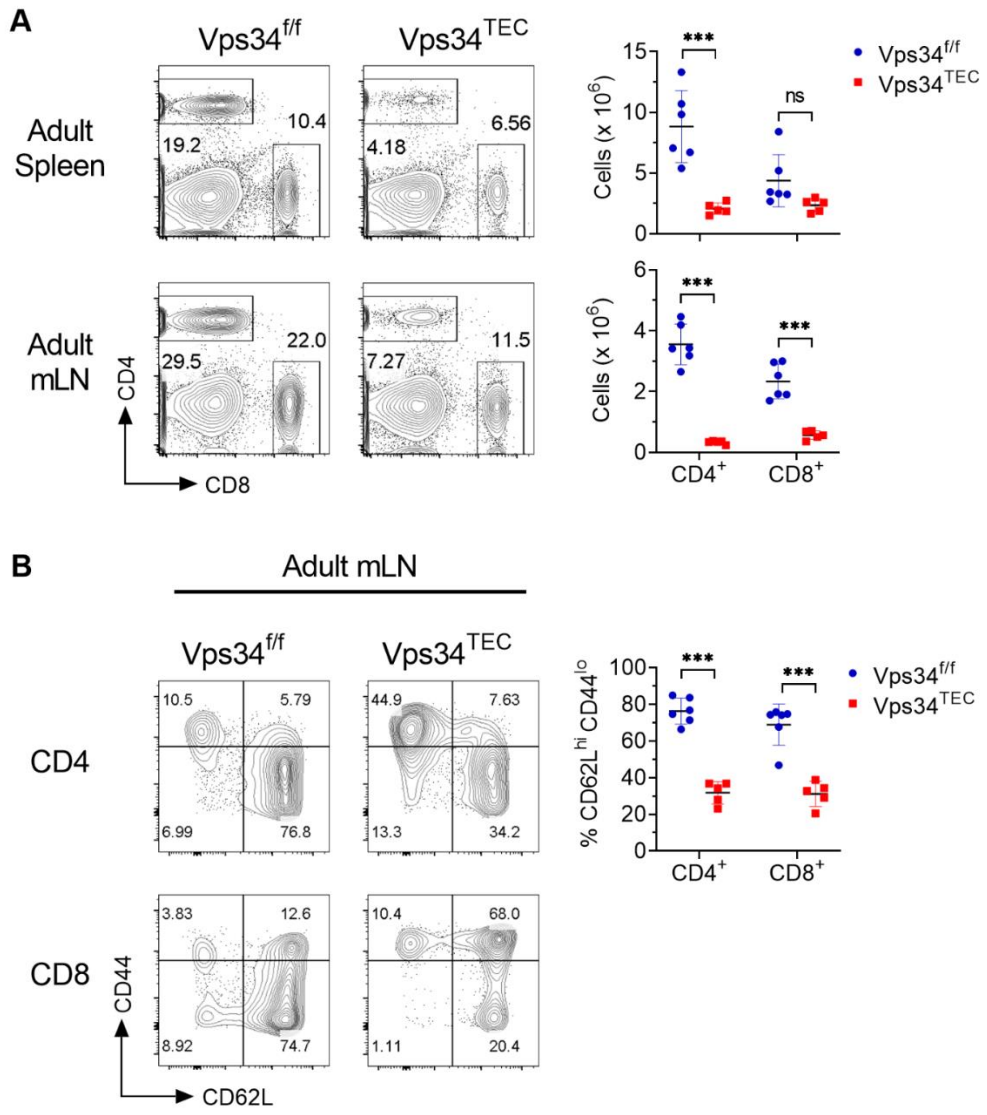


**Figure 2.3. T cell lymphopenia in adult Vps34$^{TEC}$ mice. (A)** CD4 and CD8 expression profiles of T cells isolated from spleen (top) and mesenteric lymph nodes (mLN) (bottom) in 7-week-old Vps34$^{f/f}$ or Vps34$^{TEC}$ mice. Graphs represent total CD4$^+$ T cells (CD4$^+$CD3$^+$) and CD8$^+$ T cells (CD8$^+$CD3$^+$) in the spleen (top) and mLN (bottom). **(B)** CD44 and CD62L expression profiles of T cells isolated from the mLN of 7-week-old Vps34$^{f/f}$ or Vps34$^{TEC}$ mice. Graphs represent the frequency of CD62L$^{hi}$CD44$^{lo}$ cells among total CD4$^+$ T cells (top panels) or total CD8$^+$ T cells (bottom panels). Data signify the mean ± SD. Data are representative of at least two independent experiments for each time point where each data point represents a biological replicate. ***$p < 0.001$; ns, not significant.

**TECs require Vps34 for basal autophagic flux**

Autophagy in mouse TECs occurs constitutively at levels detectable by reporter alleles, making it unique among mammalian tissue where most other cell types require inducing stimuli such as starvation to measure autophagic flux (Mizushima *et al.*, 2004). Many studies have identified a critical requirement for Vps34 expression in multiple mammalian tissues for the constitutive or induced generation of autophagy (Jaber *et al.*, 2012; Parekh *et al.*, 2017; Parekh et al., 2013; Zhou et al., 2010). Nevertheless, situations where autophagy can be induced in a Vps34-independent manner have also been described (Boukhalfa et al., 2020; McLeod et al., 2011). To measure the contribution of Vps34 to autophagy in TECs, we utilized an autophagy reporter strain that expresses transgenic LC3 (microtubule-associated protein 1A/1B-light chain 3) that is dually labelled with EGFP (enhanced green fluorescent protein) and RFP (red fluorescent protein) (Li et al., 2014). During autophagy, cytosolic LC3 is recruited to the autophagosome where it is labelled with both EGFP and RFP. As an autophagosome matures, it fuses with the lysosome and acidifies, which degrades the pH-sensitive EGFP (Figure 2.4A). Flow cytometric analysis of TECs isolated from reporter$^{+}$ wild-type controls showed an RFP$^{+}$EGFP$^{+}$ double-positive population indicating cytosolic and autophagosomal LC3 and an RFP$^{+}$EGFP$^{lo}$ population representing autolysosomes (Figure 2.4B). This confirms previous reports that autophagy is active in TECs under physiological conditions (Kasai et al., 2009; Mizushima *et al.*, 2004; Nedjic *et al.*, 2008; Schuster *et al.*, 2015; Uddin et al., 2012). In TECs isolated from reporter$^{+}$ Vps34$^{TEC}$ mice, we found a significant decrease in the frequency of EGFP$^{lo}$ cells among the RFP$^{+}$ population, indicating a block in autophagic flux and confirming an essential role for Vps34 in TEC autophagy.

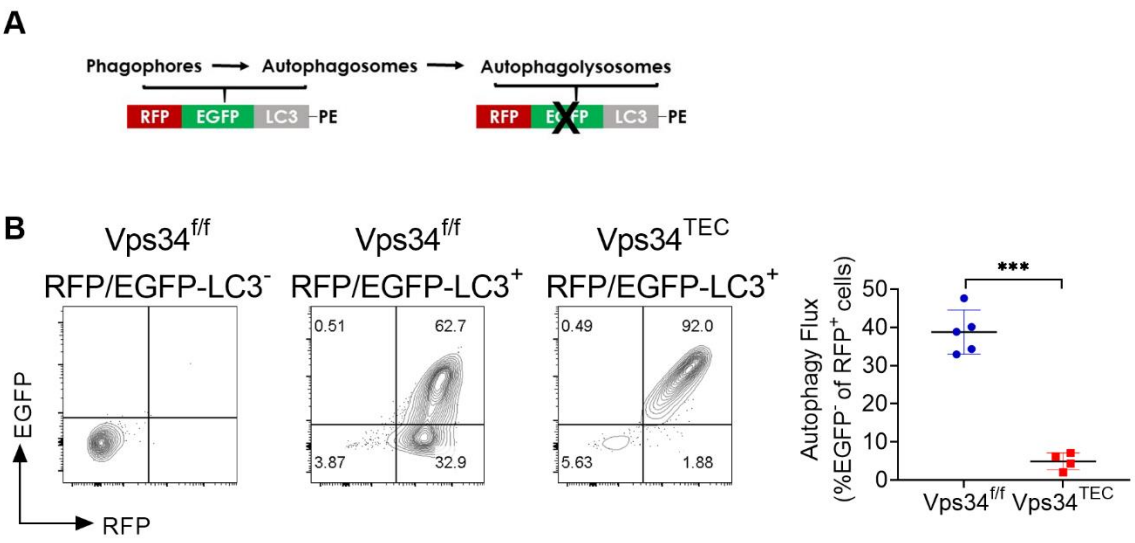


**Figure 2.4. TEC autophagy requires Vps34. (A)** Schematic of LC3-RFP-EGFP reporter. **(B)** Flow cytometric analysis of TECs ($CD45^{-}EpCAM^{+}$) for LC3-RFP/EGFP reporter expression in non-transgenic control (left), $Vps34^{f/f}$ (middle) and $Vps34^{TEC}$ (right) mice at 7-10 days of age. The graph represents percent $EGFP^{lo}$ TECs among $RFP^{+}$ TECs. Data signify the mean ± SD. Data are representative of at least two independent experiments for each time point where each data point represents a biological replicate. ***$p < 0.001$.

### Vps34 deficiency alters TEC cellularity and thymus morphology

To assess the effects of Vps34 loss on TEC cellularity and morphology, we focused our analysis to the neonatal age before extensive atrophy occurs in $Vps34^{TEC}$ mice. Histological examination of thymic morphology revealed profound disruption of thymic architecture in $Vps34^{TEC}$ mice. H&E staining and immunofluorescence analysis with the mTEC-specific markers Keratin-5 and UEA-1 showed disruption of the medulla and cortex organization in $Vps34^{TEC}$ mice resulting in smaller and more diffuse medullary islets (Figure 2.5A). To quantify these effects of Vps34 deficiency we analyzed TECs by flow cytometry, which revealed a significant decrease in the frequency and number of $EpCAM^{+}CD45^{-}$ TECs at post-natal days three and 10 (Figure 2.5B). Among TEC subsets, there was a relative loss in the frequency of mTECs ($Ly\text{-}51^{-}UEA\text{-}1^{+}$) compared to cTECs

(Ly-51$^{+}$UEA-1$^{-}$) in Vps34$^{TEC}$ mice vs. control mice (Figure 2.5C), which agreed with the histological analysis. Interestingly, mTECs isolated from mutant mice also displayed a more immature (mTEC$^{lo}$) phenotype as gleaned from lower surface expression of the antigen presentation-associated molecules MHC class II and CD80 (Figure 2.5D). These data indicate that TECs require Vps34 for normal cellularity in neonatal mice and that loss of Vps34 results in a progressive loss of TEC cellularity, with more profound effects on mTECs than cTECs.

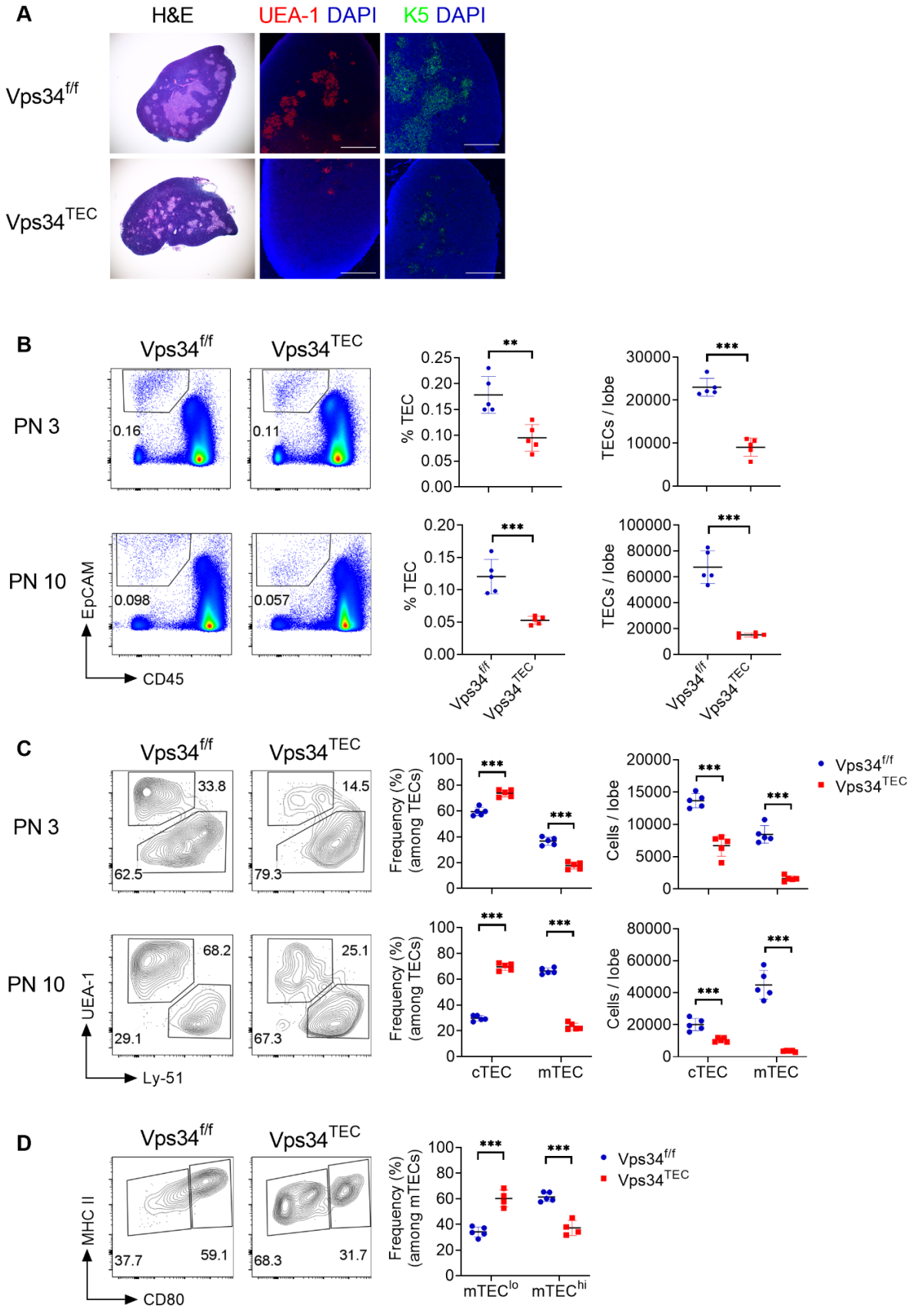
A
H&E
UEA-1 DAPI
K5 DAPI
Vps34f/f
Vps34TEC
B
Vps34f/f
Vps34TEC
PN 3
PN 10
0.16
0.11
0.098
0.057
EpCAM
CD45
% TEC
TECs / lobe
C
33.8
62.5
14.5
79.3
68.2
29.1
25.1
67.3
UEA-1
Ly-51
Frequency (%) (among TECs)
Cells / lobe
cTEC
mTEC
D
37.7
59.1
68.3
31.7
MHC II
CD80
Frequency (%) (among mTECs)
mTEClo
mTEChi

**Figure 2.5. Reduced TEC cellularity and altered morphology in Vps34$^{TEC}$ mice. (A)** Thymus tissue sections from 7- to 10-day-old Vps34$^{f/f}$ or Vps34$^{TEC}$ mice stained with H&E (2.6 x original magnification), with anti-keratin 5 (K5) (green) or UEA-1 lectin (red), and DAPI (blue) (scale bar = 100 micrometers). **(B and C)** Flow cytometric analysis of **(B)** total TECs and **(C)** TEC subsets, including mTECs (UEA-1$^{+}$Ly-51$^{-}$) and cTECs (UEA-1$^{-}$ Ly-51$^{+}$) at postnatal (pn) day 3 (top) and day 10 (bottom). Graphs represent frequency (left) and total number (right) of TECs or TEC subsets. **(D)** mTEC$^{hi}$ (MHC II$^{hi}$CD80$^{hi}$) and mTEC$^{lo}$ (MHC II$^{lo}$CD80$^{lo}$) frequency among mTECs. Data signify the mean ± SD. Data are representative of at least two independent experiments for each time point where each data point represents a biological replicate. **p < 0.01, ***p < 0.001.

We next considered that alterations in cellular proliferation may contribute to decreases in TEC cellularity in Vps34$^{TEC}$ mice. We performed flow cytometric analyses for intracellular Ki67 expression in TEC populations isolated from Vps34$^{TEC}$ neonatal mice. Compared with littermate controls, we found significant decreases in cell cycling in Vps34-deficient mTECs but not cTECs (Figure 2.6A). This suggests that the defects seen in mTEC cellularity in Vps34$^{TEC}$ mice can be partially explained by a loss of proliferating mTECs. We next aimed to measure cell death of TECs by staining with the apoptotic cell marker Annexin V. However, we found that TECs from control animals stained positive with Annexin V at an abnormally high frequency (Figure 2.6B). Importantly, CD45$^{+}$ thymocytes in the same samples bound to Annexin V at physiologically plausible frequencies confirming that the staining protocol worked well. Previous studies have suggested that enzymatic digestion of thymi artificially induces Annexin V binding of TECs and precludes the ability to assay cell death by conventional methods such as Annexin V staining (Gray et al., 2007). Taken together, the deficiency in TEC cellularity observed in Vps34$^{TEC}$ mice is due in part to a loss of proliferating cells but increased cell death may also be a significant contributor.

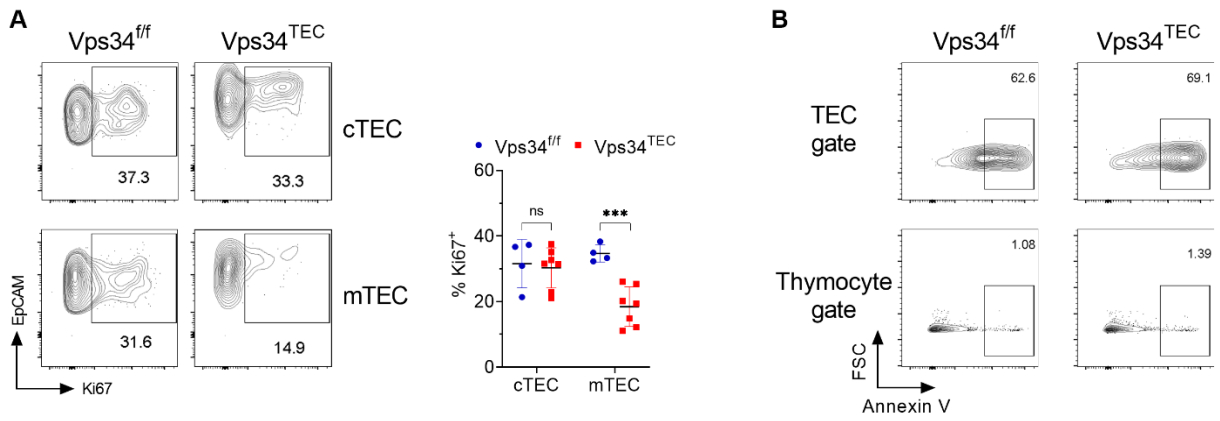


**Figure 2.6. Neonatal TEC populations differentially require Vps34 for cell cycling.** **(A)** Ki67 expression among cTECs (MHC II$^{hi}$UEA-1$^{-}$ TECs) and mTECs (MHC II$^{hi}$UEA-1$^{+}$ TECs). The graph represents frequency of Ki67$^{+}$ cells among TEC subsets. **(B)** Annexin V binding among TECs (top) and thymocytes (bottom) isolated from indicated genotypes. Data signify the mean ± SD. Data are representative of at least two independent experiments. Each data point represents a biological replicate in all graphs. ***p < 0.001; ns, not significant.

### Deleting Vps34 in adult mTECs

In Vps34$^{TEC}$ mice, mTECs are reduced in frequency from the earliest developmental time point of our analysis. This indicates that Vps34 is required by TECs to establish the mTEC compartment. However, it is unclear if Vps34 is intrinsically required for the maintenance of mTECs. To this end, we utilized a tamoxifen inducible Cre driver under the control of the endogenous Cytokeratin 5 promotor, K5-CreER$^{T2}$ (Van Keymeulen et al., 2011) to target adult mTECs. To test the fidelity of Cre activity in K5-CreER$^{T2}$ mice, we crossed this transgenic strain to the Cre reporter strain Ai14 which contains a floxed-stop-tdTomato reporter cassette knocked into the *Rosa26* locus (Madisen *et al.*, 2010). In cells expressing Cre, tdTomato is constitutively expressed. Flow cytometric analysis confirmed Cre reporter activity in a large fraction of mTECs of Cre$^{+}$ Ai14$^{+}$ mice but not Ai14$^{-}$ mice (Figure 2.7A). We next crossed K5-CreER$^{T2}$ mice with Vps34$^{f/f}$ mice to inducibly target

Vps34 in mTECs. Following tamoxifen treatment, Aire-CreER$^{T2}$ Vps34$^{f/f}$ mice survived for 7-8 days, while Vps34$^{f/f}$ controls remained healthy (Figure 2.7B). Since mTEC ablation is not lethal in adult mice (Khan et al., 2014), and K5-Cre activity is likely active in other tissues containing basal epithelial cells (including epidermis, salivary gland, and digestive tract), it is likely that Vps34 is necessary for life in adult mice due to its role in tissues other than mTECs.

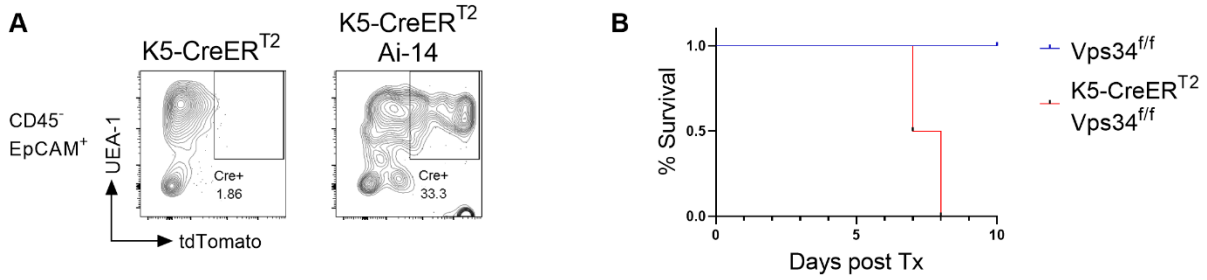


**Figure 2.7. Genetic system for inducible deletion of Vps34 in Keratin 5 expressing cells. (A)** Flow cytometric analysis of TECs (CD45$^-$EpCAM$^+$) for tdTomato expression and UEA-1 reactivity from K5-CreER$^{T2}$ Ai14$^+$ or K5-CreER$^{T2}$ mice. **(B)** K5-CreER$^{T2}$ Vps34$^{f/f}$ or Vps34$^{f/f}$ mice were administered 3 doses of tamoxifen (Tx) on consecutive days and were then monitored for survival (n= 2/genotype). Data represent two independent experiments.

In Vps34$^{TEC}$ mice, there was a reduction of mature mTEC$^{hi}$ cells among mTECs. However, it is unclear whether this defect is caused by a reduced capacity of mTEC$^{lo}$ cells to mature into mTEC$^{hi}$ cells or a reduced survival of mTEC$^{hi}$ cells. To address this problem, we used a genetic model that allows for tamoxifen inducible Cre activity in Aire expressing mTEC$^{hi}$ cells, Aire-CreER$^{T2}$ mice. We again utilized the Ai14 Cre reporter strain to assess induction of Cre activity. Flow cytometric analysis revealed Cre reporter activity in a large fraction of mTECs of Cre$^+$ Ai14$^+$ mice but not Ai14$^-$ mice (Figure 2.8A). Importantly, tdTomato expression was restricted to UEA-1$^+$ TECs indicating that Cre is not active in cTECs. To assess the role of Vps34 in mature mTECs we generated Aire-

CreER$^{T2}$ Vps34$^{f/f}$ mice. Analysis of Aire-CreER$^{T2}$ Vps34$^{f/f}$ mice treated continuously for 14 days with tamoxifen showed no significant changes in TEC frequency or cellularity (Figure 2.8B). Further, there were no changes in TEC subsets (Figure 2.8C, D). This supports a scenario where immature mTECs require Vps34 to mature into mTEC$^{hi}$ cells but not for the maintenance of mTEC$^{hi}$ cells.

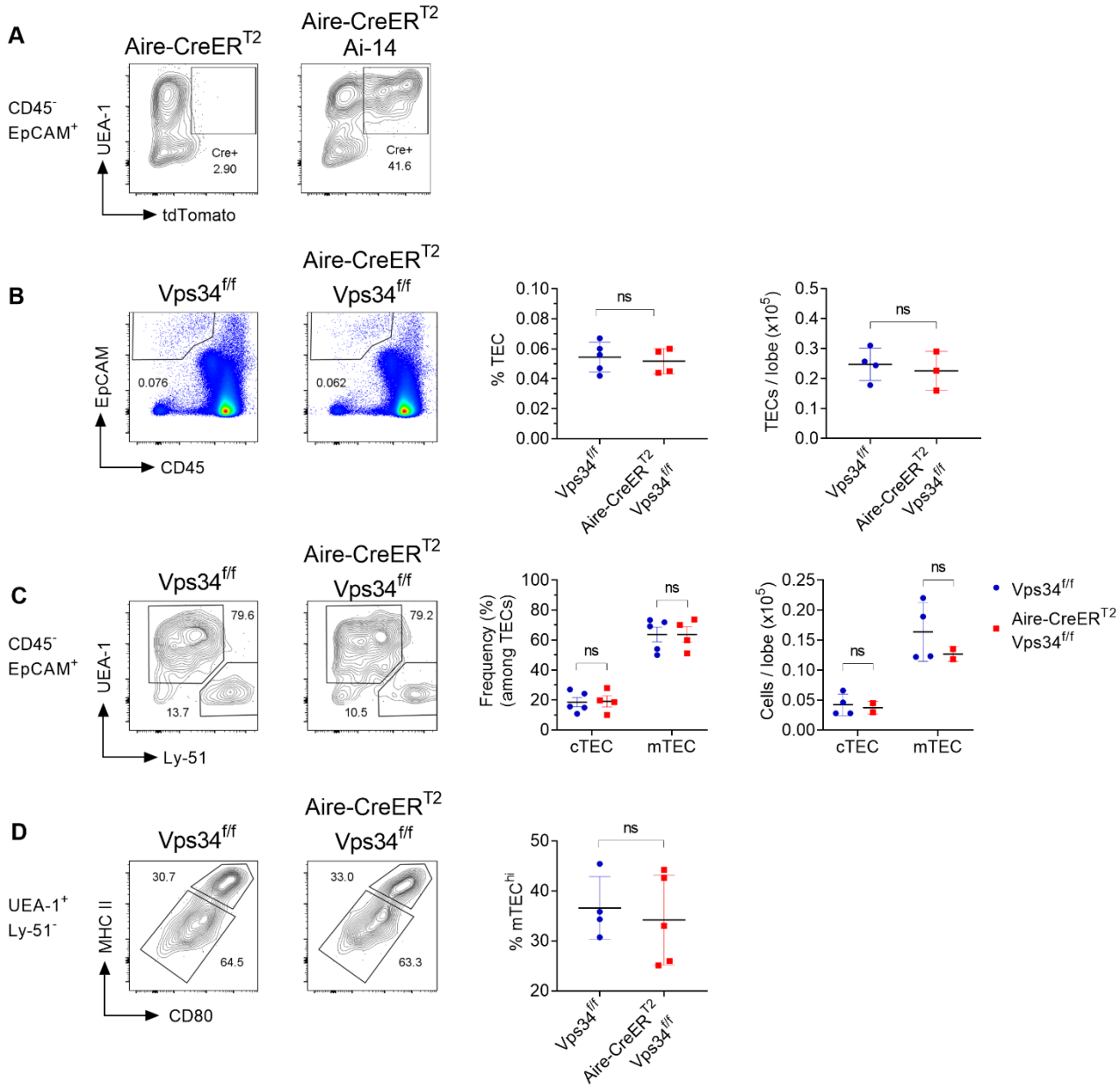


**Figure 2.8. Genetic system for inducible deletion of Vps34 in mature mTECs. (A)** Flow cytometric analysis of TECs (CD45$^-$EpCAM$^+$) for tdTomato expression and UEA-1 reactivity from Aire-CreER$^{T2}$ Ai14$^+$ or Aire-CreER$^{T2}$ mice. **(B-D)** Aire-CreER$^{T2}$ Vps34$^{f/f}$ or Vps34$^{f/f}$ mice were administered tamoxifen every other day for 14 days and were then analyzed. Flow cytometric analysis of **(B)** total TECs and **(C)** TEC subsets, including mTECs (UEA-1$^+$Ly-51$^-$) and cTECs (UEA-1$^-$Ly-51$^+$). Graphs represent frequency (left) and total number (right) of TECs or TEC subsets. **(D)** mTEC$^{hi}$ (MHC II$^{hi}$CD80$^{hi}$) frequency among mTECs. Data signify the mean ± SD. Data are representative of at least two independent experiments for each time point where each data point represents a biological replicate. ns, not significant.

**Post-natal deletion of Vps34 decreases TEC cellularity and homeostasis**

Since the hypoplastic thymi observed in Vps34$^{TEC}$ mice could be caused by a loss of TEC progenitors during development, it is unclear whether TECs require Vps34 expression to maintain their homeostasis in adulthood. To address this question, we utilized an inducible deletion system where ablation of Vps34 can be achieved specifically in the thymic stroma after the microenvironment has been fully established. Thymic lobes from newborn Rosa26-CreER$^{T2}$;Vps34$^{f/f}$ or Vps34$^{f/f}$ mice were grafted under the kidney capsule of adult C57BL/6 mice. Host hematopoietic cells were allowed to reconstitute for 3 weeks, and Cre-ER$^{T2}$-mediated deletion of Vps34 was induced by tamoxifen administration whereas control Rosa26-CreER$^{T2}$;Vps34$^{f/f}$ mice were treated with vehicle and a second control group of Vps34$^{f/f}$ mice were also treated with tamoxifen. Host kidney capsules were collected 3 weeks after administration of the last tamoxifen or vehicle dose and the grafted thymic lobes were analyzed (Figure 2.9A). The size and cellularity of grafts isolated from tamoxifen-treated Rosa26-CreER$^{T2}$;Vps34$^{f/f}$ mice were significantly reduced as compared with both groups of control mice (Figure 2.9B). Additionally, flow cytometric analysis revealed that TEC numbers were also significantly reduced in the Vps34-deficient grafts compared with the controls (Figure 2.9C). These results indicate a post-natal requirement of Vps34 in TECs to maintain thymopoiesis and TEC homeostasis.

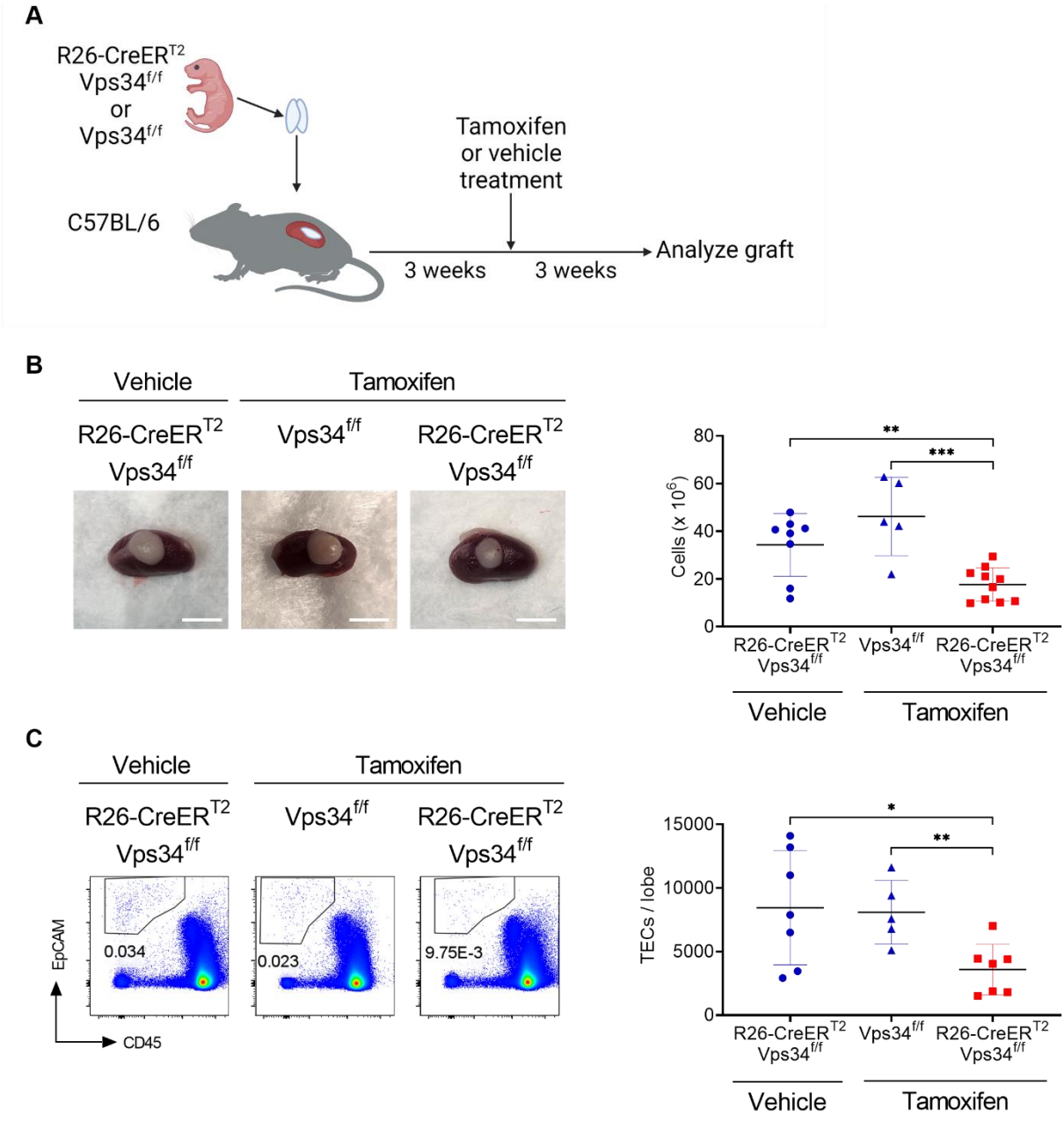


**Figure 2.9. Post-natal deletion of Vps34 in thymic stromal cells decreases cellularity and TEC homeostasis in a transplant model. (A)** Schematic of the experimental design. Thymic lobes isolated from newborn Rosa26-CreER$^{T2}$;Vps34$^{f/f}$ or Vps34$^{f/f}$ mice were transplanted under the kidney capsule of 6- to 8-week-old C57BL/6 recipient mice. Recipients were treated with tamoxifen or vehicle by oral gavage 3 weeks after grafting and were analyzed 3 weeks after the last tamoxifen treatment. **(B)** Examples of kidneys transplanted with a thymus lobe from vehicle- or tamoxifen-treated recipient mice. The graph represents total cellularity from transplanted thymi. **(C)** Flow cytometric analysis of TECs isolated from vehicle- or tamoxifen-treated mice. The graph represents total TEC cellularity (CD45$^-$EpCAM$^+$ cells) from transplanted thymi. Data signify the mean

± SD. Data are representative of at least two independent experiments where each data point represents a biological replicate. *p < 0.05, **p < 0.01, ***p < 0.001; ns, not significant.

**Vps34 promotes thymopoiesis and TEC homeostasis in a mechanism independent of canonical autophagy**

In addition to autophagy, Vps34 plays a role in endocytosis and vesicle trafficking (Backer, 2016). To investigate the role autophagy plays in maintaining thymopoiesis and TEC homeostasis, we generated mice with a TEC-specific deficiency of Atg5 ($Atg5^{TEC}$ mice), an essential component of the autophagy pathway (Levine and Kroemer, 2019), by crossing the Foxn1-Cre strain to mice with a floxed *Atg5* allele (Hara et al., 2006). We restricted our initial analysis to neonates for a better comparison with $Vps34^{TEC}$ mice.

Consistent with a recent report in adult mice (Jain et al., 2018), Atg5-deficiency in TECs did not cause a detectable change in TEC frequency or cellularity (Figure 2.10A). Further, there was no change in subset ratios or numbers (Figure 2.10B). These findings strongly suggest that Vps34 does not maintain TEC homeostasis and thymopoiesis due solely to its role in canonical autophagy.

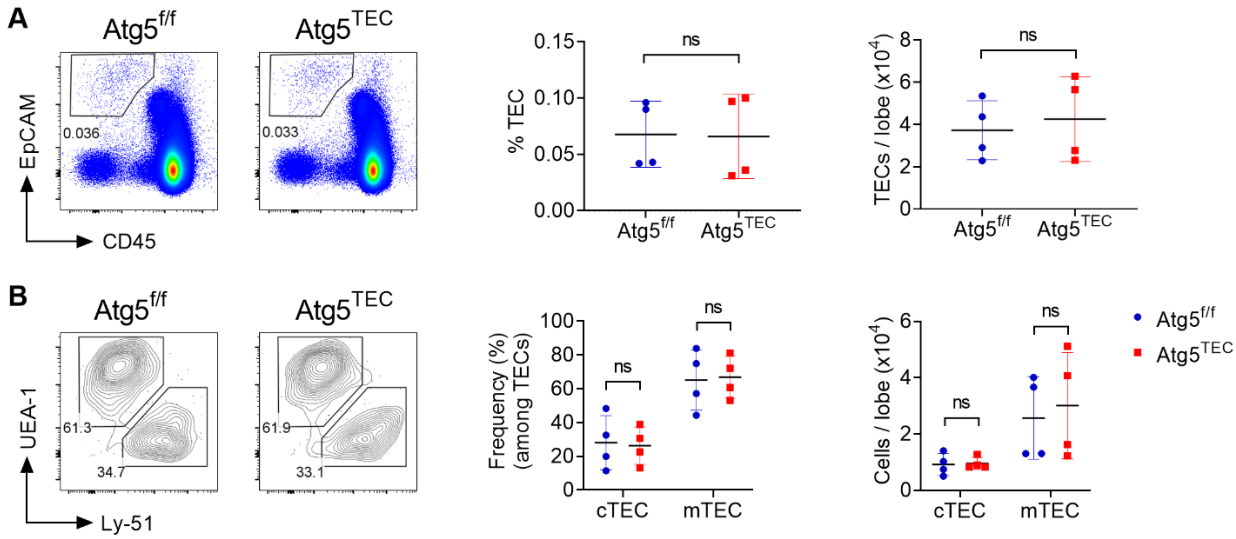


**Figure 2.10. TEC phenotype in mice with TEC-specific loss of Atg5.** Flow cytometric analysis of **(A)** total TECs (CD45$^-$EpCAM$^+$) and **(B)** TEC subsets, including mTECs (UEA-1$^+$Ly-51$^-$) and cTECs (UEA-1$^-$Ly-51$^+$) at postnatal day 10. Graphs represent frequency (left) and total number (right) of TECs or TEC subsets. Data signify the mean ± SD. Data are representative of two independent experiments where each data point represents a biological replicate. ns, not significant.

### Altered T cell development in neonatal Vps34$^{TEC}$ mice

Given the essential role Vps34 plays in endocytosis, vesicle trafficking, and the initiation of autophagy (Bilanges *et al.*, 2019), cellular processes that can influence antigen presentation (Roche and Furuta, 2015), we next investigated intrathymic development of T cells in neonatal Vps34$^{TEC}$ mice. We observed similar frequencies and numbers of DP thymocytes in mutant mice compared to controls, but a relative decrease in CD4 SP and a relative increase in CD8 SP cells (Figure 2.11). Similar shifts in the distribution of T cell subsets were observed in the spleen of mutant mice (Figure 2.11).

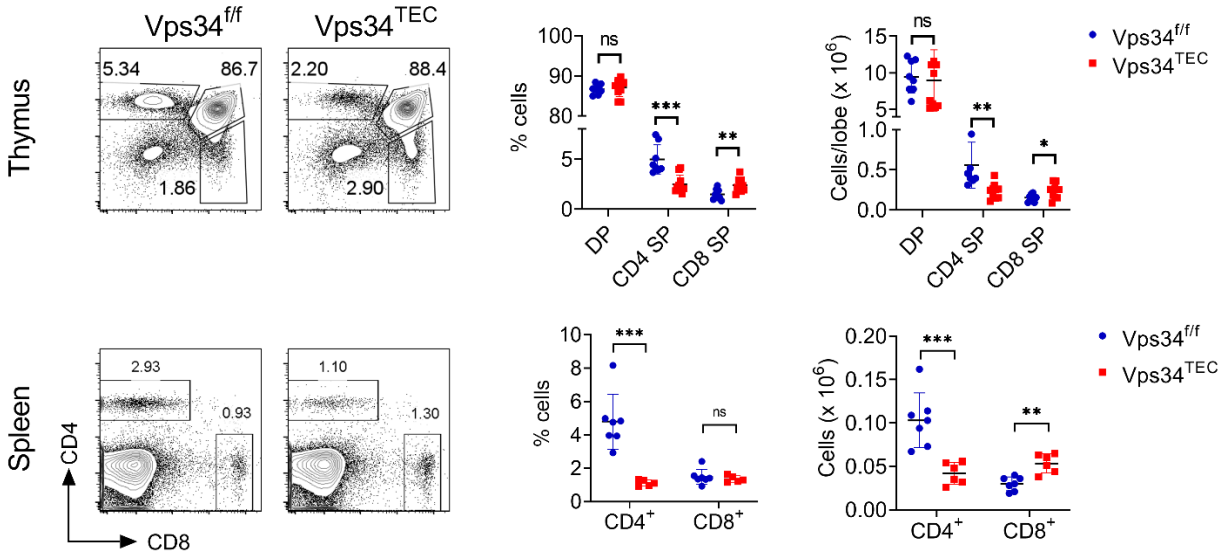


**Figure 2.11. Reduced CD4 T cells in Vps34$^{TEC}$ neonates.** Thymocytes (top) and splenocytes (bottom) from three-day-old Vps34$^{f/f}$ or Vps34$^{TEC}$ mice were analyzed by flow cytometry for CD4 and CD8 expression. Graphs represent frequency and total numbers of indicated thymocyte subsets (top) and splenic T cell subsets. Data signify the mean ± SD. Data are representative of at least two independent experiments for each time point where each data point represents a biological replicate. *p < 0.05, **p < 0.01, ***p < 0.001; ns, not significant.

To further investigate thymic selection, we analyzed CD4 and CD8 expression on developing thymocytes at discrete developmental stages. Developing thymocytes undergo sequential stages of TCRβ and CD69 cell surface expression that provide phenotypic markers of T cell positive selection (Barthlott et al., 1997). Under physiological conditions, positive selection sets off a transient upregulation of CD69 among TCRβ$^{int}$ thymocytes (stage II). In turn, these cells sequentially adopt a TCRβ$^{hi}$CD69$^{+}$ (stage III) and eventually a TCRβ$^{hi}$CD69$^{lo}$ (stage IV) cell surface phenotype as they move from the DP towards the CD4 SP or CD8 SP lineages. The relative frequencies of these distinct thymocyte populations were undisturbed in neonatal Vps34$^{TEC}$ mice (Figure 2.12A). However, at stages III and IV, there was an increase in the frequency of thymocytes that retained CD4 and CD8 DP expression. Further, the thymocytes at stages III and IV were

more skewed towards the CD8 SP lineage in Vps34$^{TEC}$ mice (Figure 2.12A). Given the alterations in SP thymocytes, we also analyzed maturation in SP subsets. Following positive selection, SP thymocytes express high surface levels of CD24 (heat-stable antigen), which they downregulate as they mature (Nikolic-Zugic and Bevan, 1990; Ramsdell et al., 1991). Interestingly, we observed no alterations in the frequency of mature TCRβ$^{hi}$CD24$^{lo}$ cells among CD4 SP thymocytes but an increase in the frequency of these cells among CD8 SP thymocytes (Figure 2.12B). This finding implies that the alterations seen in CD4 SP selection in Vps34$^{TEC}$ mice are unlikely due to defects in post-selection maturation.

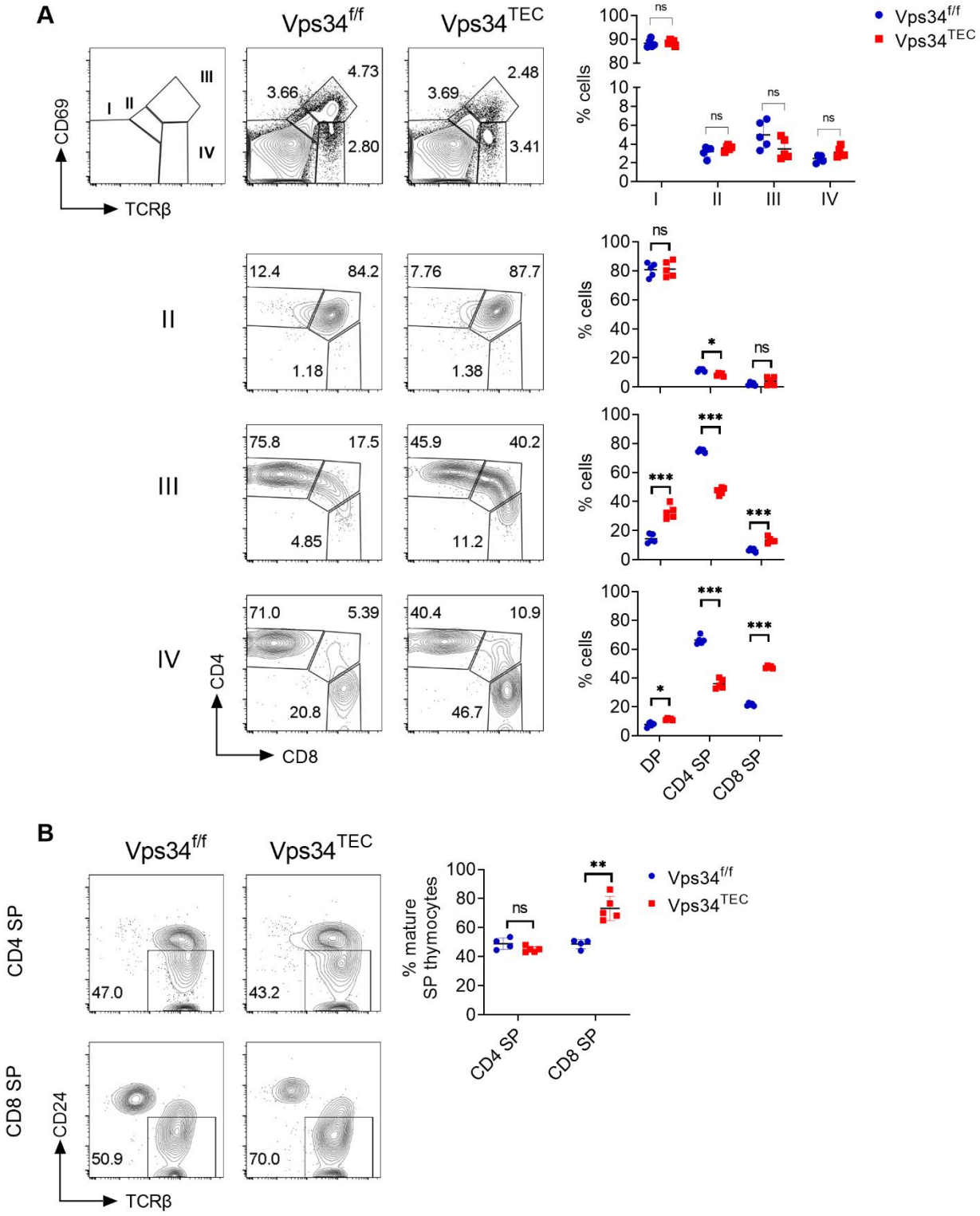


**Figure 2.12. Defective CD4⁺ T cell development in neonatal Vps34$^{TEC}$ mice.** Thymocytes from three-day-old Vps34$^{f/f}$ or Vps34$^{TEC}$ mice were analyzed by flow cytometry. **(A)** CD69 and TCRβ expression (top panel) on thymocytes was used to gate

on the indicated developmental thymocyte stages, and the percentage of cells within each stage is depicted in the graph at the top. Cells within stages II-IV were then analyzed for CD4 and CD8 surface expression. Graphs represent the frequency of DP, CD4 SP, and CD8 SP thymocytes within each specified developmental stage. **(B)** CD24 and TCRβ expression. The graph represents the frequency of mature thymocytes ($TCR\beta^{+}CD24^{lo}$) among the CD4 SP or CD8 SP subsets. Data signify the mean ± SD. Data are representative of at least two independent experiments for each time point where each data point represents a biological replicate. *p < 0.05, **p < 0.01, ***p < 0.001; ns, not significant.

An important subset of CD4 SP thymocytes is thymic regulatory T cells (tTregs), which are essential for maintaining immune tolerance and can be identified by the lineage defining transcription factor Foxp3 (Savage et al., 2020). mTECs are critical for the development of tTregs (Cowan et al., 2013). Given the observed defects in the mTEC compartment of $Vps34^{TEC}$ mice (Figure 2.5A,C), we next analyzed tTreg development in 3-day-old mice, using a Foxp3-RFP knock-in reporter line crossed onto $Vps34^{TEC}$ mice. We observed no alterations in the frequency of $Foxp3^{+}CD25^{+}$ Tregs among CD4 SP thymocytes (Figure 2.13A) or $CD4^{+}$ splenocytes (Figure 2.13B). These observations indicate that Vps34 in TECs is dispensable for the thymic development of Tregs.

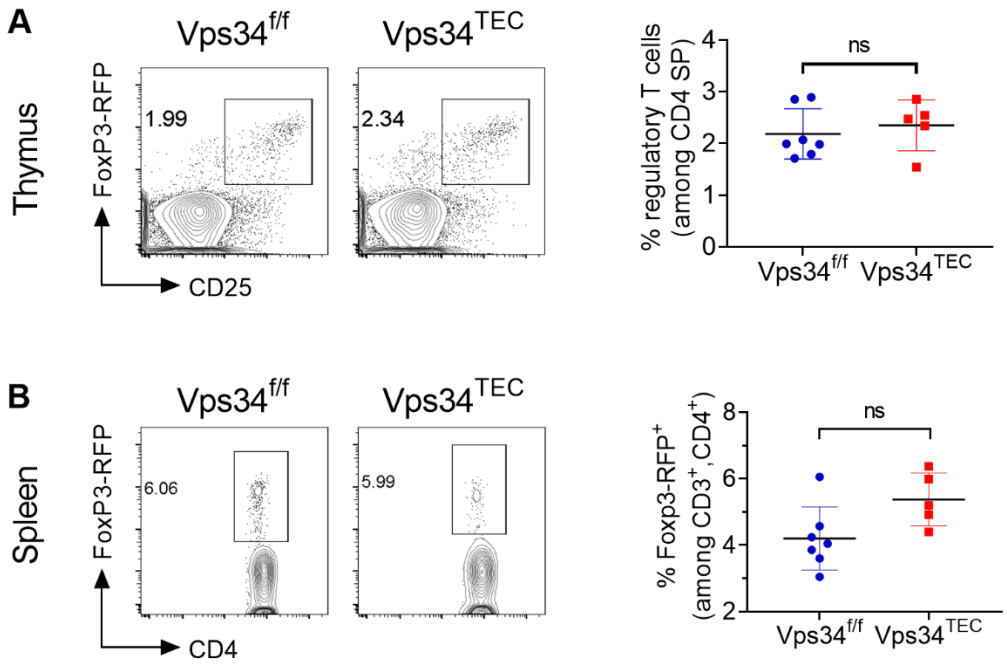


**Figure 2.13. Thymic regulatory T cell development in Vps34$^{TEC}$ mice.** Lymphocytes from three-day-old Vps34$^{f/f}$ or Vps34$^{TEC}$ mice were analyzed by flow cytometry. **(A)** Thymocytes were analyzed for Foxp3-RFP and CD25 expression of cells within the CD4 SP CD3$^+$ gate. The graph represents the frequency of thymic regulatory T cells (Foxp3-RFP$^+$CD25$^+$) among CD4 SP CD3$^+$ thymocytes. **(B)** Splenocytes were analyzed for Foxp3-RFP expression among CD4$^+$ T cells (CD3$^+$CD4$^+$). The graphs represent frequency and total numbers of Foxp3$^+$ CD4$^+$ T cells among splenocytes. Data signify the mean ± SD. Data are representative of at least two independent experiments where each data point represents a biological replicate. ns, not significant.

### Vps34 regulates positive selection of MHC class II-restricted transgenic TCRs

To further investigate the contribution of TEC-specific Vps34 to T cell positive selection, we tested the development and selection of T cells expressing antigen-specific, MHC class I- or class II-restricted TCRs in transgenic animals. Although such studies are often performed with TCR transgenic bone marrow chimeras, we opted against this approach due to the severe thymic hypoplasia in Vps34$^{TEC}$ mice. Instead, we bred individual TCR transgenic lines with the Vps34$^{TEC}$ mice and compared these animals to their Cre$^-$ littermate controls at 7 to 10 days of age. We did not observe any defects in the

frequencies or numbers of CD8 SP thymocytes for the MHC class I-restricted OTI or P14 lines (see Table 2.1 for the specificities of the transgenic TCRs). We also did not find any alterations in the expression of the clonotypic TCRs of these lines among CD8 SP cells (Figure 2.14A-C). In contrast, a near complete block in development from the DP to CD4 SP thymocyte stage occurred in each of the MHC class II-restricted TCR transgenic lines, OTII, LLO56, LLO118, and female Marilyn mice. Additionally, among the CD4 SP thymocytes, there was a decrease in the frequency of T cells expressing the clonotypic TCRs of individual transgenic lines (Figure 2.14D-H). These data indicate that Vps34 is required by TECs to positively select MHC class II-restricted but not MHC class I-restricted transgenic TCRs.

**Table 2.1: Specificity of TCR transgenic mice employed in this study.**

| TCR transgenic mouse | Restriction element | Cognate antigen |
|---|---|---|
| OTI | $K^b$ | Chicken ovalbumin 257-264 |
| P14 | $D^b$ | Lymphocytic choriomeningitis virus $gp_{33-41}$ |
| OTII | I-$A^b$ | Chicken ovalbumin 323-339 |
| LLO56 | I-$A^b$ | *Listeria monocytogenes* $LLO_{190-205}$ |
| LLO118 | I-$A^b$ | *Listeria monocytogenes* $LLO_{190-205}$ |
| Marilyn | I-$A^b$ | Male specific H-Y antigen |

Appropriate TCR signal strength is crucial for thymic selection (Gascoigne et al., 2016). Surface CD5 expression on developing thymocytes positively correlates with TCR signal strength and can be employed as a surrogate marker of TCR signal strength (Azzam et al., 1998). Interestingly, surface CD5 expression was decreased on DP thymocytes in transgenic lines expressing MHC class II-restricted but not class I-restricted

TCRs (Figure 2.14I). This finding indicates that altered TCR signaling coincides with defective positive selection. It is possible that changes in self-peptide/MHC class II displayed on Vps34-deficient TECs leads to alterations in TCR signaling on developing MHC class II-restricted transgenic thymocytes and thus causes these defects in positive selection.

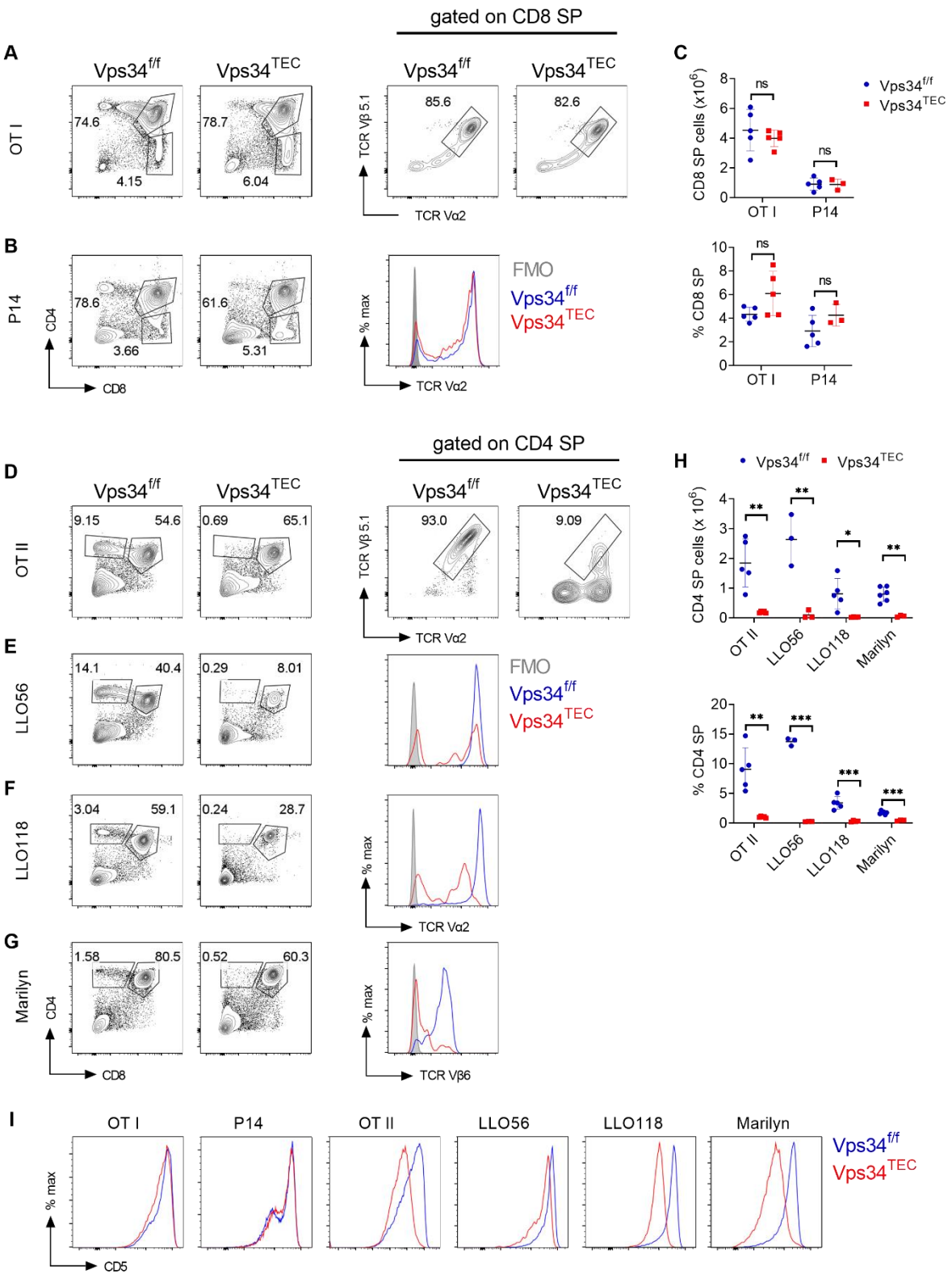


**Figure 2.14. Vps34 in TECs is critical for positive selection of MHC class II-restricted but not MHC class I-restricted transgenic TCRs.** Six separate TCR

transgenes were introgressed into the Vps34$^{TEC}$ strain and analyzed for positive selection compared with TCR transgenic Vps34$^{f/f}$ controls (see Table 2.1 for the specificities of these TCRs). **(A-G)** Flow cytometric analysis of thymocytes for CD4 and CD8 expression from the following TCR transgenic lines: **(A)** OTI, **(B)** P14, **(D)** OTII, **(E)** LLO56, **(F)** LLO118, and **(G)** Marilyn (females only). Representative flow plots or histograms show clonotypic TCR expression profiles of Vps34$^{f/f}$ (blue line), Vps34$^{TEC}$ (red line) and control staining (shaded grey) of the indicated cell populations. **(C)** Total cell number (top) and frequency (bottom) of CD8 SP thymocytes in the indicated MHC class I-restricted TCR transgenic lines. **(H)** Total cell number (top) and frequency (bottom) of CD4 SP thymocytes in the indicated MHC class II-restricted TCR transgenic lines. **(I)** Surface CD5 expression on DP thymocytes (CD4$^+$CD8$^+$) from the indicated mouse strains. Data signify the mean ± SD. Data are representative of at least two independent experiments where each data point represents a biological replicate. *$p < 0.05$, **$p < 0.01$, ***$p < 0.001$; ns, not significant.

Similar trends were observed in the spleen of the TCR transgenic animals at 7-10 days of age, where there was an almost complete absence of TCR transgenic CD4$^+$ splenocytes in Vps34$^{TEC}$ mice (Figure 2.15D-H). However, there was also a significant decrease in the frequency of splenic OTI cells and total OTI and P14 splenocytes in the mutant mice (Figure 2.15A-C). This is likely due to decreased thymopoiesis independent of selection because polyclonal Vps34$^{TEC}$ mice analyzed at a similar age range exhibited a profound decrease in thymocyte cellularity (Figure 2.2).

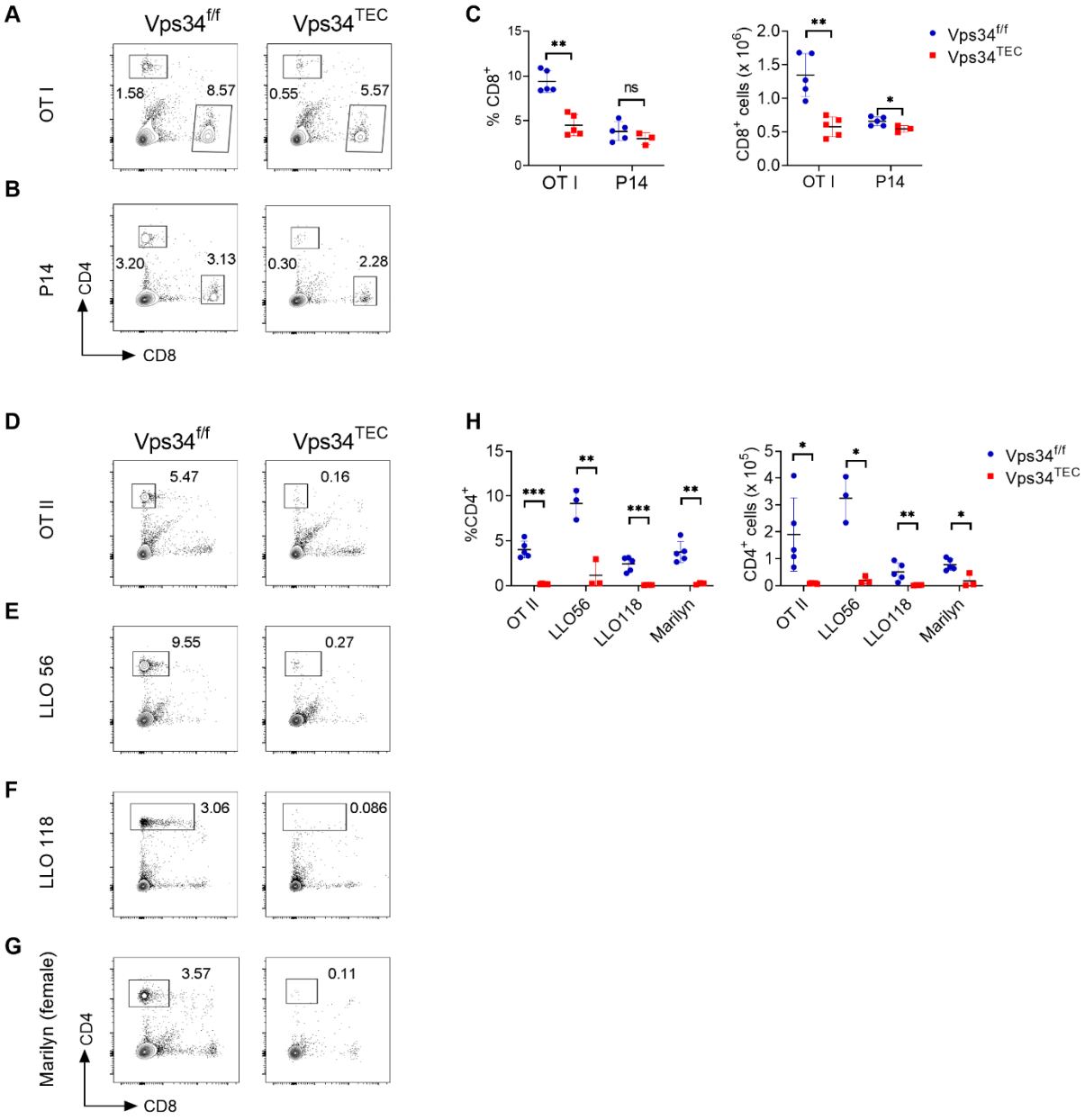


**Figure 2.15. Splenic phenotype of T cells in TCR transgenic mice. (A-C)** Flow cytometric analysis of splenocytes for CD4 and CD8 expression from the following MHC class I-restricted TCR transgenic lines: **(A)** OTI, and **(B)** P14. **(C)** Total cell number (top) and frequency (bottom) of CD8 SP cells in the indicated TCR lines. **(D-H)** Flow cytometric analysis of splenocytes for CD4 and CD8 expression from the following MHC class II-restricted TCR transgenic lines: **(D)** OTII, **(E)** LLO56, **(F)** LLO118, and **(G)** Marilyn (females only). **(H)** Total cell number (top) and frequency (bottom) of CD4 SP in the indicated transgenic TCR lines. **(I)** Marilyn thymocyte development in male Vps34$^{TEC}$ and Vps34$^{f/f}$ mice. Data signify the mean ± SD. Data are representative of at least two independent experiments where each data point represents a biological replicate. *p < 0.05, **p < 0.01, ***p < 0.001; ns, not significant.

**Altered TCRβ chain gene usage and repertoire sharing in CD4 SP thymocytes of neonatal Vps34$^{TEC}$ mice**

To explore how Vps34-mediated cellular processes in TECs impact the CD4$^{+}$ TCR repertoire, we conducted deep sequencing of the complementarity-determining region 3 (CDR3) sequences of TCR Vβ chains of genomic DNA from CD4 SP TCRβ$^{+}$ thymocytes isolated from 3 neonatal Vps34$^{TEC}$ mice and 3 littermate controls. TCR repertoire diversity was assessed using Simpson Clonality Index downsampled to 24,791 randomly chosen sequencing reads to correct for differences in the total productive templates sampled (Figure 2.16A). This analysis revealed that the repertoire diversity of CD4 SP T cells from Vps34$^{TEC}$ mice was similarly maintained as control mice (Figure 2.16B). The hypervariable CDR3 of the TCR is crucial for antigen recognition as it contacts MHC class II-peptide complexes on APCs (Adams et al., 2016; Rossjohn et al., 2015). The diversity in the CDR3 is generated through genetic recombination and by the addition of random nucleotides which produces CDR3s of variable length with a Gaussian-like distribution (Pannetier et al., 1993). Strikingly, we found that the CDR3 sequences in CD4 SP T cells from Vps34$^{TEC}$ mice were longer compared with control mice (Figure 2.16C). We next assessed TCR Vβ region gene usage and noticed significant changes in the prevalence of 6 Vβ chain gene segments (Figure 2.16D). Importantly, the altered Vβ gene segments were not of low use frequency in controls. To further assess how Vps34-deficiency in TECs impacts the CD4$^{+}$ TCR Vβ repertoire, we calculated clonal overlap using Morisita index (Figure 2.16E), which revealed significantly more clonal overlap among CD4 SP T cells from control animals than overlap between any control-mutant repertoire comparisons. Intriguingly, there was also significantly lower clonal overlap among the

repertoires of mutant animals compared to controls. Thus, while Vps34 in TECs is dispensable for maintaining $CD4^+$ TCR repertoire diversity, its absence leads to altered CDR3 length, Vβ gene usage and repertoire sharing.

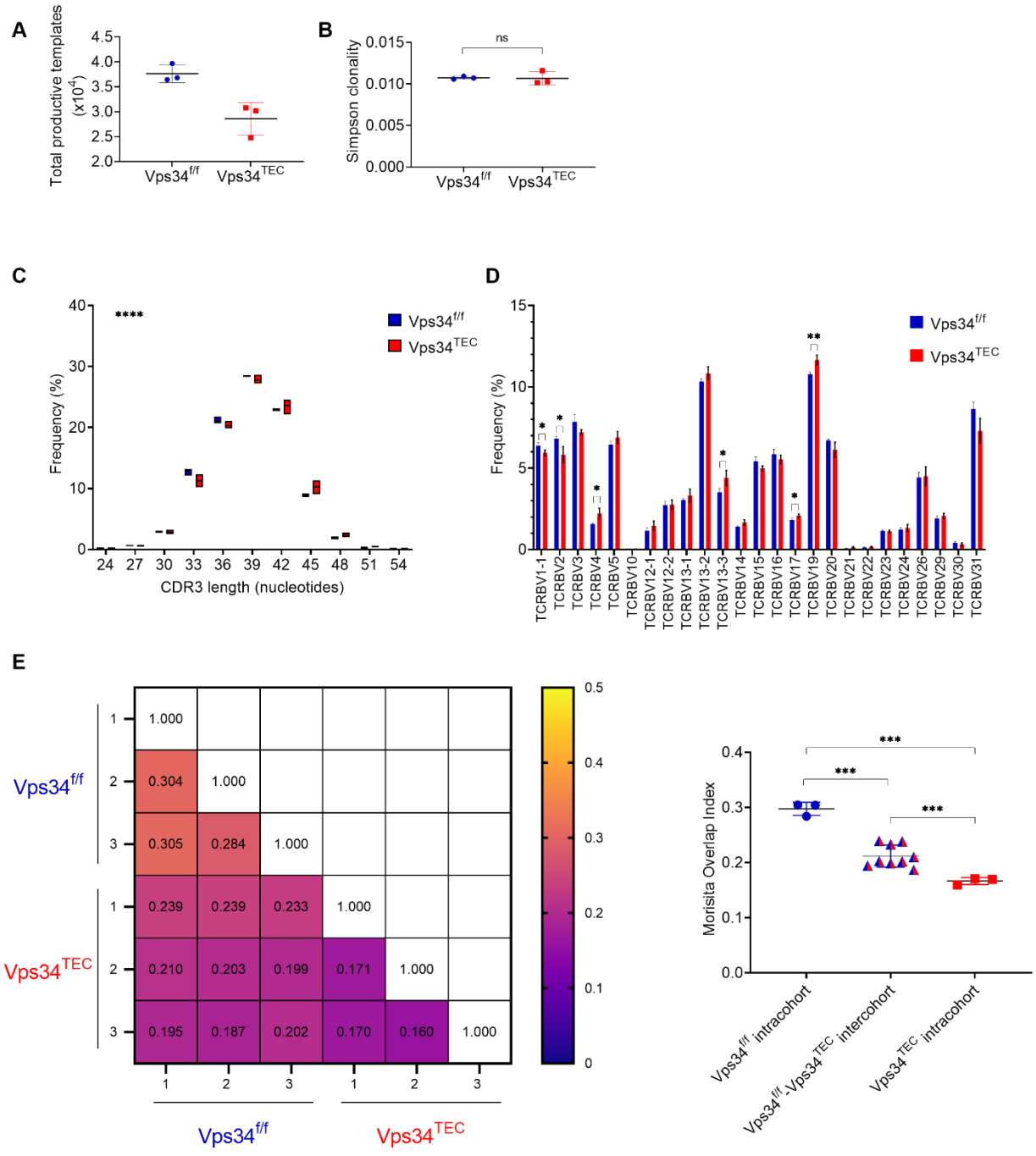


**Figure 2.16. TCRβ chains display altered gene usage and repertoire sharing in CD4 SP thymocytes of neonatal Vps34$^{TEC}$ mice.** The somatically rearranged TCRβ CDR3 sequences were amplified from genomic DNA isolated from CD4 SP TCRβ$^{+}$ thymocytes flow sorted from 4- or 6-day-old Vps34$^{f/f}$ or Vps34$^{TEC}$ mice (n= 3/ genotype). **(A)** Numbers of productive TCR sequences. **(B)** Simpson clonality indexes of TCR repertoire diversity. **(C)** Distribution of CDR3 lengths (Chi-squared test). **(D)** Distribution of TCR Vβ gene usage. **(E)** Heatmap of Morisita repertoire overlap across all samples. The graph

represents the Morisita overlap index for each individual comparison organized by group. Data signify the mean ± SD. *p < 0.05, **p < 0.01, ***p < 0.001.

**TEC Vps34-deficiency attenuates the incidence and severity of active experimental autoimmune encephalomyelitis**

To explore functional consequences of the altered $CD4^+$ T cell development and repertoire in $Vps34^{TEC}$ mice, we tested the response of these animals and littermate controls to experimental autoimmune encephalomyelitis (EAE), an animal model of human multiple sclerosis. Results showed a delayed on-set of clinical disease in $Vps34^{TEC}$ mice compared to littermate controls (Figure 2.17A). Mutant mice also experienced significantly reduced incidence and severity of disease (Figure 2.17B, C). These data indicate that Vps34 in TECs is required for a normal level of disease directed at a central nervous system autoantigen.

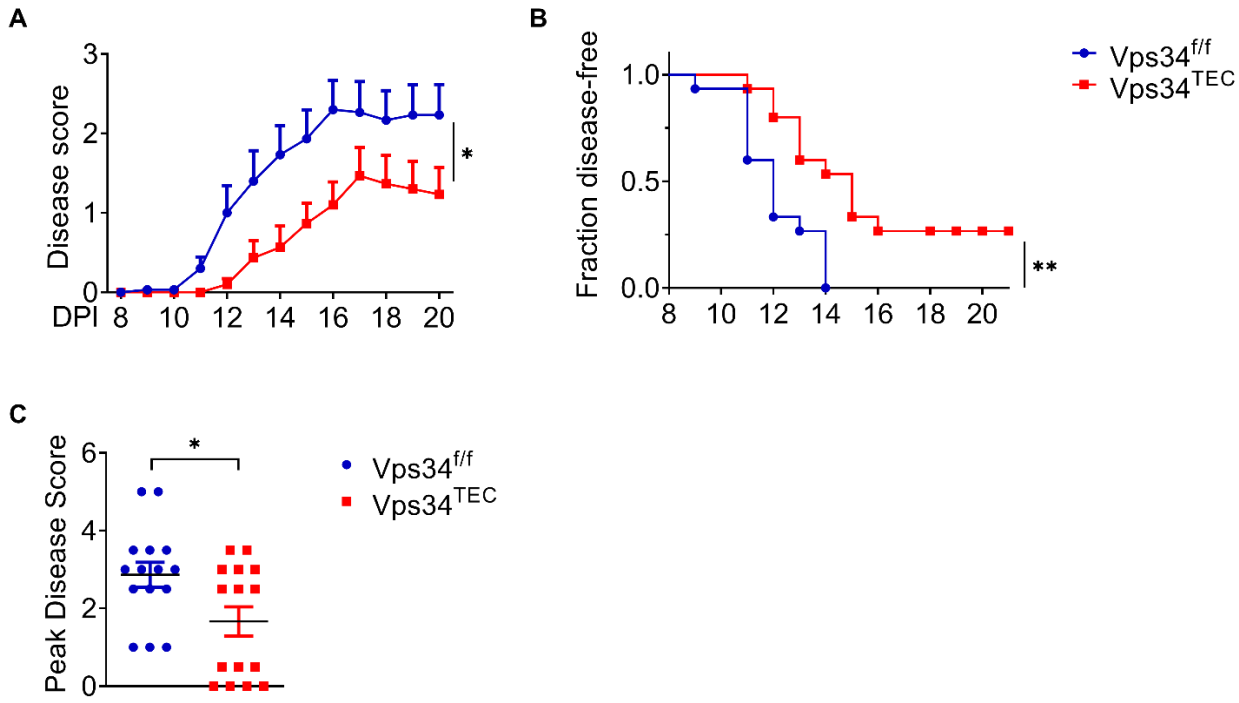


**Figure 2.17. Vps34-deficiency attenuates the incidence and severity of active EAE.** EAE was induced by active immunization with $MOG_{35-55}$ peptide. **(A)** Daily clinical score. **(B)** Disease onset. **(C)** Peak disease score. Results are accumulated from three independent experiments with a combined total of 15 mice per group. The data shown are the average ± SEM. *p < 0.05, **p < 0.01; dpi, days post-immunization.

### cTECs present increased abundance of CLIP-bound I-$A^b$ complexes in the absence of Vps34

Surface levels and turnover rates of MHC class II on cTECs are critically important for positive selection of $CD4^+$ T cells (von Rohrscheidt *et al.*, 2016). Autophagy-related proteins including Vps34 have been implicated in regulating surface expression of MHC molecules (Van Kaer *et al.*, 2019). However, we found no significant changes in the surface expression levels of either the MHC class I molecule $K^b$ or the MHC class II molecule I-$A^b$ on Vps34-deficient cTECs (Figure 2.18A, B). To investigate whether a particular MHC class II-bound peptide on cTECs was affected by loss of Vps34, we used

a monoclonal antibody (15G4) that recognizes I-A$^b$ when occupied by the invariant chain peptide derivative CLIP (Beers et al., 2005). After synthesis in the ER, MHC class II molecules contain CLIP in their peptide binding groove. In MHC class II compartments, the peptide editor DM promotes the exchange of CLIP for higher affinity peptide. However, a fraction of class II molecules is presented at the surface while containing CLIP (Denzin et al., 2017). Indeed, we found that cTECs from Vps34$^{f/f}$ animals express CLIP-bound I-A$^b$ molecules at levels above background staining of cTECs isolated from an MHC disparate strain (I-A$^d$-expressing BALB/c) (Figure 2.18C). cTECs isolated from Vps34$^{TEC}$ mice expressed significantly increased levels of CLIP-bound I-A$^b$ compared with wild-type controls. These findings indicate that Vps34 is required by cTECs to present normal surface levels of an endogenous self-peptide/MHC class II complex and suggest a role for Vps34 in generating the repertoire of self-peptides that is specialized for positive selection.

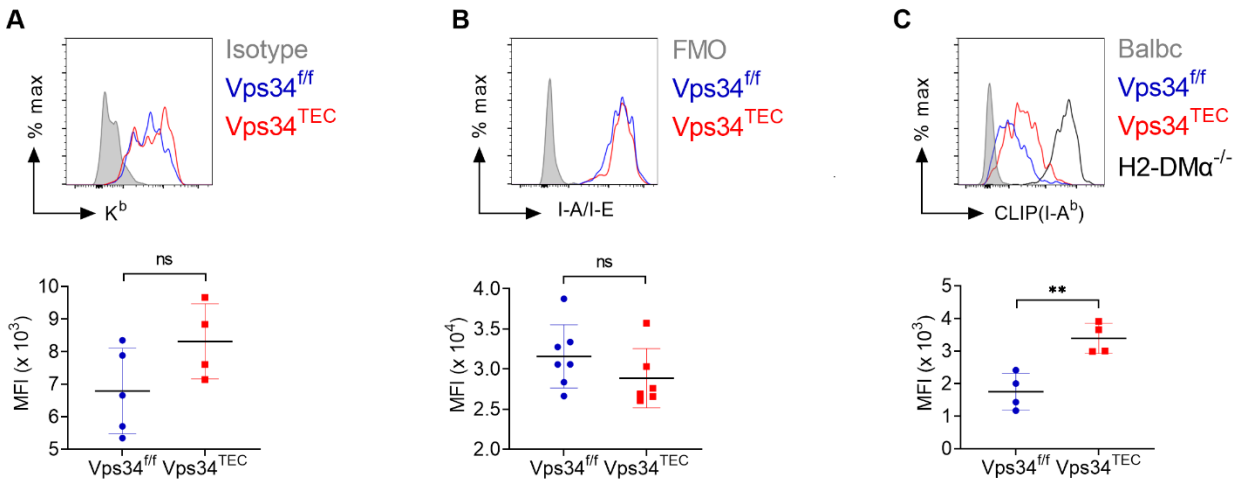


**Figure 2.18. cTECs present increased abundance of CLIP-bound I-A$^b$ complexes in the absence of Vps34. (A-C)** cTECs (CD45$^-$EpCAM$^+$Ly-51$^+$) isolated from the indicated strains (isotype and fluorescence minus one [FMO] staining are from Vps34$^{f/f}$ isolated cells) were analyzed for **(A)** MHC class I (H-2K$^b$), **(B)** MHC class II (H-2I-A/I-E), or **(C)** CLIP-bound I-A$^b$ expression by flow cytometry. Graphs represent mean fluorescence

intensity (MFI) of indicated staining. Data signify the mean ± SD. Data are representative of at least two independent experiments where each data point represents a biological replicate. **p < 0.01; ns, not significant.

**TEC Vps34 deficiency causes defects in endocytic vesicle trafficking and cathepsin L maturation**

To analyze the contribution of Vps34 to vesicle trafficking in TECs, we utilized the mouse cTEC cell line C9 (Wertheimer et al., 2018). We deleted Vps34 in C9 cells employing CRISPR/Cas9 approach, generating stable control sgLacZ cells and Vps34-deficient sgVps34 cells. Efficient deletion of Vps34 in sgVps34 cells was confirmed by significant decrease in Vps34 protein expression (Figure 2.19A). Basal autophagy was disrupted in sgVps34 cells as evidenced by the accumulation of P62, a factor that targets cargo to autophagosomes, and LC3, both of which are degraded by autophagy. Previous studies report that disruption of Vps34 expression *in vitro and in vivo* causes a vacuolization phenotype associated with defects in endosomal trafficking (Bechtel et al., 2013; Jaber *et al.*, 2016; Johnson et al., 2006). Examination of the cultures by light microscopy revealed that a significant proportion of Vps34 deficient cells accumulated numerous phase-lucent spherical cytoplasmic vacuoles (Figure 2.19B). Strikingly, H&E staining of thymic sections from neonates also revealed vacuolization caused by the absence of Vps34. To assess vesicle trafficking, we analyzed the maturation of the lysosomal protease cathepsin L, which is required by cTECs for efficient positive selection of $CD4^+$ T cells *in vivo* (Honey *et al.*, 2002; Nakagawa *et al.*, 1998). We found a significant decrease in the mature forms of cathepsin L, suggesting a significant abnormality in the ability of the lysosome to cleave immature cathepsin L (Figure 2.19A).

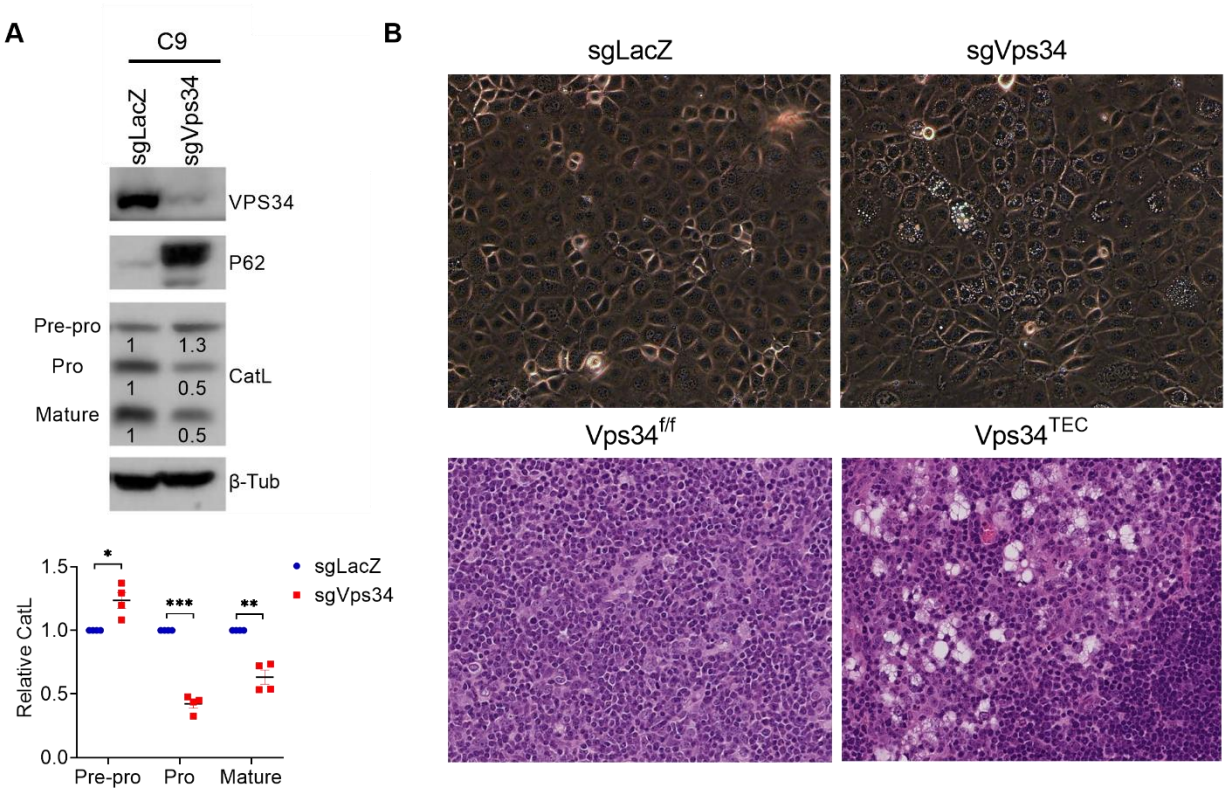


**Figure 2.19. TEC Vps34 deficiency causes defects in endocytic vesicle trafficking and Cathepsin L maturation. (A)** Proteins isolated from control and Vps34-deleted C9 cells were analyzed by western blot for markers of autophagy and vesicle trafficking. β-tubulin was used as loading control. Relative densities of pro-cathepsin L and mature-cathepsin L bands between sgLacZ and sgVps34 are indicated. Data are representative of at least two independent experiments. **(B)** Light micrograph of live control (sgLacZ) and Vps34 deleted (sgVps34) C9 cells (top). Thymus tissue sections from 7- to 10-day-old $Vps34^{f/f}$ or $Vps34^{TEC}$ mice stained with H&E (bottom, 20 x original magnification). Arrows highlight areas of significant vacuolization. n = 5 / genotype. *p < 0.05, **p < 0.01, ***p < 0.001.

## Vps34 regulates positive selection in a canonical autophagy-independent mechanism

In addition to autophagy, Vps34 plays a role in endocytosis and vesicle trafficking (Backer, 2016), both of which can contribute to antigen presentation (Kondo *et al.*, 2017). To investigate the role autophagy plays in the T cell selection phenotype observed in $Vps34^{TEC}$ mice, we analyzed T cell development and positive selection in $Atg5^{TEC}$ mice.

We restricted our initial analysis to neonates for a better comparison with Vps34$^{TEC}$ mice. Consistent with a previous report employing Atg5-deficient thymus grafts (Nedjic *et al.*, 2008), we failed to detect any difference in the intrathymic development of the polyclonal repertoire in Atg5$^{TEC}$ mice (Figure 2.20A). To test whether the autophagy pathway is necessary for positive selection of an MHC class II-restricted transgenic TCR that was dependent on Vps34 sufficiency in TECs, we investigated positive selection of OTII cells in Atg5$^{TEC}$ mice. We generated bone marrow chimeric animals by lethally irradiating either wild-type or Atg5$^{TEC}$ mice and transplanting bone marrow isolated from OTII transgenic donors. Our analysis revealed no significant change in the selection and development of OTII cells in Atg5$^{TEC}$ recipient mice (Figure 2.20B). Radiation has been shown to induce autophagy (Chaurasia et al., 2016) and it is feasible that thymic recovery following radiation is compromised in the absence of Atg5, which may confound the interpretation of these results. Further, recent reports have highlighted the changes that occur in thymic selection from early life to adulthood (Dong et al., 2017; Smith et al., 2018). Therefore, for a more direct comparison, we analyzed positive selection of OTII cells in neonatal Atg5$^{TEC}$ mice by breeding in the OTII TCR transgene to Atg5$^{TEC}$ mice. Consistent with data from the chimera experiments, we found no alteration in OTII cell positive selection between Atg5$^{TEC}$ mice and their littermate controls (Figure 2.20C). Collectively our data show that Atg5-dependent autophagy is not required by TECs to positively select a TCR that is dependent upon Vps34-mediated cell processes in TECs. Therefore, we propose that Vps34 in TECs regulates positive selection in a canonical autophagy-independent mechanism.

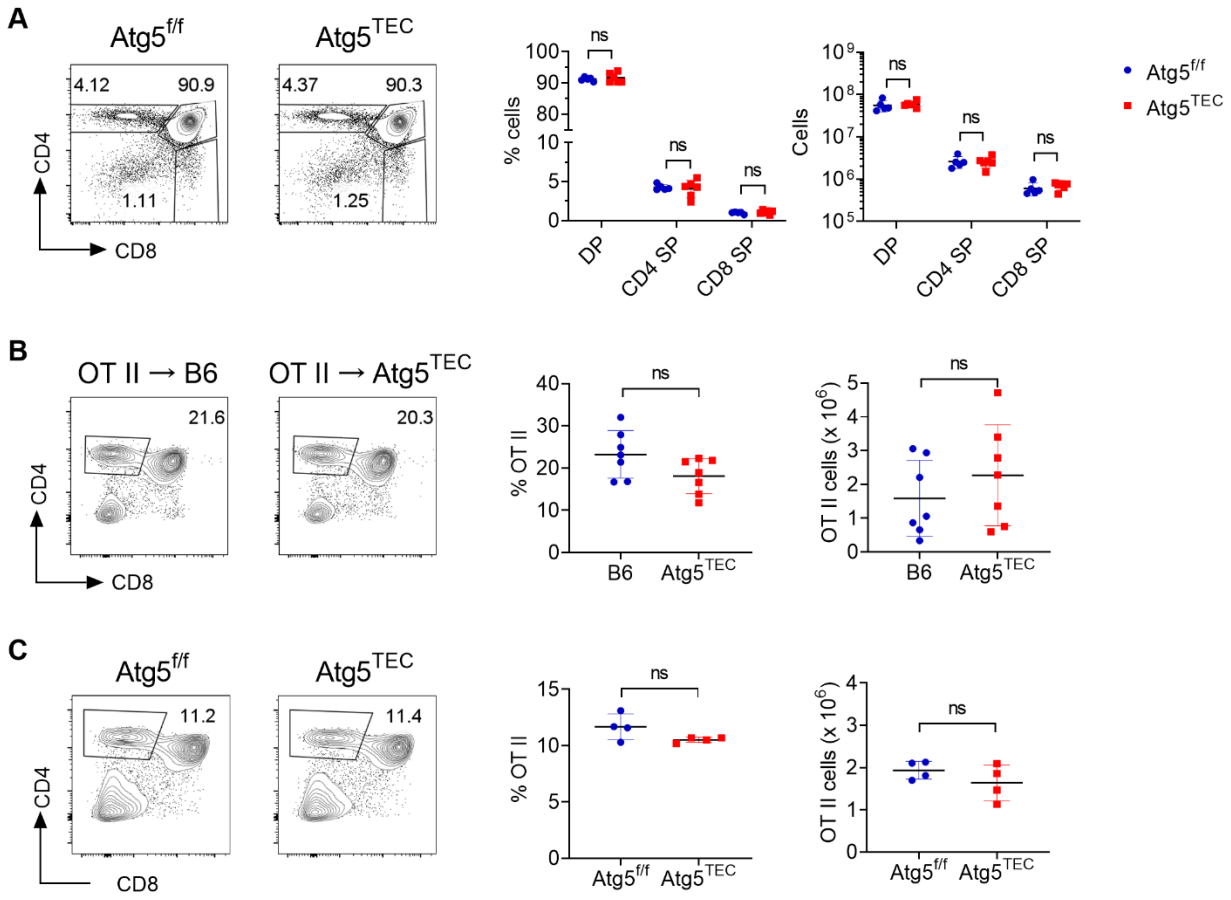


**Figure 2.20. Vps34 regulates CD4$^{+}$ T cell positive selection in a canonical autophagy-independent mechanism.** Thymocytes were analyzed for CD4 and CD8 expression by flow cytometry. **(A)** Analysis of ten-day-old Atg5$^{f/f}$ or Atg5$^{TEC}$ mice. Graphs represent frequency and total numbers of the indicated thymocyte subsets. **(B)** B6 or Atg5$^{TEC}$ mice at 5 weeks post-lethal irradiation following engraftment with OTII TCR transgenic bone marrow. Graphs represent frequency and total numbers of OTII cells (CD4 SP TCR Va2$^{hi}$). **(C)** OTII TCR transgene was introgressed into the Atg5$^{TEC}$ strain and offspring was analyzed for positive selection compared to OTII TCR transgenic Atg5$^{f/f}$ controls. Graphs represent frequency and total numbers of OTII cells (CD4 SP TCR Va2$^{hi}$). Data signify the mean ± SD. Data are representative of at least two independent experiments where each data point represents a biological replicate. ns, not significant.

### TEC Vps34 in negative selection

The Marilyn TCR transgenic system allows for the interrogation of negative selection in addition to positive selection (Lantz et al., 2000). Marilyn transgenic TCRs are specific for the male H-Y antigen. As such, developing Marilyn T cells undergo negative selection in

the thymus of male but not female mice. We did not observe any differences in the thymic selection of Marilyn T cells in male Vps34$^{TEC}$ mice compared to controls (Figure 2.21). While this may suggest that negative selection (and thus the antigen processing and presentation of the male H-Y antigen) is intact in Vps34-deficient thymi, the severe defects in positive selection in female mice confound the interpretation of these observations.

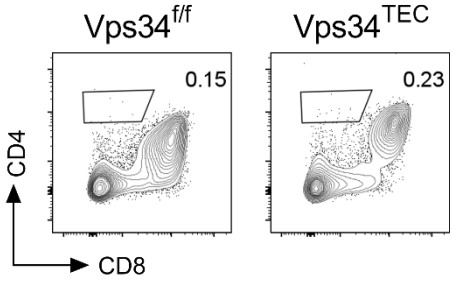


**Figure 2.21. TEC Vps34 in negative selection using Marilyn TCR$^{Tg}$ system.** Thymocytes from one-week-old Vps34$^{f/f}$ or Vps34$^{TEC}$ male mice were analyzed by flow cytometry for CD4 and CD8 expression. Data are representative of two independent experiments.

**mTEC specific targeting of Vps34 in central tolerance**

To further assess the contribution of Vps34 to TEC regulation of negative selection, we utilized Aire-CreER$^{T2}$ Vps34$^{f/f}$ mice in which Vps34 can be targeted specifically in cells required for negative selection (i.e., mature mTECs), while not disturbing cells required for positive selection (i.e., cTECs). Aire expressing mTECs have been identified as cells crucial for both negative selection and induction of tTregs to tissue specific antigens (Anderson et al., 2005; Metzger *et al.*, 2013). Flow cytometric analysis of Aire-CreER$^{T2}$ Vps34$^{f/f}$ mice showed no significant changes to thymocyte subset frequency or cellularity including CD4 SP cells and tTregs (Figure 2.22A, B). Although there were no obvious

defects in central tolerance in the polyclonal repertoire of Aire-CreER$^{T2}$ Vps34$^{f/f}$ mice, it remained possible that Vps34 mediates antigen processing and presentation of Aire-dependent tissue-restricted antigens necessary for negative selection of specific autoreactive CD4$^{+}$ T cell clones. To test this possibility, we utilized Rip-mOVA mice which express membrane bound ovalbumin (OVA) under the control of the rat insulin promoter. These mice express OVA in their mTECs which causes the negative selection of developing OTII transgenic T cells. To examine the role Vps34 plays in negative selection, we generated Aire-CreER$^{T2}$ Vps34$^{f/f}$ Rip-mOVA mice which were lethally irradiated and reconstituted with OTII TCR transgenic bone marrow. The mice were then treated with tamoxifen to delete Vps34 in mature mTECs and assessed for negative selection of developing OTII cells. We found no significant change in the cellularity of CD4 SP OTII cells in the thymus of Cre$^{+}$ mice compared to Cre$^{-}$ mice (Figure 2.23), indicating that mTECs do not require Vps34 to mediate negative selection of autoreactive T cells.

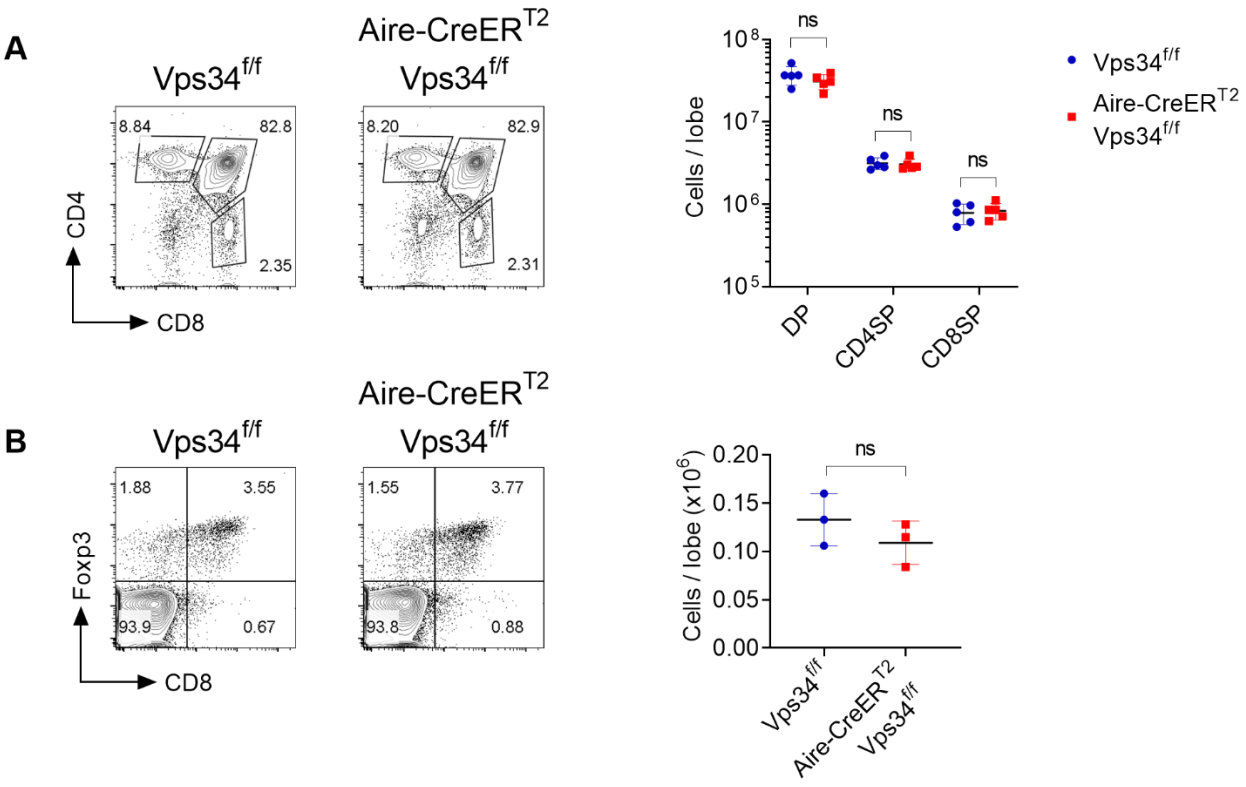


**Figure 2.22. Vps34 is dispensable in mature TECs for central tolerance.** Aire-CreER$^{T2}$ Vps34$^{f/f}$ or Vps34$^{f/f}$ mice were administered tamoxifen every other day for 14 days and then analyzed. Flow cytometric analysis of **(A)** thymocyte subsets and **(B)** thymic regulatory T cells (Foxp3$^{+}$ CD25$^{+}$) among CD4 SP cells. Graphs represent total numbers of thymocyte subsets. Data signify the mean ± SD. Each data point represents a biological replicate. ns, not significant.

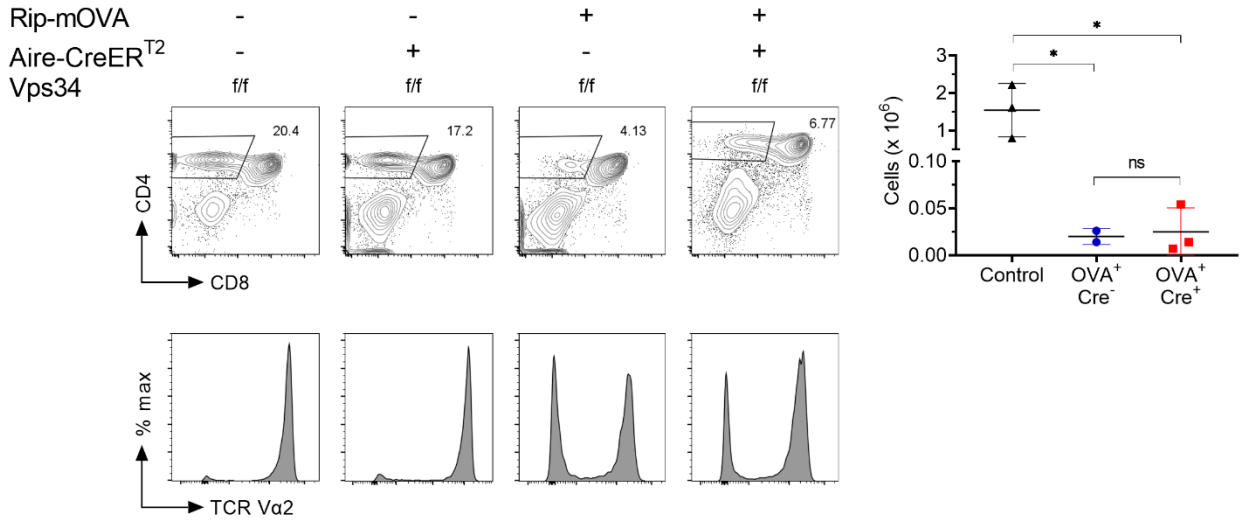


**Figure 2.23. Vps34 is not required by mTECs for negative selection of a T cell clone recognizing a neo-self-antigen.** Vps34$^{f/f}$, Aire-CreER$^{T2}$ Vps34$^{f/f}$, or Rip-mOVA Aire-CreER$^{T2}$ Vps34$^{f/f}$ mice were lethally irradiated and subsequently engrafted with OT II TCR$^{Tg}$ bone marrow. Recipients were allowed to reconstitute for 5 weeks and were then administered tamoxifen every other day for 14 days and then analyzed. Flow cytometric analysis of (top) CD4 SP thymocytes and (bottom) TCR V$\alpha$2 expression among CD4 SP. Graph represents CD4 SP cellularity per indicated recipient. Data signify the mean ± SD. Data are representative of at least two independent experiments for each time point where each data point represents a biological replicate. *p < 0.05; ns, not significant.

## 2.3 Discussion

Here we analyzed mice with TEC-specific *Vps34* gene ablation. Vps34$^{TEC}$ mice exhibited a progressive loss in thymocyte cellularity that led to T cell lymphopenia in adult animals. Peripheral T cells in adult animals exhibited an activated phenotype likely caused by homeostatic proliferation due to T cell lymphopenia. The gradual loss in thymopoiesis in Vps34$^{TEC}$ mice was preceded by a reduction in TEC cellularity suggesting that the eventual loss of DP thymocytes is likely due to insufficient TEC numbers. Using the Foxn1 promoter to drive Cre recombinase expression for gene targeting, Vps34 is likely deleted in TECs starting at the initiation of thymic organogenesis (Martinez-Ruiz et al., 2021),

which raises the possibility that the observed alterations in TEC cellularity are due to loss of TEC progenitors. Our results with a genetic system to inducibly target *Vps34* ablation in postnatal thymi indicate that TECs continue to require Vps34 for their homeostasis and to facilitate thymopoiesis after mature TECs have completed their development.

TEC-specific loss of Vps34 also caused significant alterations in thymic morphology. While conditional loss of Vps34 reduced the cellularity of both cTECs and mTECs, the latter TEC subset was relatively more profoundly impacted. We discovered a significant decrease in the frequency of Ki67 positive cells among mTECs isolated from mutant thymi. This suggests that a loss of proliferating mTECs may partially explain the defect in the mTEC compartment. However, we envision three possible scenarios to explain the relative deficiency in mTECs that will require further exploration: (1) a defect in the capacity of TEC precursors to develop into mTECs, (2) a failure of committed mTECs to expand, and/or (3) increased mTEC death. Further, among mTECs there was a reduction in mature mTECs which are critical for establishing and maintaining tolerance. We found that inducible deletion of Vps34 in mature mTECs did not alter their cellularity indicating that immature mTECs require Vps34 for maturation but not for maintenance.

Previous studies have identified TECs to have high levels of homeostatic autophagic flux (Semwal et al., 2021). Our analysis of autophagy using mice with a transgenic reporter allele confirmed constitutive autophagy in TECs under physiological conditions. Furthermore, we confirmed that Vps34 is required for homeostatic autophagy, as we observed a near complete block in TEC autophagic flux in $Vps34^{TEC}$ mice. Vps34 has been proposed to play critical roles in the initiation of autophagy as well as the fusion of the autophagosome with the lysosome for the termination of autophagy (Bilanges *et*

*al.*, 2019). However, our data using flow cytometry to analyze Vps34-deficient TECs does not allow us to discern at which steps in autophagy Vps34 is required. Future studies using fluorescent imaging of our reporter system should be able to address this issue, as the absence of $LC3^{+}$ punctae would confirm that Vps34 is essential for the initiation of autophagy. To address the role of autophagy in maintaining thymic homeostasis, we generated mice with a TEC specific loss of Atg5 which has been shown to be necessary for autophagy in TECs (Nedjic *et al.*, 2008). Consistent with previous reports, we found autophagy in TECs to be dispensable for cellular homeostasis and thymopoiesis (Jain *et al.*, 2018; Nedjic *et al.*, 2008). This suggests that Vps34 mediated cellular processes in addition to autophagy are critical for maintaining TEC homeostasis.

The class III PI3K Vps34 plays key roles in autophagy, endocytosis, and vesicle trafficking (Bilanges *et al.*, 2019), processes that control the presentation of self-antigens by TECs to developing thymocytes (Klein *et al.*, 2014). Therefore, in the present study we analyzed T cell selection in $Vps34^{TEC}$ mice. cTECs rely on unique antigen processing machinery to produce a repertoire of self-antigens that is specialized for T cell positive selection (Kondo *et al.*, 2017). While in most APCs antigens presented on MHC class II are derived from extracellular sources, cTECs present self-antigens derived from intracellular origins (Klein *et al.*, 2014). Here, we propose that TECs require Vps34-mediated cellular processes to produce a diverse collection of self-peptides needed for the development and positive selection of a broad $CD4^{+}$ T cell repertoire. Our finding that Vps34-deficient cTECs express increased surface levels of CLIP-bound MHC class II molecules provides indirect support for this possibility.

Our results show that loss of Vps34 in TECs causes defects in the development of $CD4^+$ T cells in neonatal mice. Vps34-deficient TECs were also unable to positively select MHC class II-restricted transgenic TCRs but retained their capacity to select MHC class I-restricted transgenic TCRs, providing further evidence that Vps34 is crucial in processing antigens for presentation by MHC class II but not MHC class I in cTECs. Because MHC class I-restricted TCRs were selected in $Vps34^{TEC}$ mice, it is unlikely that the defect in $CD4^+$ T cell development in neonatal mice is due to TEC dysfunction other than MHC presentation such as producing and secreting factors necessary for recruiting lymphoid progenitors, T cell lineage commitment, or T cell lineage expansion prior to positive selection.

Previous reports analyzing the TCR repertoire of mice with targeted mutations that significantly reduce the variety of self-peptides bound to MHC class II molecules have provided evidence that positive selection on a restricted collection of self-peptides is sufficient to select for a broad but distinct $CD4^+$ TCR repertoire (Pacholczyk *et al.*, 2006; Wong *et al.*, 2007). Consistent with these findings, we found a close degree of clonality maintained in the $CD4^+$ TCR repertoire in $Vps34^{TEC}$ mice compared to control mice. However, we found significantly reduced clonal sharing and altered TCR Vβ gene segment usage in $CD4^+$ T cells in the absence of Vps34 in TECs. These results indicate that Vps34-mediated cellular processes in TECs are crucial for shaping the TCR repertoire in $CD4^+$ T cells. Although the defect in the development of $CD4^+$ T cells expressing MHC class II-restricted transgenic TCRs illustrates a role for Vps34 in the positive selection of $CD4^+$ T cells, we cannot exclude that the TCR sequencing data of

the polyclonal repertoire are influenced by alterations in negative selection in Vps34$^{TEC}$ mice.

A previous report using Atg5-deficient thymic grafts argued that autophagy promotes positive selection of the CD4$^{+}$ TCR repertoire by providing selecting ligands bound to MHC class II molecules (Nedjic *et al.*, 2008). In that system, more modest effects in positive selection using transgenic TCR lines were observed compared to the positive selection defects of MHC class II-restricted transgenic TCRs reported here in Vps34$^{TEC}$ mice. Importantly, we did not observe significant changes in positive selection of OTII cells in mice with a TEC-specific Atg5 deficiency. Yet, we found a near complete block in positive selection of OTII cells in Vps34$^{TEC}$ mice. Given these observations, along with a profound block in autophagic flux in Vps34-deficient TECs, it is unlikely that the observed alterations in positive selection of CD4$^{+}$ T cells in Vps34$^{TEC}$ mice are due solely to a loss in autophagy. Nevertheless, it remains possible that Atg5-independent autophagy plays a role in the defective CD4$^{+}$ T cell selection phenotype observed in Vps34$^{TEC}$ mice. Atg5-independent autophagy has been reported in some studies (Honda et al., 2014; Ma et al., 2015; Nishida et al., 2009). Furthermore, a Vps34-dependent noncanonical form of autophagy, termed LC3-associated phagocytosis (LAP), has been described (Martinez et al., 2015). LAP supports antigen presentation in mouse macrophages by regulating the processing of endocytosed antigens for presentation to MHC class II-restricted CD4$^{+}$ T cells (Munz, 2018). Importantly, mice that are deficient in LAP due to genetic targeting of Rubicon do not display defects in T cell development (Martinez et al., 2016). Therefore, it is unlikely that Vps34 contributes to antigen presentation by TECs via LAP.

We propose that the thymic positive selection defect in Vps34$^{TEC}$ mice is caused by defects in endocytosis and/or vesicle trafficking, rather than canonical autophagy. We found that loss of Vps34 in TECs did not alter levels of MHC class II molecules on the surface of cTECs, indicating that endocytic turnover or recycling of peptide-MHC class II molecules is not the underlying cause for the defect in positive selection of CD4 T cells. However, we found an increase in the abundance of surface MHC class II molecules occupied by the invariant chain derivative peptide CLIP, indicating quantitative alterations in the repertoire of self-peptides bound to MHC class II molecules. Previous reports have identified vesicle trafficking dependent upon Vps34 catalytic activity as necessary for the endosomal processing of the protease cathepsin D into its active mature form (Jaber *et al.*, 2016; Reifler *et al.*, 2014; Ronan *et al.*, 2014; Row *et al.*, 2001). Our analysis of Vps34-deficient C9 cells provides evidence that steady-state levels of mature cathepsin L require Vps34 in cTECs. Strikingly, many of the T cell defects observed in cathepsin L knockout mice resemble those seen in Vps34$^{TEC}$ mice, including altered CD4$^{+}$ T cell selection and increased abundance of CLIP-bound MHC class II molecules on cTECs (Honey *et al.*, 2002; Nakagawa *et al.*, 1998). Taken together, our findings provide evidence that cTECs require Vps34 for the generation of the self-peptide/MHC class II repertoire in a mechanism involving Vps34-dependent proteolytic activity but likely not autophagy-mediated delivery of antigens to MHC class II-containing compartments.

In contrast to the striking defects in positive selection in mice with Vps34-deficient TECs, we failed to identify a role for Vps34 in regulating negative selection by generating mice with inducible mTEC-specific *Vps34* ablation. A previous report argued that peptide degraded by autophagy in mTECs is presented to CD4 SP thymocytes for negative

selection and tolerance induction (Aichinger *et al.*, 2013). Our data presented here along with the observation that TECs require Vps34 for basal autophagic flux, suggests that Vps34-dependent autophagy makes minor contributions if any to antigen processing and presentation in mTECs necessary for central tolerance.

In this research chapter, we address the question of what role does Vps34 play in the capacity of thymic epithelial cells for the presentation of self-peptide that is essential for positive selection of $CD4^+$ T cells. Collectively, our data identify a critical role for Vps34 in maintaining thymic function and provides new insights into the mechanisms governing the processing and presentation of self-antigens by cTECs required for thymic selection of a broad $CD4^+$ T cell repertoire (Figure 2.24). These findings also provide a rationale for targeting Vps34 activity in scenarios where enhancement of thymic function may be desired, such as during aging, recovery from radiation therapy or chemotherapy, T cell reconstitution following stem cell transplantation, and infection or inflammation that compromise T cell thymic output. A new question raised by this work is to what extent does autophagy-dependent antigen processing in thymic epithelial cells shape the repertoire of $CD4^+$ T cells.

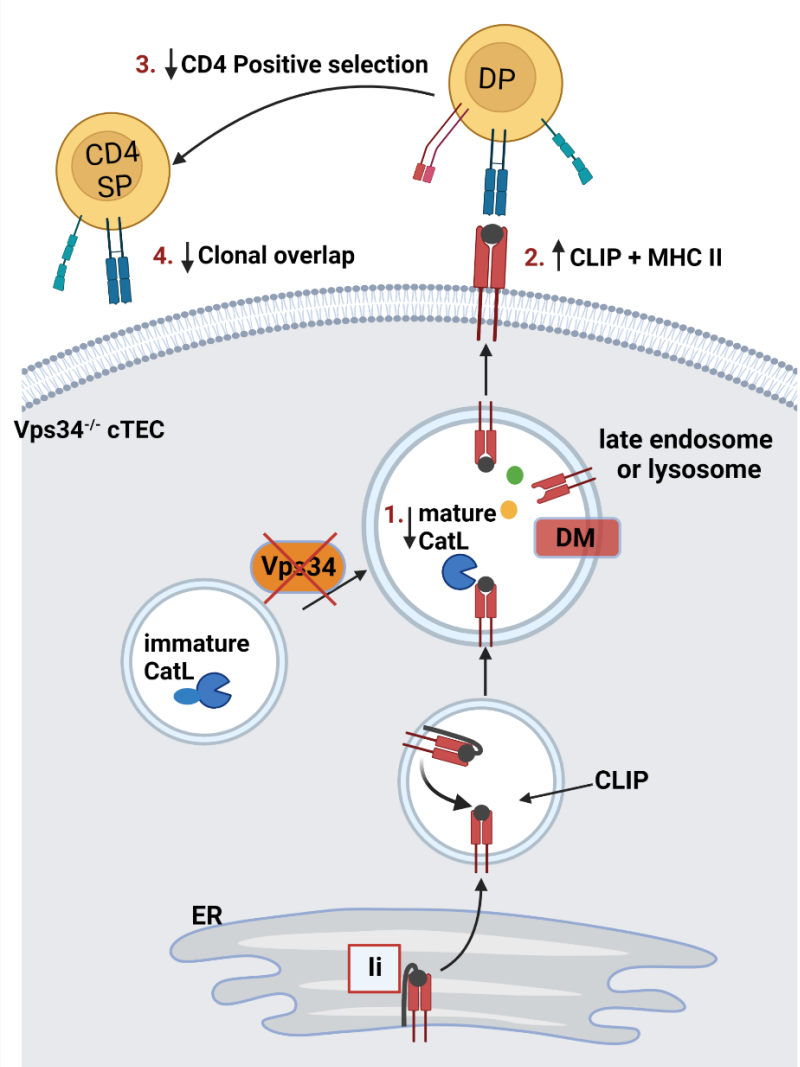


**Figure 2.24. Summary of findings related to Vps34 regulation of thymic selection in TECs.** Vps34 deficiency in cTECs causes **1.** Impaired vesicle trafficking which decreases cathepsin L (CatL) maturation. **2.** Altered antigen processing leads to a quantitative shift in the MHC II/self-peptidome and increased presentation of invariant chain (Ii) intermediates (CLIP). **3.** The altered MHC II/self-peptidome is less optimized for positive selection of CD4 SP T cells. **4.** The CD4 SP T cells that are positively selected display a TCR repertoire that is diverse but has altered properties including reduced clonal sharing. This figure was made with BioRender.com.

## 2.4 Materials and methods

### *Mice*

All mouse strains used, and their source are outlined in Table 2.2. TEC-specific deletion of *Vps34* and *Atg5* was achieved by crossing Vps34$^{f/f}$ and Atg5$^{f/f}$ mice with Foxn1-Cre mice, respectively. Tamoxifen inducible mTEC specific deletion of Vps34 was achieved by crossing Vps34$^{f/f}$ mice with K5-CreER$^{T2}$ mice. Tamoxifen inducible mature mTEC specific deletion of *Vps34* was achieved by crossing Vps34$^{f/f}$ mice with Aire-CreER$^{T2}$ mice. Tamoxifen inducible deletion of *Vps34* was achieved by crossing Vps34$^{f/f}$ mice with Rosa26-CreER$^{T2}$ mice. Cre$^{-}$ littermates were used as controls in all experiments except experiments using Rosa26-CreER$^{T2}$ to target Vps34 deletion, in which a control group was administered vehicle (as outlined below). Newborn to 10-week-old animals of both sexes were used in this study. All breeder and experimental mice were housed under specific pathogen-free conditions in compliance with guidelines from the Institutional Animal Care and Use Committee at Vanderbilt University.

**Table 2.2: Mouse strains employed in this study.**

| Mouse strain/ Genetic background | Source | Identifier/reference |
|---|---|---|
| C57BL/6J | The Jackson Laboratory | 00664 |
| BALB/cJ | The Jackson Laboratory | 00651 |
| Pik3c3$^{tm1c(EUCOMM)Wtsi}$/J (Vps34$^{f/f}$)/ C57BL/6J, 129 mixed | Dr. Jianhua Zhang, University of Alabama at Birmingham | (Jaber *et al.*, 2012) |
| B6(Cg)-Foxn1$^{tm3(cre)Nrm}$/J (Foxn1-Cre)/ C57BL/6J | Dr. Nancy Manley, University of Georgia | (Gordon *et al.*, 2007) |
| B6.129-Gt(ROSA)26Sor$^{tm1(cre/ERT2)Tyj}$/J (Rosa26-CreER$^{T2}$)/ C57BL/6J | Dr. Mark Boothby, Vanderbilt University School of Medicine | (Ventura et al., 2007) |

| | | |
|---|---|---|
| C57BL/6-Tg(TcraTcrb)1100Mjb/J (OTI)/ C57BL/6J | The Jackson Laboratory | 03831 |
| B6.Cg-Tcra$^{tm1Mom}$ Tg(TcrLCMV)327Sdz/TacMmjax (P14)/ C57BL/6J | The Jackson Laboratory | 37294 |
| B6.Cg-Tg(TcraTcrb)425Cbn/J (OTII)/ C57BL/6J | The Jackson Laboratory | 04194 |
| Tg(TcraLLO56,TcrbLLO56)#Pmal (LLO56) | Dr. Paul Allen, Washington University School of Medicine | (Milam and Allen, 2015) |
| Tg(TcraLLO118,TcrbLLO118)#Pmal (LLO118) | Dr. Paul Allen, Washington University School of Medicine | (Milam and Allen, 2015) |
| Tg(TcraH-Y,TcrbH-Y)1Pas (Marilyn) | Dr. Maria-Luisa Alegre, University of Chicago | (Lantz *et al.*, 2000) |
| C57BL/6-Tg(CAG-RFP/EGFP/Map1lc3b)1Hill/J (CAG-RFP-EGFP-LC3)/ C57BL/6J | The Jackson Laboratory | 027139 |
| B6.129S-Atg5$^{tm1Myok}$ (Atg5$^{f/f}$)/ C57BL/6J | Dr. Akiko Iwasaki, Yale University School of Medicine | (Hara *et al.*, 2006) |
| C57BL/6-Foxp3$^{tm1Flv}$/J (Foxp3-RFP)/ C57BL/6J | The Jackson Laboratory | 008374 |
| B6;129S4-H2-DMa$^{tm1Luc}$/J (H2-DMa$^{-/-}$)/ C57BL/6J | Dr. Paul Allen, Washington University School of Medicine | (Martin *et al.*, 1996) |
| B6;129S6-Gt(ROSA)26Sor$^{tm14(CAG-tdTomato)Hze}$/J (Ai14)/ C57BL/6J | Dr. Mark Anderson, University of California San Francisco Medical Center | (Madisen *et al.*, 2010) |
| B6.SJL-*Ptprc$^{a}$ Pepc$^{b}$*/BoyJ (CD45.1)/ C57BL/6J congenic strain | The Jackson Laboratory | 006785 |

| | | |
|---|---|---|
| B6.129S7-*Rag1*$^{tm1Mom}$/J (RAG$^{-/-}$)/ C57BL/6J | The Jackson Laboratory | 002014 |

***Flow cytometric analysis***

T cells from thymi, lymph nodes, and spleens were obtained by mashing the organ through a 70 μm cell strainer (Fisher Scientific International, Inc, 22-363-548) and suspended in FACS buffer (PBS containing 2% fetal bovine serum and 0.05% sodium azide) for further processing as outlined below.

For T cell analysis, cells were incubated with conjugated monoclonal antibodies against mouse CD4 (Tonbo), CD8 alpha (Tonbo), CD3 epsilon (BioLegend), CD44 (Tonbo), CD62L (BD Biosciences), CD69 (BD Biosciences), TCR beta (Tonbo), CD24 (BD Biosciences), CD25 (Tonbo), CD5 (BioLegend), TCR V alpha 2 (BioLegend), TCR V beta 5.1 (BioLegend), and/or TCR V beta 6 (BD Biosciences). For intracellular staining, cells were processed and stained for extracellular markers as described prior to fixation/permeabilization overnight using the Foxp3 transcription factor staining buffer kit (Tonbo) according to the manufacturer's protocol. Cells were then incubated with conjugated monoclonal antibody against Foxp3 (Tonbo).

For TEC analysis, thymi were dissected and digested in 1 mg/ml collagenase/dispase (Roche, Basel, Switzerland) and passed through a 100 μm mesh to remove debris. Monoclonal antibodies against mouse CD45.2 (Tonbo), EpCam (BioLegend), Ly51 (eBioscience), CD80 (BD Biosciences), $K^b$ (BD Biosciences), CLIP-bound-I-$A^b$ (clone 15G4, Santa Cruz), IgG1 (eBioscience) and I-A/I-E (eBioscience), and the UEA1 lectin (Vector Labs) were used in the TEC analysis. For intracellular staining, cells were processed and stained for extracellular markers as described prior to

fixation/permeabilization overnight using the Foxp3 transcription factor staining buffer kit (Tonbo) according to the manufacturer's protocol. Cells were then incubated with conjugated monoclonal antibody against Ki67 (Biolegend).

Flow cytometric analyses were performed using a Canto II or 4 laser Fortessa (BD Biosciences) flow cytometer. The acquired data were analyzed using FlowJo software (Version 10.0.7, Treestar, Palo Alto, CA).

***Fluorescence activated cell sorting***

Cells were stained as described for flow cytometry. ~1.1 x $10^5$ TCR$\beta^{hi}$, $CD4^+CD8^-$ thymocytes were sorted into cold HEPES buffer (PBS with 2% FBS and 0.025 M HEPES) and immediately used for genomic DNA (gDNA) isolation. Sorting was performed using a FACS Aria III (BD Biosciences) flow cytometer.

***Immunofluorescence and histology***

For cryosectioning, thymi were snap-frozen on dry ice and stored at −80°C. Tissues were sectioned at 8 µm thickness and fixed in ice-cold acetone for 2 min. Tissues were rinsed with PBS, blocked with 10% donkey serum in PBS for 30 min at room temperature, then incubated with the primary antibody anti-Keratin 5 (abcam) or biotin-labeled UEA-1 lectin (Vector Labs) overnight at 4°C. Secondary detection was performed with goat anti-rabbit IgG (Jackson ImmunoResearch) and Streptavidin-Cy3 (Vector Labs). Sections were examined by fluorescent microscopy using a Zeiss LSM 710 confocal microscope.

For paraffin sectioning, tissues were collected and fixed in 10% PFA for formalin overnight. Tissues were dehydrated through an ethanol series and embedded in paraffin

wax using standard procedures. Sections (8 mm) were cut and rinsed in xylene before rehydration through a reverse ethanol series. Hematoxylin and eosin staining was performed on paraffin sections using standard procedures; sections were then imaged on a Nikon AZ 100M widefield microscope.

### *Thymus grafts*

Thymic lobes were dissected from newborn Rosa26-CreER$^{T2}$ mice and placed in ice cold PBS. Thymi were separated into single lobes and connective tissue removed. A single lobe was transplanted under the kidney capsule of each 6-week-old male C57BL/6 recipient, as described (Jain et al., 2017). Grafts were allowed to reconstitute for 3 weeks, then mice were orally gavaged with 3 mg of tamoxifen (Sigma-Aldrich) in peanut oil for three alternate days and analyzed 3 weeks after the final dose.

### *TCR sequencing and analysis*

*Sample preparation*

Genomic DNA was prepared from CD4$^{+}$CD8$^{-}$ TCRβ$^{hi}$ thymocytes sorted from 4- or 6-day-old mice using a standard Qiagen® DNA extraction kit according to the manufacturer's instructions. Library preparation and sequencing sample data were generated using the immunoSEQ® Assay (Adaptive Biotechnologies, Seattle, WA). The somatically rearranged mouse TCRβ CDR3 regions were amplified from genomic DNA using a two-step, amplification bias-controlled multiplex PCR approach. The first PCR consisted of forward and reverse amplification primers specific for every known V and J gene segment and amplified the hypervariable CDR3 of the immune receptor locus. The second PCR

added a proprietary barcode sequence and Illumina® adapter sequences. In addition, reference gene primers were included in the PCR reaction to quantify total sequenceable nucleated cells and to accurately measure the fraction of T cells in each sample. CDR3 and reference gene libraries were sequenced on an Illumina® instrument according to the manufacturer's instructions.

*Data analysis*

Raw sequence reads were demultiplexed according to Adaptive's proprietary barcode sequences. Demultiplexed reads were then further processed to remove adapter and primer sequences, and to identify and remove primer dimers, germline, and other contaminant sequences. The filtered data were clustered using both the relative frequency ratio between similar clones and a modified nearest-neighbor algorithm, to merge closely related sequences to correct for technical errors introduced through PCR and sequencing. The resulting sequences were sufficient to allow annotation of the V, D, and J genes and the N1 and N2 regions constituting each unique CDR3 and the translation of the encoded CDR3 amino acid sequence. Gene definitions were based on annotation in accordance with the IMGT database (www.imgt.org). The set of observed biological TCRβ CDR3 sequences was normalized to correct for residual multiplex PCR amplification bias and quantified against a set of synthetic TCRβ CDR3 sequence analogues. Data were analyzed using the immunoSEQ Analyzer toolset. Data were imported into GraphPad Prism 6.0 for statistical analyses and graph generation.

### *Induction and evaluation of active EAE*

Six- to eight-week-old animals were used for EAE induction, as described (Miller et al., 2010). Under isoflurane anesthesia, the animals were subcutaneously injected at two sites into the flank with 200 µl of 1 mg/ml $MOG_{35-55}$ (MEVGWYRSPFSRVVHLYRNGK) peptide (Biomatik) emulsified in Freund's complete adjuvant [2 mg/ml *Mycobacterium tuberculosis* extract H37Ra in incomplete Freund's adjuvant (BD bioscience, 263910)]. Immediately after immunization and 48 h later, all mice received 400 ng of pertussis toxin (Calbiochem, 516560) by i.p. injection. Mice were scored daily in a blinded manner according to the following scale: 0, no clinical signs; 0.5, partially limp tail; 1, paralyzed tail; 1.5, paralyzed tail and hind leg inhibition; 2, loss in coordinated movement, hind limb paresis; 2.5, one hind limb paralyzed; 3; both hind limbs paralyzed; 3.5, hind limbs paralyzed, weakness in forelimbs; 4, forelimbs paralyzed; 5, moribund.

### *TEC culture*

C9 cells (Wertheimer *et al.*, 2018) (kindly provided by Dr. M. van den Brink from Memorial Sloan Kettering Cancer Center) were cultured in Dulbecco's modified Eagle's medium (DMEM) supplemented with 10% (v/v) fetal bovine serum (FBS; HyClone Fetal Clone III), 100 units per ml penicillin, and 100 mg/ml streptomycin.

### *CRISPR-Cas9 editing of Vps34 in C9 cells*

For excision of the *Vps34* gene, we used a lentivirus harboring either lentiCRISPR v2 empty vector (Addgene, #52961) or lentiCRISPR v2 sgVps34. We amplified lentiviruses as described (Song et al., 2014). Parental C9 cells were transfected with the respective

virus to produce control sgLacZ cells and stable Vps34-deficient sgVps34 cells. gRNA sequences for Vps34 were TCTCGTAGCATGTTTCGCCA. Efficient gene deletion was confirmed by western analysis.

***Western blotting***

C9 cells were lysed in RIPA buffer (Sigma Aldrich) containing a cocktail of protease inhibitors (Roche) with brief sonication. Total proteins (50 µg) were separated on SDS-PAGE gels, transferred onto PVDF membranes, and incubated with primary antibodies. Secondary antibodies were subsequently applied and proteins were detected with ECL substrate (Clarity$^{TM}$, Bio-Rad) or using an LI-COR Odyssey Infrared Imaging System.

***Generation of bone marrow chimeras***

Recipient mice were lethally irradiated (1,000 cGy) and 6 hours later injected with ~$10^7$ bone marrow cells derived from donor mice. Mice were used for experiments at 5 to 6 weeks after injection of bone marrow cells.

***OTII x Rip-mOVA system to test negative selection***

Following reconstitution with OTII TCR$^{Tg}$ bone marrow, recipient mice (Vps34$^{f/f}$, Aire-CreER$^{T2}$ Vps34$^{f/f}$, Aire-CreER$^{T2}$ Vps34$^{f/f}$ Rip-mOVA) were treated with tamoxifen suspended in peanut oil (3 mg) by oral gavage every other day for 14 days and then analyzed.

### *Statistical analysis*

Statistical analysis was performed with GraphPad Prism 6.0 (GraphPad Software). Data are presented as mean ± S.D. N was at least two for each genotype in each experiment, as indicated in the text and/or figure legends. Comparisons between two groups were made using two-tailed student's t-test; $p < 0.05$ was considered significant.

*EAE*

EAE clinical scores and disease incidence were analyzed using ANOVA and Kaplan-Meier curves by log-rank test. Peak disease score was analyzed by two-tailed student's t-test. $p < 0.05$ was considered significant.

*TCR sequencing*

Clonality, gene usage, and overlap comparisons were analyzed by two-tailed student's t-test. CDR3 length was analyzed by Chi-squared test (Miqueu et al., 2007). $p < 0.05$ was considered significant.

# Chapter 3

# VPS34 PROMOTES MATURE B CELL HOMEOSTASIS YET RESTRICTS GERMINAL CENTER FORMATION

## 3.1 Introduction

B cell responses are critical for effectively containing pathogens through antibody and cytokine secretion and by presenting antigens to T cells (Murphy and Weaver, 2016). The class III PI3K Vps34 has been implicated in diverse cellular processes such as autophagy, endosomal sorting, phagocytosis, and micropinocytosis through association with specific protein complexes and by producing PI3P in different subcellular compartments (Backer, 2016; Bilanges *et al.*, 2019). Vps34 is necessary for the homeostasis and function of a wide array of mammalian tissues. Whole body or cell specific Vps34-deficiency results in various pathologies typically associated with altered autophagy and endocytic vesicle trafficking (Bilanges *et al.*, 2019). In T cells, loss of Vps34 results in T cell lymphopenia associated with impaired autophagy and reduced IL-7Rα expression (McLeod *et al.*, 2011; Parekh *et al.*, 2013; Willinger and Flavell, 2012). Vps34 has also been shown to be important for MHC class II antigen processing in DCs and TECs ((Parekh *et al.*, 2017; Postoak et al., 2022; Yang *et al.*, 2021); see chapter 2), which raises the possibility of Vps34 playing a role in T cell-dependent B cell responses. A recent study reports that Vps34-independent noncanonical autophagy in B cells restrains germinal center (GC) responses (Martinez-Martin *et al.*, 2017). However, the role of Vps34 in GC responses was not directly tested. Recently, inhibition of phosphatidylinositol-3-phosphate 5-kinase (PIKfyve) lipid kinase, which uses PI3P as

substrate, was shown to have selective cytotoxic activity in B-cell non-Hodgkin lymphoma compared with normal cells. Inhibition of PIKfyve caused significant lysosomal dysfunction which was critical to the mechanism of action (Gayle et al., 2017). Despite the accumulating evidence that Vps34 and its product PI3P are critical to maintaining immune cell function, the role Vps34 plays in B cell biology has remained understudied, including the organismal consequences of B cell-specific Vps34 deficiency.

In the present study, we analyzed mice with a B cell-specific loss of *Vps34* to determine its effects on the development, homeostasis, and function of B cells. Our data reveal that Vps34 promotes the homeostasis of mature B cells and that Vps34 deficiency causes defects in autophagy and mitochondrial function. We further show that mice harboring a B cell-specific deletion of Vps34 generate a humoral response with an increased GC phenotype in response to immunization with a T cell-dependent antigen.

## 3.2 Results

### B cells require Vps34 for starvation-induced autophagy

To understand the role Vps34 plays in B cell biology, we generated mice in which Vps34 is specifically ablated in the B lymphocyte lineage by crossing mice harboring floxed *Vps34* alleles to the CD19-Cre knock-in/knock-out strain (Rickert et al., 1997) – hereafter referred to as B cell$^{\Delta Vps34}$ mice (Figure 3.1A). Western blot analysis showed significantly reduced Vps34 expression in splenic B cells isolated from B cell$^{\Delta Vps34}$ mice (Figure 3.1B), confirming efficient knockdown.

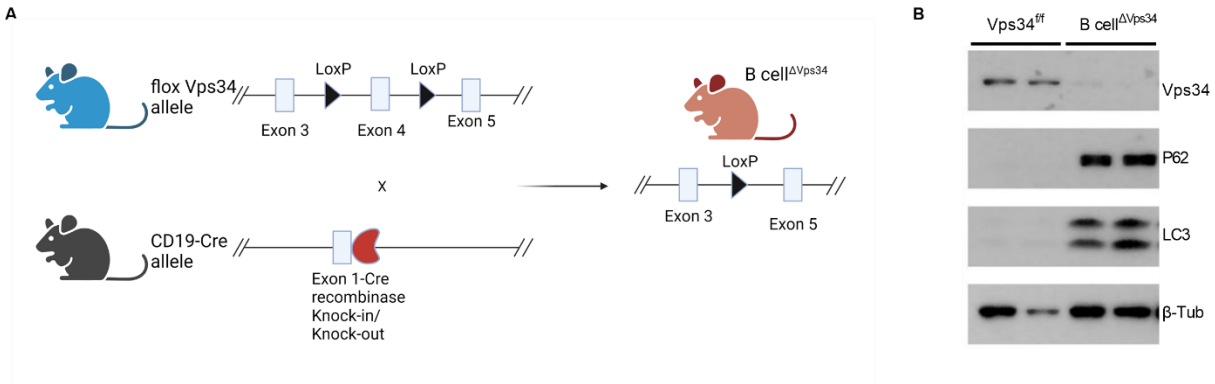


**Figure 3.1. Generation of mouse strain with B cell-specific Vps34 ablation. (A)** Vps34$^{f/f}$ mice were crossed to CD19-Cre knock-in mice to generate mice with B cell-specific loss of Vps34 (B cell$^{\Delta Vps34}$). **(B)** Expression of Vps34, LC3, and P62 by immunoblot in freshly isolated B cells from B cell$^{\Delta Vps34}$ and Vps34$^{f/f}$ mice. Data are representative of two independent experiments with n=2 per experiment.

During canonical autophagy, Vps34 is required for the nucleation of the phagophore which precedes the generation of autophagosomes containing membrane bound, lipidated LC3b-II (Galluzzi and Green, 2019). Therefore, it was unexpected to observe accumulation of the autophagy-related molecules LC3-I, LC3-II (microtubule-associated protein 1A/1B-light chain 3), and P62 (Sequestosome-1) in Vps34-deficient splenic B cells (Figure 3.1B). While this indicates that mature B cells require Vps34 to maintain normal levels of autophagy under homeostatic conditions, higher expression of P62 and LC3-I,-II can also indicate increased rates of autophagy, not a block in autophagy (Yoshii and Mizushima, 2017). In addition, Vps34-independent autophagy has been observed (Boukhalfa *et al.*, 2020; McLeod *et al.*, 2011). Interestingly, we noted an increase in cell size and granularity in Vps34-deficient B cells (Figure 3.2A), observations that have been linked to decreased autophagy (Wang and Levine, 2010). Therefore, to measure the contribution of Vps34 to B cell autophagy more directly, we utilized an autophagy reporter strain that expresses transgenic LC3 that is dually labelled with EGFP

and RFP (Li *et al.*, 2014). In this system, cytosolic and autophagosomal LC3 are labelled with EGFP and RFP. As the autophagosome matures, it fuses with the lysosome (termed autolysosome) and quenches EGFP signal. This allows for the interrogation of autophagic flux as assessed by the ratio of EGFP to RFP signal. Consistent with western blot analysis, Vps34-deficient B cells showed increased levels of LC3 at steady state as measured by RFP expression (Figure 3.2B). To measure canonical autophagy flux, autophagy was induced via starvation and the ratio of EGFP to RFP signal was assessed by flow cytometry. Indeed, in control cells isolated from starved mice there was a reduction in the ratio of EGFP to RFP compared to fed mice, indicating an increased rate of autophagosome to autolysosome formation upon starvation (Figure 3.2C). However, there was a significant reduction in autophagic flux in cells isolated from starved B cell$^{\Delta Vps34}$ mice (Figure 3.2C).

To test for a functional consequence of disrupted autophagy, we next evaluated mitochondrial function as autophagy has been linked to maintaining organelles such as mitochondria (Arbogast and Gros, 2018). We conducted extracellular flux assays on B cells stimulated for 48 hours with LPS (lipopolysaccharide), BAFF (B-cell-activating factor), and IL-4. Our results showed that B cells isolated from B cell$^{\Delta Vps34}$ mice have significantly reduced maximal and spare mitochondrial oxygen consumption rates (OCR) compared to control B cells (Figure 3.2D). Mitochondria-selective autophagy (termed mitophagy) also limits the generation of reactive oxygen species (ROS) (Metur and Klionsky, 2021), therefore we measured mitochondrial ROS in freshly isolated B cells using mitoSOX dye. Our data indicated increased mitochondrial ROS in Vps34-deficient B cells (Figure 3.2E).

In sum, while LC3 lipidation can occur in the absence of Vps34 in B cells, Vps34 is required for normal levels of autophagy under homeostatic conditions and in response to starvation. Furthermore, Vps34 promotes mitochondrial function in activated B cells and restrains accumulation of mitochondrial ROS in naïve B cells. Our data support a link between Vps34-mediated autophagy and mitochondrial homeostasis.

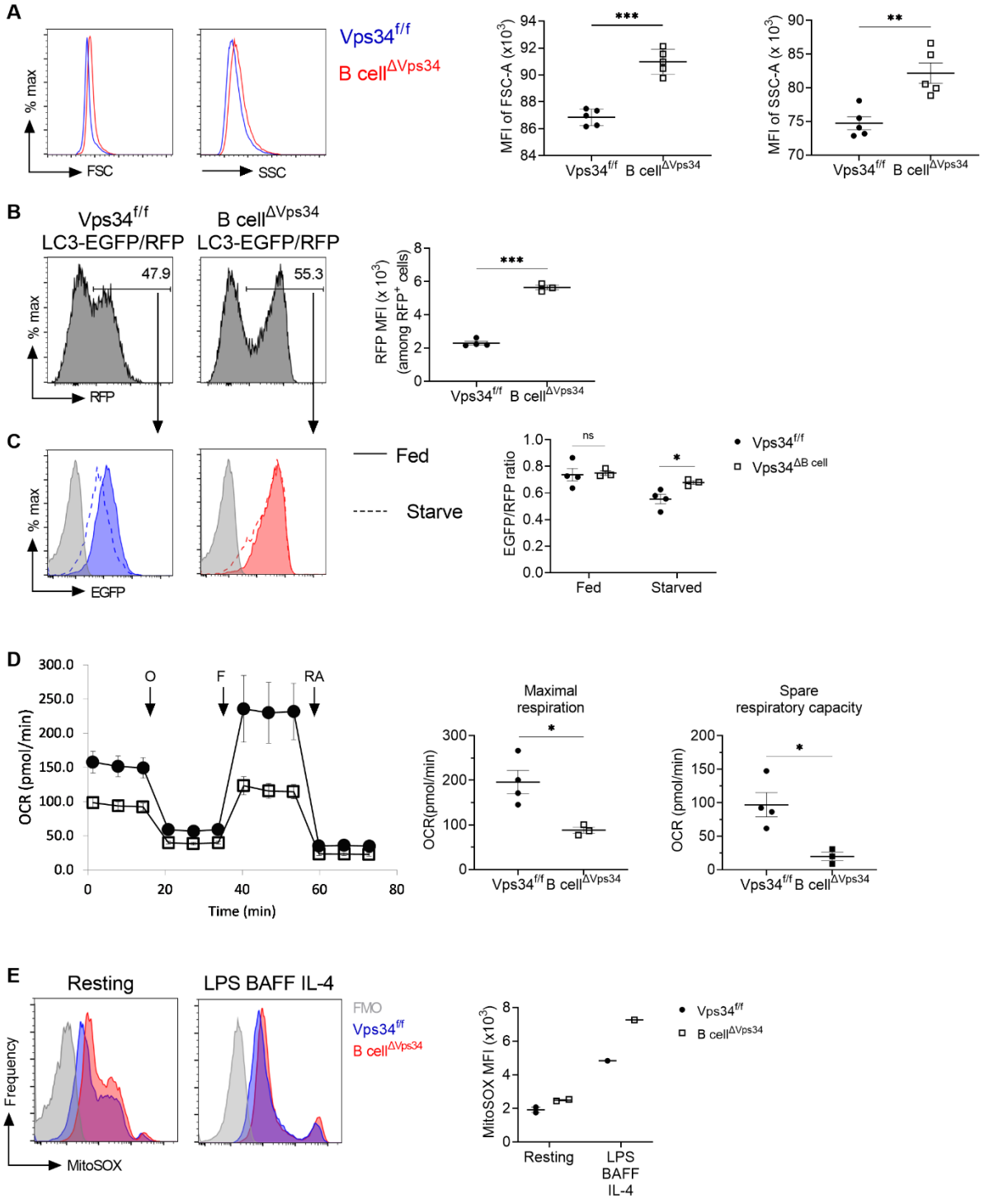


**Figure 3.2. B cells require Vps34 for starvation-induced autophagy and to maintain mitochondrial quality. (A)** Splenic B cells (B220$^{+}$CD93$^{-}$) isolated from Vps34$^{f/f}$ and B cell$^{\Delta Vps34}$ mice were analyzed for size by forward scatter (FSC) and granularity by side scatter (SSC). Graphs represent the mean fluorescent intensity (MFI) of both

measurements. **(B-C)** Splenic B cells isolated from LC3-EGFP/RFP Vps34$^{f/f}$ and LC3-EGFP/RFP B cell$^{\Delta Vps34}$ mice were analyzed by flow cytometry for reporter expression. **(B)** RFP expression. The graph represents MFI of RFP among RFP$^{+}$ cells. **(C)** EGFP expression in cells isolated from fed (solid, filled histogram) or starved (dotted, empty histogram) mice. The graph represents the ratio of EGFP to RFP MFI among RFP$^{+}$ cells. Data are representative of at least two independent experiments. **(D)** Mitochondrial stress test of B cells isolated from Vps34$^{f/f}$ and B cell$^{\Delta Vps34}$ mice activated for 2 d with BAFF, IL-4, and LPS. Maximal respiration and spare respiratory capacity calculated by Seahorse report generator (right). Data represent two independent experiments. **(E)** Mitochondrial ROS levels in freshly isolated splenic B cells (B220$^{+}$) from Vps34$^{f/f}$ and B cell$^{\Delta Vps34}$ mice measured by MitoSOX staining. The graph represents MitoSOX staining MFI. Each data point represents a biological replicate in all graphs. *p < 0.05, **p < 0.01, ***p < 0.001; ns, not significant.

### B cell development in B cell$^{\Delta Vps34}$ mice

Given the role that Vps34 plays in the development of αβ T and invariant natural killer T (iNKT) cell lineages (McLeod *et al.*, 2011; Parekh *et al.*, 2013), we next assessed developing B cell populations in B cell$^{\Delta Vps34}$ mice. Flow cytometric analysis revealed normal numbers of cells at the pro-B cell, pre-B cell and immature B cell stages of development in mutant mice (Figure 3.3A). After immature B cells egress the bone marrow to finalize maturation and populate peripheral lymphoid organs, some return to the bone marrow as mature recirculating B cells, which were significantly reduced in B cell$^{\Delta Vps34}$ mice (Figure 3.3A). This indicates that B cells can develop and mature normally in the bone marrow of B cell$^{\Delta Vps34}$ mice. Although the expression of Cre from the CD19 promoter is reported to effectively delete loxP-flanked DNA in mature B cells (90–95%), it results in incomplete DNA rearrangement in pre-B cells (75-80%) (Rickert *et al.*, 1997). Therefore, it remains possible that Vps34 contributes to B cell development but is not apparent by CD19-Cre driven ablation.

To further evaluate whether Vps34 contributes to the fitness of developing B cells, we performed competitive reconstitution experiments with mixed bone marrow chimeric

mice (Figure 3.3B). Wild-type mice (CD45.2) were lethally irradiated and transplanted with a 1:1 mixture of bone marrow cells isolated from congenic wild-type mice (CD45.1) and B cell$^{\Delta Vps34}$ mice (CD45.2) or control Vps34$^{f/f}$ mice (CD45.2). Our analysis showed a significant reduction in the relative frequency of Vps34-deficient developing B cells beginning at the immature stage with the defect becoming more apparent at the mature stage and in splenic B cells (Figure 3.3C). Therefore, while CD19-Cre driven deletion of Vps34 results in normal numbers of developing B cells, Vps34 promotes the competitive fitness of immature B cells.

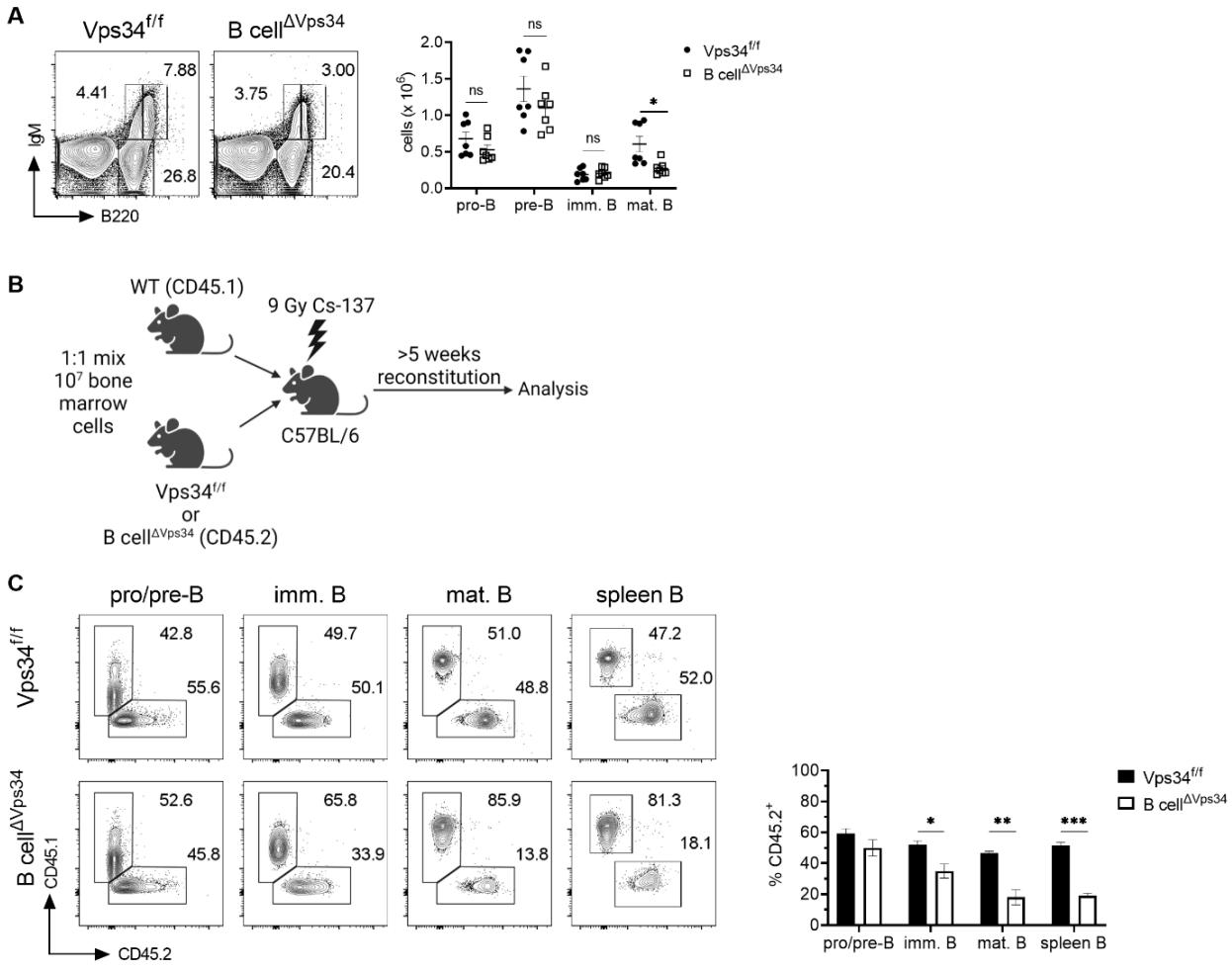


**Figure 3.3. Vps34 promotes competitive fitness of immature B cells. (A-C)** Bone marrow cells isolated from Vps34$^{f/f}$ or B cell$^{\Delta Vps34}$ mice were analyzed by flow cytometry

for developmental markers. **(A)** Flow plots representing B220 and IgM expression. Graphs represent the total number of cells at pro-B ($B220^{+}IgM^{-}CD43^{+}$) pre-B ($B220^{+}IgM^{-}CD43^{-}$), immature ($B200^{int}IgM^{+}$), and mature ($B220^{+}IgM^{hi}$) stages of development. **(B)** Schematic of competitive reconstitution experiment. Recipient wild-type CD45.2 mice (C57BL/6) were lethally irradiated and then transplanted with a 1:1 mixture of bone marrow cells isolated from wild-type (CD45.1) and B cell$^{\Delta Vps34}$ or control ($Vps34^{f/f}$) (CD45.2) mice. Transplanted mice were rested for >5 weeks and then bone marrow and spleen were harvested for flow cytometric analysis. **(C)** Representative flow plots of the relative frequencies of $CD45.1^{+}$ and $CD45.2^{+}$ B cells at indicated stages of development. The graph represents the frequency of $CD45.2^{+}$ cells among B cells at the indicated stages. Data are representative of two independent experiments. Each data point represents a biological replicate in all graphs. *$p < 0.05$, ***$p < 0.001$; ns, not significant.

### Vps34 promotes mature B cell survival and homeostatic proliferation

The reduced numbers of mature B cells isolated from the bone marrow of B cell$^{\Delta Vps34}$ mice suggests that B cells may require Vps34 for mature homeostasis. Therefore, we next assessed mature B cell populations in the periphery. B cells in the spleens of B cell$^{\Delta Vps34}$ mice were reduced in numbers and showed specific decreases in follicular B cells and marginal zone B cells (Figure 3.4A, B). Next, we determined the cellularity of B1 B cells, an innate-like subset of B cells that are enriched in the peritoneum (Baumgarth, 2017). We found significant reductions of total B cells and of B1 B cells in the peritoneal cavity of mutant mice (Figure 3.4C, D). Among B1 B cells, there was a significant reduction in the frequency of CD5 expressing B1a B cells. This is consistent with previous studies that report an essential role for autophagy in maintaining normal levels of B1a cellularity (Arnold *et al.*, 2016; Clarke *et al.*, 2018; Miller *et al.*, 2008).

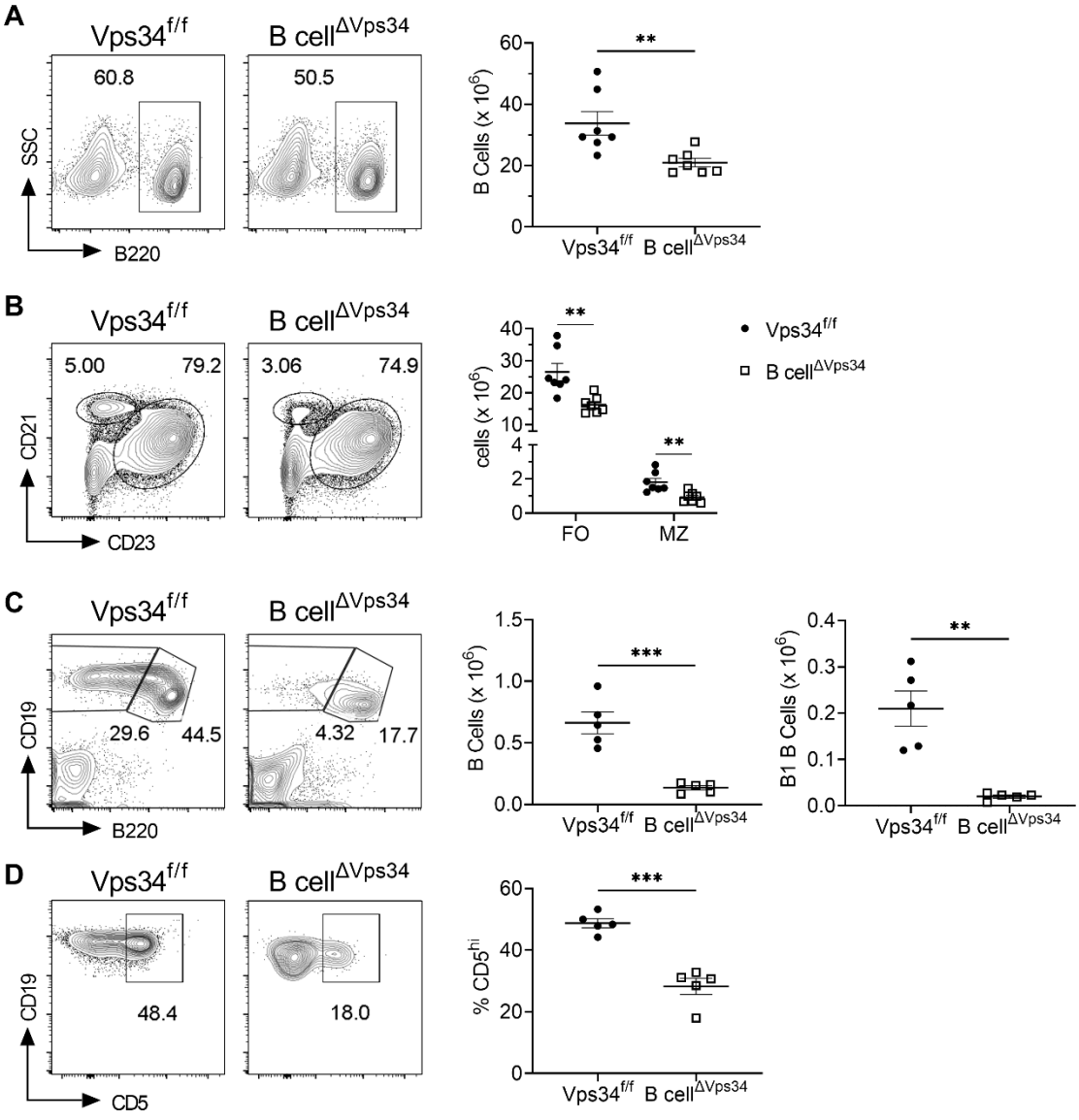


**Figure 3.4. Peripheral B cells are decreased in B cell$^{\Delta Vps34}$ mice.** Flow cytometric analysis of peripheral B cells from Vps34$^{f/f}$ and B cell$^{\Delta Vps34}$ mice. **(A)** Total number of splenic B cells (B220$^{+}$). **(B)** Total number of splenic B cell subsets including transitional 1 (T1), transitional 2 (T2), marginal zone (MZ), and follicular (FO) B cells. Representative flow plots show gate frequencies of T1 (CD21$^{lo}$IgM$^{hi}$), T2/MZ (CD21$^{hi}$IgM$^{hi}$), and FO (CD21$^{int}$IgM$^{+}$) within B220$^{+}$ gate. **(C)** Total number of peritoneal B cells (CD19$^{+}$). **(D)** Total number of peritoneal B1 B cells (CD19$^{+}$B220$^{int}$). Data are representative of two independent experiments. Each data point represents a biological replicate in all graphs. **p < 0.01, ***p < 0.001.

To further test the role Vps34 plays in mature peripheral B cells, we employed a model of CreER$^{T2}$ mediated gene deletion after adoptive transfer of B cells into B cell-deficient RAG knock out recipients. To confirm efficient Cre induction in adoptively transferred B cells, we crossed Rosa26-CreER$^{T2}$ mice to the Ai14 Cre reporter strain which contains a floxed-STOP-tdTomato cassette knocked into the *Rosa26* locus. After adoptive transfer of B cells isolated from Rosa26-CreER$^{T2}$; Ai14$^{Tg}$; Vps34$^{f/f}$ mice, RAG-deficient recipients were treated with tamoxifen by oral gavage. Splenic B cells were then isolated one week after the final dose and analyzed by flow cytometry for tdTomato expression (Figure 3.5A). High percentages of tdTomato$^{+}$ B cells were isolated from recipients that received tamoxifen but not from control mice that were administered vehicle (Figure 3.5B), confirming efficient Cre induction. We then tested the competitive homeostasis of Vps34-deficient mature B cells (CD45.2) by co-transferring with an equal ratio of B cells isolated from wild-type CD45.1 mice to RAG knockout mice (CD45.2). Recipients were analyzed three weeks after tamoxifen treatment (Figure 3.5C). Our analysis showed that the ratio of Vps34-depleted B cells (tamoxifen treated group) had dropped substantially compared to co-transferred wild-type CD45.1 B cells, whereas control cells (vehicle treated group) remained at normal ratios (Figure 3.5D).

In addition to autophagy and endocytic vesicle trafficking, there is accumulating evidence to suggest Vps34 plays a role in cell cycle control, growth, and cytokinesis (Furuya et al., 2010; Gulati *et al.*, 2008; Sagona et al., 2010; Thoresen et al., 2010). Naive B cells undergo homeostatic proliferation in response to lymphopenic environments (Cabatingan et al., 2002). To test if B cells require Vps34 for homeostatic proliferation, we stained Rosa26-CreER$^{T2}$; Vps34$^{f/f}$ B cells with CFSE immediately prior to transfer to

RAG$^{-/-}$ recipients (Figure 3.5E). Flow cytometric analyses showed that B cells recovered from tamoxifen treated recipients had undergone significantly fewer cell divisions compared to B cells isolated from vehicle treated mice (Figure 3.5F).

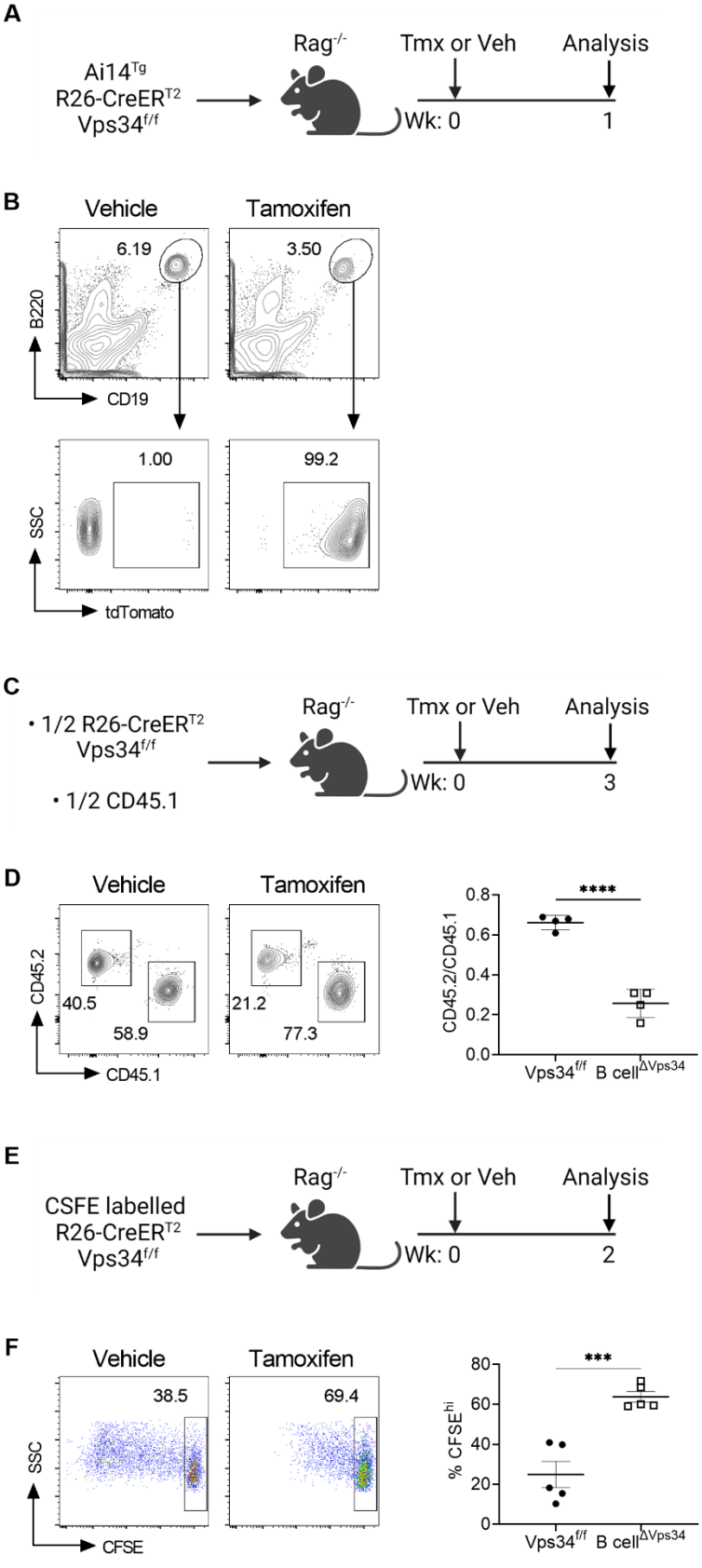
A
Ai14Tg
R26-CreERT2
Vps34f/f
Rag-/-
Tmx or Veh
Analysis
Wk: 0
1
B
Vehicle
Tamoxifen
6.19
3.50
B220
CD19
1.00
99.2
SSC
tdTomato
C
• 1/2 R26-CreERT2 Vps34f/f
• 1/2 CD45.1
Rag-/-
Tmx or Veh
Analysis
Wk: 0
3
D
Vehicle
Tamoxifen
CD45.2
40.5
58.9
21.2
77.3
CD45.1
****
CD45.2/CD45.1
0.8
0.6
0.4
0.2
0.0
Vps34f/f B cell
ΔVps34
E
CSFE labelled
R26-CreERT2
Vps34f/f
Rag-/-
Tmx or Veh
Analysis
Wk: 0
2
F
Vehicle
Tamoxifen
38.5
69.4
SSC
CFSE
***
% CFSEhi
80
60
40
20
0
Vps34f/f B cell
ΔVps34

**Figure 3.5. Vps34 promotes mature B cell survival and homeostatic proliferation.** **(A)** Schematic of tamoxifen (Tmx) induced Cre reporter activity in mature B cells adoptively transferred to Rag-deficient hosts. **(B)** Flow cytometric analysis of splenic B cells ($B220^{+}CD19^{+}$) for Cre (tdTomato) activity. **(C)** Schematic of experimental system to test competitive fitness of Vps34-deficient mature B cells (CD45.2) compared to congenically labelled wild-type (CD45.1) B cells. **(D)** Relative frequency of Vps34-deficient (CD45.2) and wild-type (CD45.1) B cells present in the spleen of hosts three weeks post Tmx treatment. **(E)** Schematic of experimental system to measure the homeostatic proliferation of carboxyfluorescein succinimidyl ester (CFSE) labelled Vps34-deficient mature B cells. **(F)** Flow cytometric analysis of splenic B cells for CFSE dilution. The graph represents the frequency of $CFSE^{hi}$ cells. Data are representative of two independent experiments. Each data point represents a biological replicate in all graphs. ***p < 0.001, ****p < 0.0001.

Peripheral homeostasis of mature B cells is maintained by continual signaling via the BCR and the receptor for BAFF (Boothby and Rickert, 2017; Smulski and Eibel, 2018). To address whether Vps34 is required to respond to cell survival signals via BAFF, we cultured B cells in LPS + BAFF and IL-4 and assayed apoptosis by Annexin V binding. Our results showed that Vps34-deficient B cells undergo significantly more apoptosis when stimulated with LPS + BAFF and IL-4 (Figure 3.6). Taken together, our findings reveal that B cells require Vps34 for mature homeostasis and homeostatic proliferation.

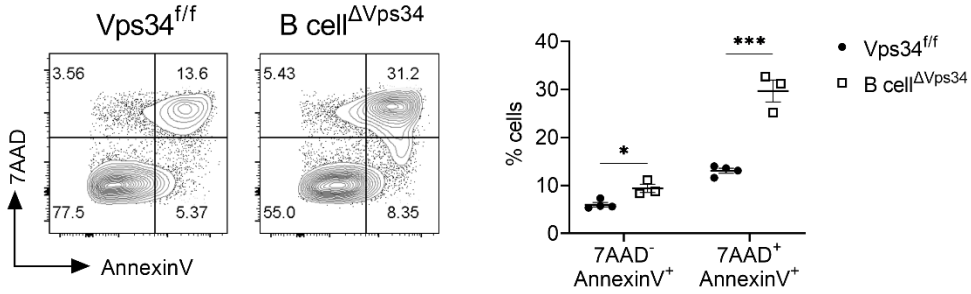


**Figure 3.6. Increased *ex vivo* apoptosis in Vps34-deficient B cells.** Purified B cells from the spleen of $Vps34^{f/f}$ and $B\ cell^{\Delta Vps34}$ mice were cultured for two days in the presence of LPS, BAFF, and IL-4. Apoptosis was assessed by AnnexinV and 7AAD binding by flow cytometry. The graph represents the frequency of cells that are early apoptosis ($AnnexinV^{+}7AAD^{-}$) and late apoptosis ($AnnexinV^{+}7AAD^{+}$). Data signify the mean ± SEM. Data are representative of at least two independent experiments where each data point represents a biological replicate. *p < 0.05, ***p < 0.001.

**B cell$^{\Delta Vps34}$ mice display enhanced germinal center formation in response to immunization with T cell-dependent antigen**

To test the contribution of Vps34 to B cell function, we immunized mice with the model T cell-dependent antigen sheep red blood cells (SRBC) and analyzed splenic B cells for GC formation and serum levels of antigen-specific antibody titers. One week post-immunization, B cell$^{\Delta Vps34}$ mice contained a significantly enhanced frequency of B cells displaying a GC phenotype (GL7$^{+}$CD95$^{+}$) among all splenic B220$^{+}$ B cells (Figure 3.7A). However, due to the defect in total peripheral B cells, the total number of GC B cells per spleen was not significantly altered (Figure 3.7A). We next assessed the antibody response to SRBC immunization by measuring serum levels of antigen-specific antibodies. We found a significant reduction in SRBC-specific IgM antibodies but no alterations in SRBC-specific IgG1 antibodies in B cell$^{\Delta Vps34}$ mice (Figure 3.7B). Overall, the data indicate that B cells require Vps34 for a normal response to T cell-dependent immunization.

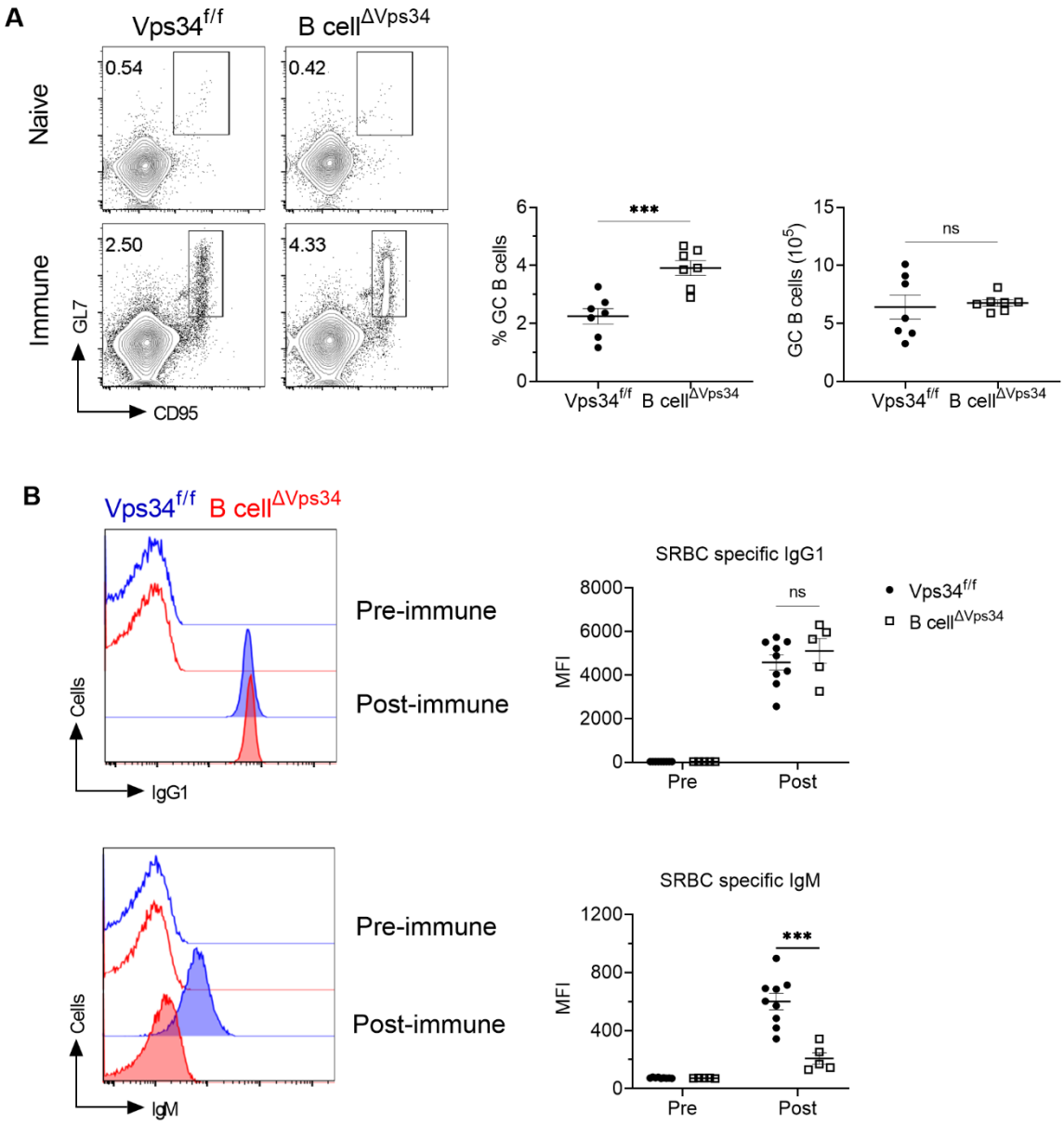


**Figure 3.7. B cell$^{\Delta Vps34\ mice}$ show enhanced germinal center formation in response to immunization with T cell-dependent antigen.** Vps34$^{f/f}$ and B cell$^{\Delta Vps34}$ mice were immunized with SRBC and analyzed 7 days later. **(A)** Splenic B cells analyzed for GL7 and CD95 expression by flow cytometry. The graphs represent frequency (left) and total number (right) of germinal center B cells (GL7$^{+}$CD95$^{+}$) in the spleens of immunized mice. **(B)** SRBC-binding IgM and IgG1 in the sera of pre-immune (open histograms) and post-immune (closed histograms) mice of the indicated genotypes; plotted MFIs as measured by flow cytometry. ***p < 0.001; ns, not significant.

**Capacity of Vps34-deficient B cells to process and present antigens to MHC class II-restricted T cells**

Previous work from our group has demonstrated a role for Vps34 in maintaining the capacity of APCs to process and present antigen to MHC II-restricted $CD4^+$ T cells (Parekh *et al.*, 2017; Yang *et al.*, 2021). Furthermore, given the alterations in the B cell response to the T cell-dependent antigen SRBC in B cell$^{\Delta Vps34}$ mice, we next sought to assess whether Vps34-deficient B cells display alterations in antigen processing and presentation. Mature B cells from B cell$^{\Delta Vps34}$ mice expressed a modest but reproducible increase in surface MHC II molecules (Figure 3.8A), a phenotype also observed in Vps34-deficient DCs (Parekh *et al.*, 2017). To investigate whether a particular endogenously derived MHC class II-bound peptide on B cells was affected by loss of Vps34, we used a monoclonal antibody (15G4) that recognizes the MHC class II molecule I-$A^b$ when occupied by the invariant chain peptide derivative CLIP (Beers *et al.*, 2005). After synthesis in the ER, MHC class II molecules contain CLIP in their peptide binding groove. In MHC class II compartments, the peptide editor DM promotes the exchange of CLIP for higher affinity peptide. However, in B cells a fraction of class II molecules is presented at the surface while containing CLIP (Denzin *et al.*, 2017). Indeed, we found that B cells from Vps34$^{f/f}$ animals express CLIP-bound I-$A^b$ molecules at levels above background staining of B cells isolated from an MHC disparate strain (I-$A^d$-expressing BALB/c), yet significantly lower levels compared to H2-DM deficient B cells (Figure 3.8A), confirming the veracity of the assay. B cells isolated from B cell$^{\Delta Vps34}$ mice expressed significantly reduced levels of CLIP-bound I-$A^b$ than wild-type controls (Figure 3.8A). These findings indicate that Vps34 is required by B cells to present normal surface levels of an

endogenous self-peptide/MHC class II complex. To further characterize the role Vps34 plays in maintaining the MHC II-immunopeptidome in naïve B cells, we stained B cells with a monoclonal antibody that reacts with the I-$A^b$ alloantigen (KH74). Although the specific peptide(s) complexed with I-$A^b$ that KH74 recognizes is unknown, the peptide specificity of the monoclonal antibody was validated by its significantly reduced reactivity to B cells isolated from DM-knockout mice (which ostensibly only express I-$A^b$ occupied by CLIP) (Figure 3.8A). Interestingly, there were no significant changes in the surface expression of MHC II molecules that react with KH74 in Vps34-deficient B cells (Figure 3.8A). Taken together the data suggest a role for Vps34 in maintaining a normal repertoire of MHC II-bound peptides in naïve B cells.

Cathepsin proteases contribute to antigen processing by generating antigenic peptides that are loaded onto MHC II molecules as well as invariant chain degradation and dissociation from MHC II (Roche and Furuta, 2015). The steady-state expression levels of cathepsins varies among APCs with B cells expressing relatively low levels (Delamarre et al., 2005). Therefore, protease activity is regulated in a lineage-specific manner to optimize epitope generation for MHC II processing. Given the alterations observed in CLIP-bound MHC II expression in Vps34-deficient B cells, we analyzed the expression of cathepsin L, a protease with relatively high expression in B cells (Delamarre *et al.*, 2005). Western blot analysis showed significantly increased levels of the mature form of cathepsin L protein in B cells isolated from B cell$^{\Delta Vps34}$ mice (Figure 3.8B). This finding suggests a role for Vps34 in maintaining normal endolysosomal protease activity in B cells with implications for MHC II epitope generation.

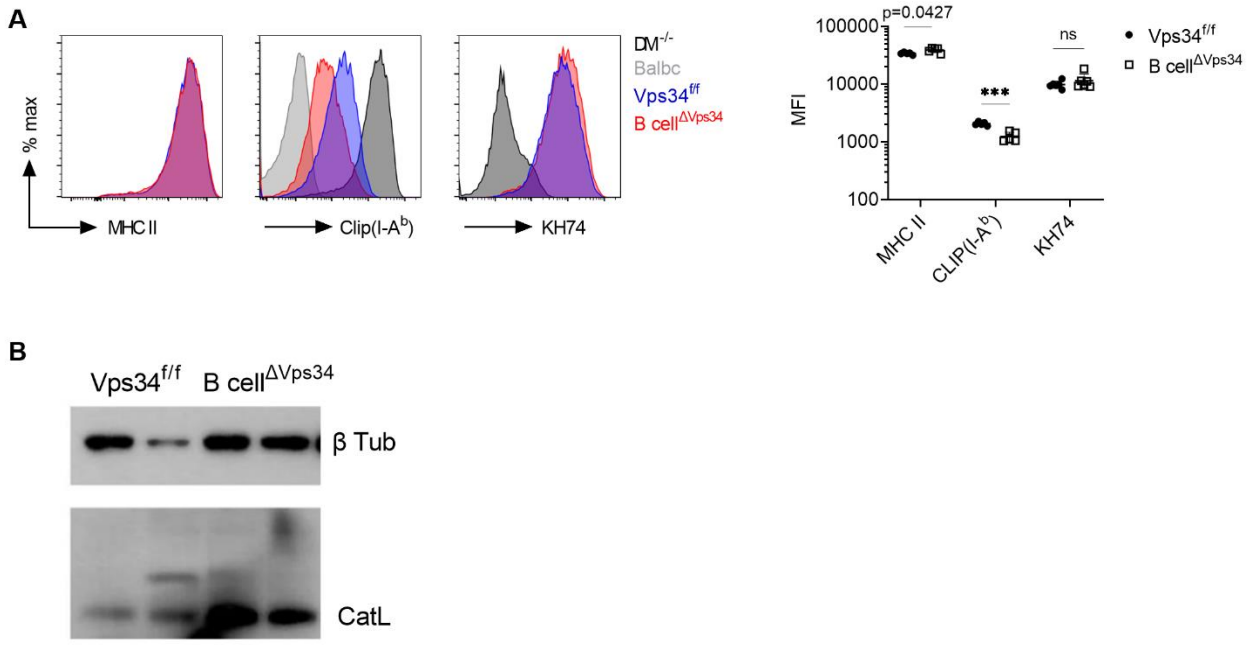


**Figure 3.8. Altered MHC class II-mediated presentation of an endogenous peptide in Vps34-deficient B cells. (A)** Splenic B cells (B220$^+$CD93$^-$) isolated from mice of the indicated genotypes were analyzed by flow cytometry for surface expression of MHC II, Clip(I-A$^b$) and the MHC class II epitope recognized by the KH74 antibody. The graph represents the MFI of each measurement. **(B)** Protein isolated from control and Vps34-deficient B cells was analyzed by western blot for cathepsin L expression. β-tubulin was used as loading control. Data are representative of at least two independent experiments. ***p < 0.001; ns, not significant.

### 3.3 Discussion

In the present study we analyzed mice with B cell-specific *Vps34* gene ablation. The cellularity of developing B cell populations was unperturbed in the bone marrow of B cell$^{\Delta Vps34}$ mice. It is plausible that CD19-Cre driven loxP recombination is inefficient in developing B cells thus obfuscating a role for Vps34 in promoting B cell development in B cell$^{\Delta Vps34}$ mice. To investigate the role Vps34 plays in B cell development more rigorously, we analyzed the competitive reconstitution of the B cell compartment in irradiated chimeras transplanted with a mixture of bone marrow derived from B cell$^{\Delta Vps34}$

mice and wild-type mice. We found a relative decrease in the frequency of immature and mature B cells derived from mutant bone marrow. Our results support a role for Vps34 in maintaining the competitive fitness of immature B cells and the reconstitution of mature B cells.

Our analysis of mature peripheral B cells revealed significant defects in the cellularity of follicular and marginal zone B cells. Furthermore, in a series of adoptive transfer experiments, we observed significant defects in the competitive survival and homeostatic proliferation of mature B cells with an acute deletion of *Vps34*. Although it is clear that B cells require Vps34 for homeostatic proliferation, further studies will be required to discern whether Vps34 promotes homeostatic proliferation by directly impacting cell cycling or Vps34 indirectly controls proliferation by improving the survival of proliferating B cells. The survival of mature B cells depends on prosurvival signals derived from BAFF signaling and tonic BCR signaling. In *in vitro* experiments, we found that BAFF stimulated Vps34-deficient B cells were significantly more susceptible to apoptosis compared to wild-type cells. Together, our results show that Vps34 is essential for B cell homeostasis.

Using mice with an autophagy reporter transgene, we confirmed that Vps34 is necessary in B cells to execute normal autophagic flux in response to starvation, a prototypical autophagy-inducing stimulus. However, we found that splenic B cells freshly isolated from mutant animals expressed significantly increased amounts of both LC3b-I and -II, indicating that LC3 conjugation can occur independently of Vps34 activity, an observation that is inconsistent with the canonical model of autophagy in which Vps34 initiates the nucleation of the autophagosome prior to an elongation step that is

hallmarked by LC3 lipidation. We also observed that Vps34-deficient B cells were increased in size under homeostatic conditions, an observation linked to defective autophagy in other cell types (Wang and Levine, 2010). Furthermore, innate-like B1 B cells were also significantly reduced in B cell$^{\Delta Vps34}$ mice, consistent with previous reports detailing an essential role for autophagy in B1 cell maintenance by analyzing mice with B cell specific loss of the canonical autophagy-essential molecules Atg5, Atg16L1, and Atg7 (Arnold *et al.*, 2016; Chen *et al.*, 2014; Clarke *et al.*, 2018; Martinez-Martin *et al.*, 2017; Miller *et al.*, 2008).

We immunized B cell$^{\Delta Vps34}$ mice to assess the functional consequences of Vps34 deficiency in B cells. We observed an increase in the frequency of B cells displaying a GC phenotype. This was a surprising result, given the survival defects of naïve and TLR agonist-stimulated Vps34-deficient B cells. The sera of immunized mice contained similar levels of antigen-specific IgG1 but reduced levels of antigen-specific IgM, providing evidence of an altered humoral response. Previous studies analyzing mice with B cell-specific loss of Atg5, Atg7 and Atg16L1 have produced conflicting results on the importance of canonical autophagy in primary humoral responses to T cell dependent antigen (Arnold *et al.*, 2016; Chen *et al.*, 2014; Conway et al., 2013; Martinez-Martin *et al.*, 2017; Pengo *et al.*, 2013). Increased GC formation in response to immunization is a phenomenon unique to Vps34 conditional loss among autophagy-related molecules so far reported. However, it should also be noted that none of the previous reports measured B cell responses to SRBCs, as we did here. Therefore, it remains possible that autophagy-related molecules uniquely restrain GC formation in response to SRBC immunization. Since Vps34 restrains the capacity of DCs to present soluble antigen via

the MHC class II pathway (Parekh *et al.*, 2017), it is plausible that altered antigen presentation may contribute to the enhanced GC formation observed in B cell$^{\Delta Vps34}$ mice. Vps34-deficient naïve B cells exhibited a modest increase in surface levels of MHC class II, but significantly lower expression of MHC class II molecules containing the invariant chain derivative CLIP. This suggests altered antigen processing under homeostatic conditions. It is unclear however, how exactly Vps34-mediated cell processes contribute to MHC II antigen presentation. Possible mechanisms include modulating delivery of antigen to MHC class II containing compartments, altering protease activity responsible for generating MHC class II epitopes, or contributing to invariant chain degradation. We did not observe changes in the surface levels of MHC class II molecules occupied by $H2^b$ alloantigen, raising the possibility that there may not be widespread changes in the immunopeptidome of Vps34-deficient B cells but that changes are specific to CLIP. Previous reports have identified vesicle trafficking dependent upon Vps34 catalytic activity as necessary for the endosomal processing of the protease cathepsin D into its active mature form (Jaber *et al.*, 2016; Reifler *et al.*, 2014; Ronan *et al.*, 2014; Row *et al.*, 2001). Our analysis revealed a significant increase in steady-state levels of mature cathepsin L in Vps34-deficient B cells. Therefore, it is possible that altered protease activity contributes to the alterations in GC formation observed in B cell$^{\Delta Vps34}$ mice.

In sum, we have identified a novel role for the lipid kinase Vps34 in promoting the competitive fitness of immature B cells and the homeostasis of mature B cells. Further, we provide evidence that Vps34 modulates GC formation in response to T cell dependent immunization (Figure 3.9). This work opens exciting avenues to further understand the contribution of autophagy-related cellular processes to B cell biology.

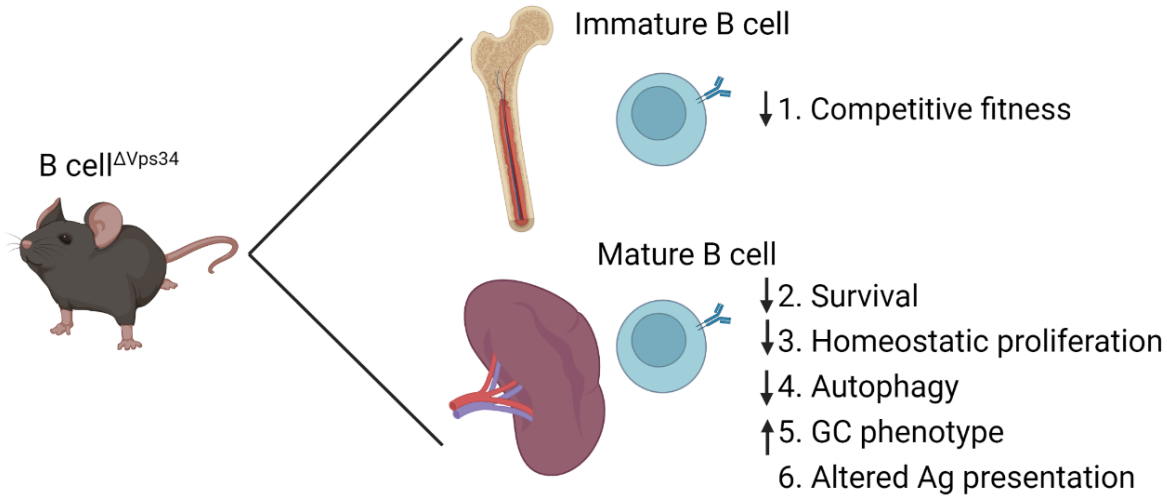


**Figure 3.9. Summary of findings related to Vps34 regulation of B cell development and function.** Vps34-deficiency in B cells causes **(1)** Reduced competitive fitness of immature B cells in the bone marrow, **(2)** Attenuated survival of mature peripheral B cells, **(3)** Reduced homeostatic proliferation, **(4)** Defective autophagy flux, **(5)** Enhanced germinal center formation in response to T cell-dependent immunization associated with **(6)** Altered antigen processing and protease expression. This figure was made with BioRender.com.

## 3.4 Materials and methods

### *Mice*

B cell-specific deletion of *Vps34* was achieved by crossing Vps34$^{f/f}$ mice with CD19-Cre mice (Rickert *et al.*, 1997). Tamoxifen inducible deletion of *Vps34* was achieved by crossing Vps34$^{f/f}$ mice with Rosa26-CreER$^{T2}$ mice. Cre$^{-}$ littermates were used as controls in all experiments except experiments using Rosa26-CreER$^{T2}$ to target Vps34 deletion, in which a control group was administered vehicle (as outlined below). Six- to 10-week-old animals of both sexes were used in this study. All breeder and experimental mice were housed under specific pathogen-free conditions in compliance with guidelines from the Institutional Animal Care and Use Committee at Vanderbilt University.

### *Flow cytometric analysis*

Single cell suspensions from blood, spleen, lymph nodes or bone marrow were treated with lysis buffer (BD Bioscience) to remove red blood cells before staining. Fc receptors were blocked using an anti-CD16/32 antibody (eBiosciences). Cells were stained for 20 minutes at 4°C using the appropriate combination of antibodies suspended in cold FACS buffer (PBS, 1%FBS, 0.05% sodium azide). For analysis of B cell development, bone marrow cells were stained with anti- B220, -IgM, -CD43, -IgD, and -CD23. For analysis of competitive reconstitution, bone marrow cells were stained with anti-B220, -IgM, -CD45.1, and -CD45.2. For analysis of splenic B cell populations, splenocytes were stained with anti-B220, -CD93, -CD23, and -CD21. For analysis of peritoneal B cell populations, cells isolated by peritoneal wash were stained with anti-CD19, -B220, and -CD5. Analysis of B cell MHC II was performed on splenocytes stained with anti-CD93, -B220, -MHC II (clone

M5/114.15.2), or -CLIP-bound-I-$A^b$ (clone 15G4, Santa Cruz Biotechnology), or with KH74. For analysis of germinal center B cells, splenocytes were stained with anti-B220, -IgD, -CD95, and -GL7. Apoptosis assays were performed using Annexin V apoptosis detection kit (BD Biosciences). Unless otherwise specified, all mAbs were from BD Pharmingen, Life Technologies, eBioscience, or Tonbo Biosciences.

Flow cytometric analyses were performed using a Canto II or 4 laser Fortessa (BD Biosciences) flow cytometer. The acquired data were analyzed using FlowJo software (Version 10.0.7, Treestar, Palo Alto, CA).

***In vitro B cell culture***

B cells from the spleen were enriched using MACS B cell isolation kit (Miltenyi Biotec). Cells were cultured in RPMI supplemented with 10% FBS (MilliporeSigma), 1x penicillin-streptomycin, 1x MEM Nonessential Amino Acids (Corning), 1 mM sodium pyruvate, 2 mM GlutaMax, and 55 mM 2-ME (Thermo Fisher Scientific). The following concentrations were used for cell stimulation: 5 µg/mL LPS, 10 ng/mL rBAFF, 20 ng/mL rIL-4. Cells were seeded in 6-well plates at $2.5x10^6$ cells/mL in a total volume of 2 mL culture media.

***Western blotting***

B cells isolated from spleens were lysed in RIPA buffer (Sigma Aldrich) containing a cocktail of protease inhibitors (Roche) with brief sonication. Total proteins (50 µg) were separated on SDS-PAGE gels, transferred onto PVDF membranes, and incubated with primary antibodies. Secondary antibodies were subsequently applied, and proteins were

detected with ECL substrate (Clarity$^{TM}$, Bio-Rad) or using an LI-COR Odyssey Infrared Imaging System.

***Generation of bone marrow chimeras***

Recipient mice were lethally irradiated (1,000 cGy) and 8 hours later injected with ~$10^7$ bone marrow cells derived from donor mice as described in Figure 3.3B. Irradiated recipients were subsequently maintained on a sterile diet. Mice were used for experiments at 5 to 6 weeks after injection of bone marrow cells.

***Seahorse assays***

Mitochondrial respiration of Vps34-deficient B cells was determined with Extracellular Flux Analyzer XFe96 (Seahorse Bioscience). Resting splenic B cells were isolated with a B cell isolation kit according to the manufacturer's protocol (catalog number:130-090-862, Miltenyi Biotec), and stimulated at 5x$10^6$ cells/mL in 2 mL on 6-well plates for two days with BAFF (10 ng/mL), IL-4 (20 ng/ml), and LPS (5 µg/mL). Activated B cells were plated (250,000 cells/well) in a Cell-Tak (25 µL at 5 µg/mL; Corning) coated XF-96 cell culture microplates (Seahorse Bioscience). The plate was then incubated in a NON-$CO_2$ 37 °C incubator for 1 hour to finish coating. The mitochondrial stress assay was performed in XF DMEM assay medium supplemented with 10 mM glucose, 1 mM sodium pyruvate (Fisher Scientific International, Inc, 11360070), and 2 mM glutamine (pH 7.4). During OCR (oxygen consumption rate) analysis, cells were treated with oligomycin (10 µM), carbonyl cyanide-4-(trifluoromethoxy) phenylhydrazone (FCCP; 10 µM; Sigma-Aldrich Corporation, C2920-10 MG) and rotenone and antimycin (both 5 µM; Sigma-Aldrich

Corporation, R8875, and A8674). The maximal OCR is attained by stimulating the respiratory chain with uncoupler FCCP. Spare respiratory capacity is calculated by subtracting average basal OCR from the corresponding average maximal OCR. Analyses were completed by the manufacturer's recommended program and the data files were plotted with Prism.

***Detection of mitochondrial reactive oxygen species***

For flow analyses of mitochondrial ROS, $1x10^6$ splenocytes were washed in PBS and stained with MitoSOX (5 μM; Invitrogen) in PBS for 20 min at 37˚C, then washed three times (1% BSA in PBS) and further stained with anti-B220 antibodies.

***Immunization***

After collection of pre-immune sera, mice were immunized with SRBCs ($2×10^8$ cells per mouse; Thermo Fisher Scientific, Waltham MA) and analyzed 1 week after immunization. Analysis of antigen-specific antibody production in the sera of immunized mice was performed according to the method described (McAllister et al., 2017).

***Adoptive transfer of mature B cells***

B cells isolated from the spleen of donor mice were enriched using MACS B cell isolation kit (Miltenyi Biotec). Donor cells ($5\text{-}10x10^6$) were injected intravenously into $RAG1^{-/-}$ recipients. In homeostatic proliferation experiments, donor cells were stained for 10 minutes at room temperature with CFSE (5 μM in PBS) (Thermofisher) prior to injection. Recipients were treated with Tamoxifen (3 mg) suspended in corn oil or vehicle by oral

gavage the same day as the adoptive transfer and two subsequent times with a single day in between each treatment. After the indicated amount of time (individual experimental schema represented in Figure 3.5) spleens from recipient mice were collected for analysis.

***Statistical analysis***

Statistical analysis was performed with GraphPad Prism 6.0 (GraphPad Software). Data are presented as mean ± S.D. N was at least two for each genotype in each experiment, as indicated in the text and/or figure legends. Comparisons between two groups were made using two-tailed student's t-test; $p < 0.05$ was considered significant.

# Chapter 4

# SUMMARY AND CONCLUSIONS

## 4.1 Synopsis of findings

This dissertation examines how cell processes mediated by the autophagy-related molecule Vps34 contribute to the homeostasis and function of two distinct professional APCs, namely TECs and B cells. In Chapter 2, we examine mice with TEC-specific loss of Vps34 to further characterize the unique molecular machinery employed by cTECs to produce peptide/MHC II molecules that are optimized for the generation of a broad and appropriately populated T cell compartment. We found that Vps34 promotes the homeostasis of TECs and is required to maintain normal levels of T cell lymphopoiesis beyond the neonatal stage of development. Before extensive thymic hypotrophy occurred in mutant mice, we found significant defects in the positive selection of $CD4^+$ but not $CD8^+$ T cells. We utilized TCR transgenic animals and TCR sequencing to show that Vps34 is necessary for the selection of specific TCR clones. These results highlight the requirement of TEC-specific Vps34 for controlling T cell commitment to the helper lineage. These findings were not recapitulated in mice with a TEC-specific loss of Atg5, suggesting that endocytosis and/or vesicle trafficking were responsible for the phenotypes observed in $Vps34^{\Delta TEC}$ mice. Alternatively, it is also possible that a combination of Vps34-mediated endocytosis, vesicle trafficking, and autophagy in TECs are necessary for positive selection of $CD4^+$ T cells. Analyzing mice with mTEC-specific ablation of Vps34 revealed no significant alterations in negative selection or tTreg induction in the polyclonal repertoire or a TCR clone specific to a model neoantigen transgenically expressed in the

thymus. Therefore, our data support the hypothesis that Vps34 activity in TECs is more important for positive selection than negative selection.

In chapter 3, we generated and characterized a novel mouse strain with a B cell-specific ablation of Vps34. Using mixed bone marrow chimeras, we provide evidence for Vps34 in promoting the competitive fitness of immature B cells. We further show that Vps34 is necessary for the homeostasis of mature B cells and their capacity to perform autophagy in response to starvation. Finally, we report that Vps34 in B cells restrains a GC phenotype in response to immunization with a T cell-dependent antigen and is associated with an altered antigen-specific antibody response.

A commonality between the two studies is the finding that Vps34 is necessary for maintaining normal levels of MHC II occupied by CLIP but does not significantly alter total surface expression levels of MHC II. We also found that Vps34 was required for normal expression of mature cathepsin L under homeostatic conditions. These findings provide evidence that dysregulated protease activity in Vps34-deficient APCs contributes to the alterations in MHC class II antigen presentation observed in the two research chapters reported here. These findings are summarized in Figure 4.1.

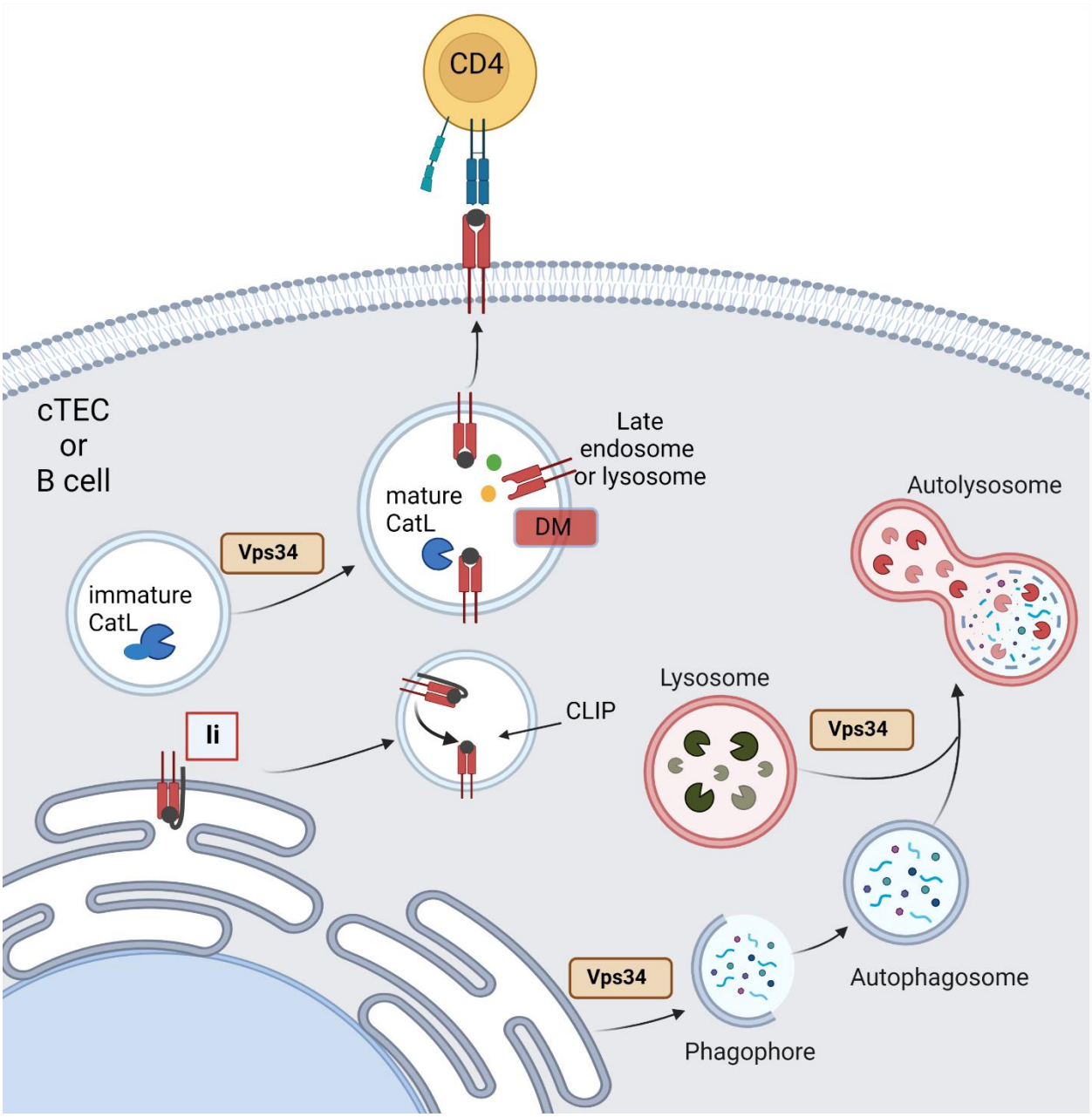


**Figure 4.1. Graphical summary of dissertation results.** In chapters 2 and 3 we found that Vps34 promotes homeostasis of mature TECs and B cells. Vps34 is critical for autophagic flux in these cells. We also found that Vps34 is necessary for the presentation of peptides that facilitate positive selection of $CD4^+$ T cells. In both cell types, we found that the absence of Vps34 causes alterations in the MHC class II ligandome and is associated with altered levels of mature cathepsin L (catL). This figure was made with BioRender.com.

### 4.2 Implications, limitations, and future directions

Traditionally, MHC II molecules present peptides from exogenous and membrane-bound sources, but they also can present peptide from intracellular sources. Indeed, approximately 10–30% of the peptides that are eluted from MHC class II are derived from cytosolic or nuclear proteins (Adamopoulou et al., 2013; Chicz et al., 1993; Dongre et al., 2001). However, the underlying processes for the intracellular route of MHC class II presentation are less clear.

Soon after the molecular elucidation of the autophagic pathway in the 1990's, it became apparent that autophagy impinges on cellular processes that also contribute to antigen presentation. Early work showed that starvation, a strong autophagy-inducing stimulus, altered the immunopeptidome in B cells and promoted the MHC class II presentation of peptides from intracellular and lysosomal source proteins (Dengjel et al., 2005). Around this time, observational studies reported that autophagosomes constantly fuse with MHC class II compartment (MIIC) vesicles in a variety of APCs and that targeting of antigens for autophagic degradation can enhance $CD4^+$ T cell recognition (Kasai *et al.*, 2009; Schmid *et al.*, 2007). Mechanistically, the prevailing thought began to emerge that protein cargo targeted to autophagosomes are then delivered to MIICs allowing for the presentation by MHC class II to $CD4^+$ T cells (Crotzer and Blum, 2010). Following the generation of mice with knockout or transgenic floxed alleles of autophagy-essential genes, significant efforts were made to define the contribution of autophagy to *in vivo* immune responses.

**TECs**

In 2004, Yoshinori Ohsumi's group generated a transgenic autophagy reporter mouse strain allowing for *in vivo* monitoring of autophagy in mammalian tissues. Ohsumi's group reported that a limited number of tissues were constitutively active in autophagy, including TECs (Mizushima *et al.*, 2004), a finding that was subsequently confirmed by our group in Chapter 2 and by others (Nedjic *et al.*, 2008; Rodrigues et al., 2022; Schuster *et al.*, 2015). Of note, Mizushima et al. also reported that the cortex of the thymus was most active among TECs and that autophagy in the thymus was higher in neonates compared to adults. The observation that TECs are constitutively highly active in autophagy suggested that this process may play an important role in TEC function. In 2008, Ludger Klein's group reported the first *in vivo* role for an autophagy-related gene, *Atg5,* in thymus function (Nedjic *et al.*, 2008). Since germline mutations in Atg5 are perinatal lethal in mice (Kuma et al., 2004), Nedjic et al. utilized a thymus transplant model in which thymic stromal tissues isolated from $Atg5^{-/-}$ embryos were transplanted under the renal capsule of host mice. In this model, the host hematopoietic system reconstitutes the ectopic thymus allowing for the interrogation of T cell development and selection. Two main findings were made in this landmark study: (1) While there were no overt changes in the selection of a polyclonal repertoire in $Atg5^{-/-}$ grafts, Atg5 deficiency had a significant effect on individual MHC class II-restricted but not class I-restricted TCR specificities. Depending on the model TCR examined, autophagy had a positive, neutral, or deleterious effect on the selection of MHC class II-restricted TCR transgenic thymocytes. (2) Transplantation of Atg5-deficient grafts into nude mice (that have severely compromised thymic function) resulted in severe colitis and multi-organ inflammation.

The work presented in Chapter 2 contributes to our further understanding of the role that autophagy and related cellular processes play in TEC function. While the effect TEC-Atg5 had on positive selection of certain MHC class II-restricted transgenic TCRs was varied and relatively mild, we observed a near complete block in the positive selection of each of the four MHC class II-restricted transgenic TCRs crossed to $Vps34^{TEC}$ mice. Our data also show that TECs do not require Atg5 for selection of OT-II thymocytes, providing more evidence that Vps34 plays a more dominant role than Atg5 in promoting positive selection by TECs. Furthermore, no alterations in the TCR Vβ usage were observed in the repertoire of $CD4^+$ T cells selected on $Atg5^{-/-}$ thymic stromal cells. However, our analysis of the TCR repertoire using bulk sequencing revealed that, while the diversity of the $CD4^+$ TCR repertoire was maintained in $Vps34^{TEC}$ mice, there was a significant change in clonal overlap and CDR3 length, observations consistent with selection on a limited TEC immunopeptidome (Pacholczyk *et al.*, 2006; Wong *et al.*, 2007). The differences observed between Vps34 and Atg5 mutants highlight the phenotypic differences that can be observed by genetic suppression of separate autophagy-related molecules, a phenomenon that is becoming increasingly appreciated (Galluzzi and Green, 2019). Indeed, a recent study analyzed T cell selection in thymic grafts deficient in lysosomal associated membrane protein 2 (Lamp2) (Rodrigues *et al.*, 2022), a lysosomal protein that has been implicated in chaperone-mediated autophagy, macroautophagy and lysosomal function (Kaushik and Cuervo, 2018; Sudhakar et al., 2020). Lamp2 was shown to be necessary for cTEC autophagy, normal cathepsin L activity, and CD4 but not CD8 T cell selection. Considering the similarities of this phenotype with the defects reported in chapter 2 with $Vps34^{TEC}$ mice, it is tempting to

speculate that Lamp2 and Vps34 modulate TEC cell function by similar mechanisms. Using a cTEC derived cell line, we provide evidence that Vps34-mediated vesicle trafficking was necessary for maintaining normal levels of cathepsin L. In future studies, it will be important to extend these findings to primary cTECs. Furthermore, we assayed total cell lysates for cathepsin L expression. We presume most cathepsin L is localized to the endo/lysosome in mutant cells where it could participate in antigen processing, but it remains possible that Vps34 is required to maintain lysosomal integrity and to keep proteases from leaking into the cytosol. Also, while we observed decreases in expression of mature cathepsin L, we provided no evidence that it altered cathepsin L activity. Follow up studies using cathepsin L activity probes *in vivo* or *ex vivo* should provide further clarity on how and the extent to which Vps34-deficiency alters cathepsin L activity in cTECs.

The question of whether autophagy in TECs modulates the generation of a T cell repertoire more prone to autoimmunity or autoinflammation has produced conflicting answers. While Nedjic et al. observed severe intestinal inflammation in their thymus transplant model, others reported that epithelial cell-specific (including TECs) deletion of Atg5 or Atg7 resulted in no apparent disease (Sukseree et al., 2012; Sukseree et al., 2013). Furthermore, genetic knockdown of the autoimmunity-associated gene C-type lectin domain containing 16A (Clec16a) in the nonobese diabetic model for type 1 diabetes resulted in protection from autoimmunity, which was attributed to T cell hyporeactivity resulting from altered selection on autophagy-impaired TECs (Schuster *et al.*, 2015). While we did not observe development of spontaneous pathology in $Vps34^{TEC}$ mice, it is possible that a diseased state may arise as the mice age. We also tested $Vps34^{TEC}$ mice for their capacity to mount a response to a CNS-derived autoantigen in an

animal model of multiple sclerosis. Vps34$^{TEC}$ mice exhibited a delayed and reduced disease course. Therefore, it is possible that Vps34-mediated antigen processing is required for the generation of self-peptide/MHC II complexes specialized to promote reactivity of CD4$^{+}$ T cells. However, since Vps34$^{TEC}$ mice display significant T cell lymphopenia, we cannot exclude the possibility that Vps34$^{TEC}$ mice were protected from disease simply because there was a smaller pool of total T cells in the periphery for encephalitogenic T cells to emerge from. Also, the reactivity of T cells in Vps34$^{TEC}$ mice may be altered by a history of increased homeostatic proliferation. And finally, homeostatic proliferation in Vps34$^{TEC}$ mice may skew the peripheral TCR repertoire to enhanced self-reactivity (Moses et al., 2003). Future studies will be required to more carefully examine whether Vps34 in TECs directly influences the reactivity of mature T cells. One potential approach would be to utilize a system similar to Nedjic et al., by transplanting Vps34-deficient thymic stroma (depleted of hematopoietic cells) onto the renal capsule of syngeneic nude mice and monitor for disease development. This approach may not reveal differences in T cell hyporeactivity, however. A definitive approach would be to leverage the Vps34$^{TEC}$ Foxp3-RFP reporter mice generated in chapter 2. Intrinsic differences in T cell reactivity could be revealed by adoptive transfer of Foxp3-RFP$^{-}$CD25$^{-}$CD4$^{+}$ sorted mature thymocytes isolated from Vps34$^{TEC}$ mice or littermates to RAG-deficient hosts and monitor for weight loss and colitis. This would be illuminative not only for the case of Vps34-dependent antigen processing in the thymus specifically, but the broader question of what role the peptides thymocytes are selected on play in controlling their function when they emerge in the periphery. Accumulating evidence suggests that the MHC class I immunopeptidome and TCR affinity in the thymus

influence mature $CD8^+$ T cell function (Fulton et al., 2015; Mandl et al., 2013; Nitta et al., 2010; Takada *et al.*, 2015). However, there is less evidence to-date for a similar scenario involving $CD4^+$ T cells (Persaud et al., 2014; Takahama et al., 2019). $Vps34^{TEC}$ mice offer a system to address this outstanding question in the field.

**B cells**

Vps34 is necessary for the homeostasis and function of a wide array of mammalian tissues (Bilanges *et al.*, 2019). Despite the accumulating evidence that Vps34 is critical to maintaining immune cell function, the role Vps34 plays in B cell development and function has remained understudied, including the organismal consequences of B cell-specific Vps34 deficiency. In chapter 3, we begin to describe a role for Vps34 in B cell biology by generating and analyzing a conditional knock-out strain.

Using a CD19-Cre driver, we provide evidence that Vps34 promotes the competitive fitness of immature B cells. However, we did not examine a role for Vps34 in early B cell development. Additional studies utilizing a Cre-driver that is expressed early in B cell development (e.g., Mb1-Cre/CD79a-Cre) would permit us to assess whether Vps34 is required for B cells to develop normally. Alternatively, an approach that would not require generating an additional mouse strain would be to analyze B cell development in radiation bone marrow chimeras transplanted with bone marrow derived from a combination of Rosa26-$CreER^{T2}$ $Vps34^{f/f}$ mice and a B cell-deficient strain (e.g., $\mu MT^{-/-}$ or $RAG^{-/-}$). In this system, tamoxifen-induced targeted gene ablation would occur only in the B lineage. Deletion of Vps34 early in T cell development causes reduced T cell development that was attributed to defects in IL-7 receptor signaling (McLeod *et al.*,

2011). Since, B cell development is arrested at the pre-pro B cell stage in IL-7 receptor knockout mice (Kikuchi et al., 2005), it will be interesting to interrogate a role for Vps34 in IL-7 receptor signaling during B cell lymphopoiesis.

Our studies analyzing acute ablation of Vps34 in mature B cells revealed an essential role for Vps34 in maintaining mature B cell homeostasis. However, the mechanism by which Vps34 contributes to B cell homeostasis has yet to be established. B cell homeostasis depends on tonic and induced BCR signaling and receptors sensitive to trophic factors, such as BAFF-R during development and maintenance (Khan, 2009). While Vps34 is not a direct signal transducer, similar to the class II PI3Ks, it can indirectly regulate signaling through its function in regulating endosomal trafficking (Bilanges *et al.*, 2019). Therefore, *in vitro* apoptosis assays should be performed to test if Vps34 is required in B cells for BCR or BAFF-R mediated homeostasis. Since BCR and BAFF-R signaling both involve downstream NF-κB activation, Vps34-deficient B cells can be tested for NF-κB signaling after stimulation with anti-BCR antibodies and recombinant BAFF.

While previous studies analyzing the contribution of B cell-autophagy in primary humoral responses to T cell dependent immunization have produced conflicting results, it is generally thought that B cell-canonical autophagy plays a negligible role in the primary response to most antigens and a more substantial role in the memory response (Arbogast and Gros, 2018; Sandoval et al., 2018). Therefore, the increased GC formation in B cell$^{\Delta Vps34}$ mice in response to SRBC immunization was surprising as no previous study reports a role for an autophagy-related factor in restraining GC formation in response to T cell dependent immunization. However, it should also be noted that none of the previous

reports measured B cell responses to SRBCs, as we did in chapter 3. Therefore, it remains possible that autophagy-related molecules uniquely restrain GC formation in response to SRBC immunization – if this is indeed the case, this would indicate the existence of autophagy-dependent substrate in T cell dependent germinal center responses. Future studies analyzing the response of mice with a B cell-specific deletion of an essential factor for canonical autophagy (e.g., Atg5 or Atg7) to SRBC immunization will permit a direct comparison with B cell$^{\Delta Vps34}$ mice. B cell lymphopenia in B cell$^{\Delta Vps34}$ mice further confounds the interpretation of the GC response to SRBC immunization. Therefore, a genetic system in which Vps34 can be inducibly targeted in mature B cells (i.e., huCD20-CreER$^{T2}$ Vps34$^{f/f}$ mice) will improve our understanding of B cell-specific Vps34 in T cell-dependent GC responses. While immunization with model antigens is inexpensive and technically less challenging, it will be important to test the function of Vps34-deficient B cells in a clinically relevant disease model such as their response to challenge with a pathogen (e.g., influenza A virus). A recent study reports that B cell autophagy is upregulated in patients with systemic lupus erythematosus (SLE) and in the New Zealand (black×white) $F_1$ hybrid mouse (NZB/W) model of spontaneous lupus like disease (Clarke et al., 2015). Furthermore, genome-wide association studies have linked nucleotide polymorphisms in autophagy-related genes to susceptibility for SLE (Han et al., 2009; International Consortium for Systemic Lupus Erythematosus et al., 2008). Interestingly, mice with a B cell-specific deletion of Atg5 are protected from lupus-like disease in the Fas$^{lpr}$ model which was associated with defects in the survival of long-lived plasma cells. Considering that B cell$^{\Delta Vps34}$ mice have defects in survival of mature B cells yet enhanced GC formation, it will be of great interest to interrogate the role B cell-Vps34

plays in an autoimmune response characterized by autoantibody mediated pathology. The $Fas^{lpr}$ model is especially attractive since this mutation is available on the same genetic background (C57BL/6J) as B $cell^{\Delta Vps34}$ mice.

Finally, future studies should further study the role Vps34 plays in MHC class II-mediated antigen processing and presentation by B cells. Our results show that Vps34-deficient B cells display reduced surface levels of MHC II/CLIP complexes. We have inferred from this observation that the MHC II-ligandome is altered in the absence of Vps34. This hypothesis can be directly tested by mass spectrometry powered immunopeptidome analysis of peptides eluted from MHC II molecules isolated from Vps34-deficient B cells and compared to the immunopeptidome of wild-type littermates. A landmark study using immunopeptidome analysis of Human B-lymphoblastoid Awells cell lines reported an increase in intracellular and lysosomal derived peptides bound by MHC II following induction of autophagy via starvation (Dengjel *et al.*, 2005). However, starvation may induce other stress-related responses in addition to autophagy that could influence antigen presentation, therefore it will be revealing to analyze primary B cells with a genetic suppression of autophagy. In addition to MHC II/CLIP, we also analyzed surface levels of MHC II bound to the $H\text{-}2^{b}$ alloantigen. The observation that Vps34 deficiency in B cells does not alter surface expression of MHC II/$H\text{-}2^{b}$ alloantigen raises the possibility that there may be presentation of specific peptides that are influenced by Vps34, but not others. Considering cathepsin proteases contribute to invariant chain processing necessary for normal levels of surface MHC II/CLIP, along with the observation of increased levels of mature cathepsin L in Vps34-deficient B cells, it is possible that Vps34 is required by B cells for the degradation of invariant chain. It is well

established that cathepsin S plays an essential role in B cell antigen presenting functions due in part to its role in invariant chain degradation (Nakagawa et al., 1999; Riese et al., 1998; Shi et al., 1999). Therefore, future studies measuring invariant chain degradation in pulse-chase experiments with radiolabeled amino acids should provide insights into how Vps34 contributes to antigen presentation.

**Overall conclusions**

The results of this dissertation represent the first extensive examination of the role Vps34 plays in TECs and B cells, two important APC populations. While the evidence presented here strongly suggests that Vps34 plays a critical role in controlling MHC class II presentation in both TECs and B cells, whether Vps34 promotes or restrains antigen presentation appears to depend on the APC type and/or the route of delivery of antigen to the APC (i.e., endocytosis vs endogenous) and perhaps even the localization of antigen from discrete cellular compartments (e.g., membrane bound, cytosolic, or mitochondrial) in the case of endogenous antigen. Furthermore, previous work from the Van Kaer group found that Vps34 restrains the capacity of DCs to present the model antigen soluble ovalbumin to $CD4^+$ T cells yet promotes the stimulatory capacity of DCs in the MHC class II-restricted presentation of a central nervous system-derived autoantigen to $CD4^+$ T cells, indicating *in vivo* conditions such as disease state may also influence how Vps34 controls antigen presentation within a single APC lineage. Collectively, these findings highlight the importance of examining the role of Vps34 in presenting antigen derived from multiple sources in various APC cell populations *in vivo*. Such work will inform the development of therapeutics that leverage the presentation of antigen to T cells.

## REFERENCES


Abramson, J., and Anderson, G. (2017). Thymic Epithelial Cells. Annu Rev Immunol *35*, 85-118. 10.1146/annurev-immunol-051116-052320.

Adamopoulou, E., Tenzer, S., Hillen, N., Klug, P., Rota, I.A., Tietz, S., Gebhardt, M., Stevanovic, S., Schild, H., Tolosa, E., et al. (2013). Exploring the MHC-peptide matrix of central tolerance in the human thymus. Nat Commun *4*, 2039. 10.1038/ncomms3039.

Adams, J.J., Narayanan, S., Birnbaum, M.E., Sidhu, S.S., Blevins, S.J., Gee, M.H., Sibener, L.V., Baker, B.M., Kranz, D.M., and Garcia, K.C. (2016). Structural interplay between germline interactions and adaptive recognition determines the bandwidth of TCR-peptide-MHC cross-reactivity. Nat Immunol *17*, 87-94. 10.1038/ni.3310.

Aichinger, M., Wu, C., Nedjic, J., and Klein, L. (2013). Macroautophagy substrates are loaded onto MHC class II of medullary thymic epithelial cells for central tolerance. J Exp Med *210*, 287-300. 10.1084/jem.20122149.

Akkaya, M., Kwak, K., and Pierce, S.K. (2020). B cell memory: building two walls of protection against pathogens. Nat Rev Immunol *20*, 229-238. 10.1038/s41577-019-0244-2.

Alberts, B. (2002). Molecular biology of the cell, 4th Edition (Garland Science).

Allman, D., and Pillai, S. (2008). Peripheral B cell subsets. Curr Opin Immunol *20*, 149-157. 10.1016/j.coi.2008.03.014.

Alves, N.L., Richard-Le Goff, O., Huntington, N.D., Sousa, A.P., Ribeiro, V.S., Bordack, A., Vives, F.L., Peduto, L., Chidgey, A., Cumano, A., et al. (2009). Characterization of the thymic IL-7 niche in vivo. Proc Natl Acad Sci U S A *106*, 1512-1517. 10.1073/pnas.0809559106.

Anderson, M.S., Venanzi, E.S., Chen, Z., Berzins, S.P., Benoist, C., and Mathis, D. (2005). The cellular mechanism of Aire control of T cell tolerance. Immunity *23*, 227-239. 10.1016/j.immuni.2005.07.005.

Anderson, M.S., Venanzi, E.S., Klein, L., Chen, Z., Berzins, S.P., Turley, S.J., von Boehmer, H., Bronson, R., Dierich, A., Benoist, C., and Mathis, D. (2002). Projection of an immunological self shadow within the thymus by the aire protein. Science *298*, 1395-1401. 10.1126/science.1075958.

Arbogast, F., and Gros, F. (2018). Lymphocyte Autophagy in Homeostasis, Activation, and Inflammatory Diseases. Front Immunol *9*, 1801. 10.3389/fimmu.2018.01801.

Arnold, J., Murera, D., Arbogast, F., Fauny, J.D., Muller, S., and Gros, F. (2016). Autophagy is dispensable for B-cell development but essential for humoral autoimmune responses. Cell Death Differ *23*, 853-864. 10.1038/cdd.2015.149.

Audiger, C., Rahman, M.J., Yun, T.J., Tarbell, K.V., and Lesage, S. (2017). The Importance of Dendritic Cells in Maintaining Immune Tolerance. J Immunol *198*, 2223-2231. 10.4049/jimmunol.1601629.

Azzam, H.S., Grinberg, A., Lui, K., Shen, H., Shores, E.W., and Love, P.E. (1998). CD5 expression is developmentally regulated by T cell receptor (TCR) signals and TCR avidity. J Exp Med *188*, 2301-2311. 10.1084/jem.188.12.2301.

Backer, J.M. (2016). The intricate regulation and complex functions of the Class III phosphoinositide 3-kinase Vps34. Biochem J *473*, 2251-2271. 10.1042/BCJ20160170.

Baran-Gale, J., Morgan, M.D., Maio, S., Dhalla, F., Calvo-Asensio, I., Deadman, M.E., Handel, A.E., Maynard, A., Chen, S., Green, F., et al. (2020). Ageing compromises mouse thymus function and remodels epithelial cell differentiation. Elife *9*. 10.7554/eLife.56221.

Barthlott, T., Kohler, H., and Eichmann, K. (1997). Asynchronous coreceptor downregulation after positive thymic selection: prolonged maintenance of the double positive state in CD8 lineage differentiation due to sustained biosynthesis of the CD4 coreceptor. J Exp Med *185*, 357-362. 10.1084/jem.185.2.357.

Baumgarth, N. (2016). B-1 Cell Heterogeneity and the Regulation of Natural and Antigen-Induced IgM Production. Front Immunol *7*, 324. 10.3389/fimmu.2016.00324.

Baumgarth, N. (2017). A Hard(y) Look at B-1 Cell Development and Function. J Immunol *199*, 3387-3394. 10.4049/jimmunol.1700943.

Bechtel, W., Helmstadter, M., Balica, J., Hartleben, B., Kiefer, B., Hrnjic, F., Schell, C., Kretz, O., Liu, S., Geist, F., et al. (2013). Vps34 deficiency reveals the importance of endocytosis for podocyte homeostasis. J Am Soc Nephrol *24*, 727-743. 10.1681/ASN.2012070700.

Beers, C., Burich, A., Kleijmeer, M.J., Griffith, J.M., Wong, P., and Rudensky, A.Y. (2005). Cathepsin S controls MHC class II-mediated antigen presentation by epithelial cells in vivo. J Immunol *174*, 1205-1212. 10.4049/jimmunol.174.3.1205.

Besnard, M., Padonou, F., Provin, N., Giraud, M., and Guillonneau, C. (2021). AIRE deficiency, from preclinical models to human APECED disease. Dis Model Mech *14*. 10.1242/dmm.046359.

Bilanges, B., Alliouachene, S., Pearce, W., Morelli, D., Szabadkai, G., Chung, Y.L., Chicanne, G., Valet, C., Hill, J.M., Voshol, P.J., et al. (2017). Vps34 PI 3-kinase inactivation enhances insulin sensitivity through reprogramming of mitochondrial metabolism. Nat Commun *8*, 1804. 10.1038/s41467-017-01969-4.

Bilanges, B., Posor, Y., and Vanhaesebroeck, B. (2019). PI3K isoforms in cell signalling and vesicle trafficking. Nat Rev Mol Cell Biol *20*, 515-534. 10.1038/s41580-019-0129-z.

Blum, J.S., Wearsch, P.A., and Cresswell, P. (2013). Pathways of antigen processing. Annu Rev Immunol *31*, 443-473. 10.1146/annurev-immunol-032712-095910.

Boothby, M., and Rickert, R.C. (2017). Metabolic Regulation of the Immune Humoral Response. Immunity *46*, 743-755. 10.1016/j.immuni.2017.04.009.

Boukhalfa, A., Nascimbeni, A.C., Ramel, D., Dupont, N., Hirsch, E., Gayral, S., Laffargue, M., Codogno, P., and Morel, E. (2020). PI3KC2alpha-dependent and VPS34-independent generation of PI3P controls primary cilium-mediated autophagy in response to shear stress. Nat Commun *11*, 294. 10.1038/s41467-019-14086-1.

Breed, E.R., Lee, S.T., and Hogquist, K.A. (2018). Directing T cell fate: How thymic antigen presenting cells coordinate thymocyte selection. Semin Cell Dev Biol *84*, 2-10. 10.1016/j.semcdb.2017.07.045.

Brisson, L., and Carrier, A. (2015). A novel actor in antitumoral immunity: The thymus-specific serine protease TSSP/PRSS16 involved in CD4(+) T-cell maturation. Oncoimmunology *4*, e1026536. 10.1080/2162402X.2015.1026536.

Busch, R., Rinderknecht, C.H., Roh, S., Lee, A.W., Harding, J.J., Burster, T., Hornell, T.M., and Mellins, E.D. (2005). Achieving stability through editing and chaperoning: regulation of MHC class II peptide binding and expression. Immunol Rev *207*, 242-260. 10.1111/j.0105-2896.2005.00306.x.

Byfield, M.P., Murray, J.T., and Backer, J.M. (2005). hVps34 is a nutrient-regulated lipid kinase required for activation of p70 S6 kinase. J Biol Chem *280*, 33076-33082. 10.1074/jbc.M507201200.

Cabatingan, M.S., Schmidt, M.R., Sen, R., and Woodland, R.T. (2002). Naive B lymphocytes undergo homeostatic proliferation in response to B cell deficit. J Immunol *169*, 6795-6805. 10.4049/jimmunol.169.12.6795.

Castaneda, J., Hidalgo, Y., Sauma, D., Rosemblatt, M., Bono, M.R., and Nunez, S. (2021). The Multifaceted Roles of B Cells in the Thymus: From Immune Tolerance to Autoimmunity. Front Immunol *12*, 766698. 10.3389/fimmu.2021.766698.

Cepeda, S., Cantu, C., Orozco, S., Xiao, Y., Brown, Z., Semwal, M.K., Venables, T., Anderson, M.S., and Griffith, A.V. (2018). Age-Associated Decline in Thymic B Cell Expression of Aire and Aire-Dependent Self-Antigens. Cell Rep *22*, 1276-1287. 10.1016/j.celrep.2018.01.015.

Chaurasia, M., Bhatt, A.N., Das, A., Dwarakanath, B.S., and Sharma, K. (2016). Radiation-induced autophagy: mechanisms and consequences. Free Radic Res *50*, 273-290. 10.3109/10715762.2015.1129534.

Chen, M., Hong, M.J., Sun, H., Wang, L., Shi, X., Gilbert, B.E., Corry, D.B., Kheradmand, F., and Wang, J. (2014). Essential role for autophagy in the maintenance of

immunological memory against influenza infection. Nat Med *20*, 503-510. 10.1038/nm.3521.

Chen, M., Kodali, S., Jang, A., Kuai, L., and Wang, J. (2015). Requirement for autophagy in the long-term persistence but not initial formation of memory B cells. J Immunol *194*, 2607-2615. 10.4049/jimmunol.1403001.

Cheng, M., and Anderson, M.S. (2018). Thymic tolerance as a key brake on autoimmunity. Nat Immunol *19*, 659-664. 10.1038/s41590-018-0128-9.

Chicz, R.M., Urban, R.G., Gorga, J.C., Vignali, D.A., Lane, W.S., and Strominger, J.L. (1993). Specificity and promiscuity among naturally processed peptides bound to HLA-DR alleles. J Exp Med *178*, 27-47. 10.1084/jem.178.1.27.

Christoforidis, S., Miaczynska, M., Ashman, K., Wilm, M., Zhao, L., Yip, S.C., Waterfield, M.D., Backer, J.M., and Zerial, M. (1999). Phosphatidylinositol-3-OH kinases are Rab5 effectors. Nat Cell Biol *1*, 249-252. 10.1038/12075.

Clarke, A.J., Ellinghaus, U., Cortini, A., Stranks, A., Simon, A.K., Botto, M., and Vyse, T.J. (2015). Autophagy is activated in systemic lupus erythematosus and required for plasmablast development. Ann Rheum Dis *74*, 912-920. 10.1136/annrheumdis-2013-204343.

Clarke, A.J., Riffelmacher, T., Braas, D., Cornall, R.J., and Simon, A.K. (2018). B1a B cells require autophagy for metabolic homeostasis and self-renewal. J Exp Med *215*, 399-413. 10.1084/jem.20170771.

Conway, K.L., Kuballa, P., Khor, B., Zhang, M., Shi, H.N., Virgin, H.W., and Xavier, R.J. (2013). ATG5 regulates plasma cell differentiation. Autophagy *9*, 528-537. 10.4161/auto.23484.

Cowan, J.E., Parnell, S.M., Nakamura, K., Caamano, J.H., Lane, P.J., Jenkinson, E.J., Jenkinson, W.E., and Anderson, G. (2013). The thymic medulla is required for Foxp3+ regulatory but not conventional CD4+ thymocyte development. J Exp Med *210*, 675-681. 10.1084/jem.20122070.

Crotzer, V.L., and Blum, J.S. (2010). Autophagy and adaptive immunity. Immunology *131*, 9-17. 10.1111/j.1365-2567.2010.03321.x.

Delamarre, L., Pack, M., Chang, H., Mellman, I., and Trombetta, E.S. (2005). Differential lysosomal proteolysis in antigen-presenting cells determines antigen fate. Science *307*, 1630-1634. 10.1126/science.1108003.

Dengjel, J., Schoor, O., Fischer, R., Reich, M., Kraus, M., Muller, M., Kreymborg, K., Altenberend, F., Brandenburg, J., Kalbacher, H., et al. (2005). Autophagy promotes MHC class II presentation of peptides from intracellular source proteins. Proc Natl Acad Sci U S A *102*, 7922-7927. 10.1073/pnas.0501190102.

Denzin, L.K., Khan, A.A., Virdis, F., Wilks, J., Kane, M., Beilinson, H.A., Dikiy, S., Case, L.K., Roopenian, D., Witkowski, M., et al. (2017). Neutralizing Antibody Responses to Viral Infections Are Linked to the Non-classical MHC Class II Gene H2-Ob. Immunity *47*, 310-322 e317. 10.1016/j.immuni.2017.07.013.

Dong, M., Artusa, P., Kelly, S.A., Fournier, M., Baldwin, T.A., Mandl, J.N., and Melichar, H.J. (2017). Alterations in the Thymic Selection Threshold Skew the Self-Reactivity of the TCR Repertoire in Neonates. J Immunol *199*, 965-973. 10.4049/jimmunol.1602137.

Dongre, A.R., Kovats, S., deRoos, P., McCormack, A.L., Nakagawa, T., Paharkova-Vatchkova, V., Eng, J., Caldwell, H., Yates, J.R., 3rd, and Rudensky, A.Y. (2001). In vivo MHC class II presentation of cytosolic proteins revealed by rapid automated tandem mass spectrometry and functional analyses. Eur J Immunol *31*, 1485-1494. 10.1002/1521-4141(200105)31:5<1485::AID-IMMU1485>3.0.CO;2-A.

Fulton, R.B., Hamilton, S.E., Xing, Y., Best, J.A., Goldrath, A.W., Hogquist, K.A., and Jameson, S.C. (2015). The TCR's sensitivity to self peptide-MHC dictates the ability of naive CD8(+) T cells to respond to foreign antigens. Nat Immunol *16*, 107-117. 10.1038/ni.3043.

Fung-Leung, W.P., Surh, C.D., Liljedahl, M., Pang, J., Leturcq, D., Peterson, P.A., Webb, S.R., and Karlsson, L. (1996). Antigen presentation and T cell development in H2-M-deficient mice. Science *271*, 1278-1281. 10.1126/science.271.5253.1278.

Furuya, T., Kim, M., Lipinski, M., Li, J., Kim, D., Lu, T., Shen, Y., Rameh, L., Yankner, B., Tsai, L.H., and Yuan, J. (2010). Negative regulation of Vps34 by Cdk mediated phosphorylation. Mol Cell *38*, 500-511. 10.1016/j.molcel.2010.05.009.

Galluzzi, L., and Green, D.R. (2019). Autophagy-Independent Functions of the Autophagy Machinery. Cell *177*, 1682-1699. 10.1016/j.cell.2019.05.026.

Gascoigne, N.R., Rybakin, V., Acuto, O., and Brzostek, J. (2016). TCR Signal Strength and T Cell Development. Annu Rev Cell Dev Biol *32*, 327-348. 10.1146/annurev-cellbio-111315-125324.

Gayle, S., Landrette, S., Beeharry, N., Conrad, C., Hernandez, M., Beckett, P., Ferguson, S.M., Mandelkern, T., Zheng, M., Xu, T., et al. (2017). Identification of apilimod as a first-in-class PIKfyve kinase inhibitor for treatment of B-cell non-Hodgkin lymphoma. Blood *129*, 1768-1778. 10.1182/blood-2016-09-736892.

Gies, V., Guffroy, A., Danion, F., Billaud, P., Keime, C., Fauny, J.D., Susini, S., Soley, A., Martin, T., Pasquali, J.L., et al. (2017). B cells differentiate in human thymus and express AIRE. J Allergy Clin Immunol *139*, 1049-1052 e1012. 10.1016/j.jaci.2016.09.044.

Gommeaux, J., Gregoire, C., Nguessan, P., Richelme, M., Malissen, M., Guerder, S., Malissen, B., and Carrier, A. (2009). Thymus-specific serine protease regulates positive selection of a subset of CD4+ thymocytes. Eur J Immunol *39*, 956-964. 10.1002/eji.200839175.

Gordon, J., Xiao, S., Hughes, B., 3rd, Su, D.M., Navarre, S.P., Condie, B.G., and Manley, N.R. (2007). Specific expression of lacZ and cre recombinase in fetal thymic epithelial cells by multiplex gene targeting at the Foxn1 locus. BMC Dev Biol *7*, 69. 10.1186/1471-213X-7-69.

Gossens, K., Naus, S., Corbel, S.Y., Lin, S., Rossi, F.M., Kast, J., and Ziltener, H.J. (2009). Thymic progenitor homing and lymphocyte homeostasis are linked via S1P-controlled expression of thymic P-selectin/CCL25. J Exp Med *206*, 761-778. 10.1084/jem.20082502.

Gray, D., Abramson, J., Benoist, C., and Mathis, D. (2007). Proliferative arrest and rapid turnover of thymic epithelial cells expressing Aire. J Exp Med *204*, 2521-2528. 10.1084/jem.20070795.

Groll, M., Ditzel, L., Lowe, J., Stock, D., Bochtler, M., Bartunik, H.D., and Huber, R. (1997). Structure of 20S proteasome from yeast at 2.4 A resolution. Nature *386*, 463-471. 10.1038/386463a0.

Gulati, P., Gaspers, L.D., Dann, S.G., Joaquin, M., Nobukuni, T., Natt, F., Kozma, S.C., Thomas, A.P., and Thomas, G. (2008). Amino acids activate mTOR complex 1 via Ca2+/CaM signaling to hVps34. Cell Metab *7*, 456-465. 10.1016/j.cmet.2008.03.002.

Han, J., and Zuniga-Pflucker, J.C. (2021). A 2020 View of Thymus Stromal Cells in T Cell Development. J Immunol *206*, 249-256. 10.4049/jimmunol.2000889.

Han, J.W., Zheng, H.F., Cui, Y., Sun, L.D., Ye, D.Q., Hu, Z., Xu, J.H., Cai, Z.M., Huang, W., Zhao, G.P., et al. (2009). Genome-wide association study in a Chinese Han population identifies nine new susceptibility loci for systemic lupus erythematosus. Nat Genet *41*, 1234-1237. 10.1038/ng.472.

Hara, T., Nakamura, K., Matsui, M., Yamamoto, A., Nakahara, Y., Suzuki-Migishima, R., Yokoyama, M., Mishima, K., Saito, I., Okano, H., and Mizushima, N. (2006). Suppression of basal autophagy in neural cells causes neurodegenerative disease in mice. Nature *441*, 885-889. 10.1038/nature04724.

Herman, P.K., and Emr, S.D. (1990). Characterization of VPS34, a gene required for vacuolar protein sorting and vacuole segregation in Saccharomyces cerevisiae. Mol Cell Biol *10*, 6742-6754. 10.1128/mcb.10.12.6742-6754.1990.

Honda, S., Arakawa, S., Nishida, Y., Yamaguchi, H., Ishii, E., and Shimizu, S. (2014). Ulk1-mediated Atg5-independent macroautophagy mediates elimination of mitochondria from embryonic reticulocytes. Nat Commun *5*, 4004. 10.1038/ncomms5004.

Honey, K., Nakagawa, T., Peters, C., and Rudensky, A. (2002). Cathepsin L regulates CD4+ T cell selection independently of its effect on invariant chain: a role in the generation of positively selecting peptide ligands. J Exp Med *195*, 1349-1358. 10.1084/jem.20011904.

Hong, Z., Pedersen, N.M., Wang, L., Torgersen, M.L., Stenmark, H., and Raiborg, C. (2017). PtdIns3P controls mTORC1 signaling through lysosomal positioning. J Cell Biol *216*, 4217-4233. 10.1083/jcb.201611073.

Hozumi, K., Mailhos, C., Negishi, N., Hirano, K., Yahata, T., Ando, K., Zuklys, S., Hollander, G.A., Shima, D.T., and Habu, S. (2008). Delta-like 4 is indispensable in thymic environment specific for T cell development. J Exp Med *205*, 2507-2513. 10.1084/jem.20080134.

International Consortium for Systemic Lupus Erythematosus, G., Harley, J.B., Alarcon-Riquelme, M.E., Criswell, L.A., Jacob, C.O., Kimberly, R.P., Moser, K.L., Tsao, B.P., Vyse, T.J., Langefeld, C.D., et al. (2008). Genome-wide association scan in women with systemic lupus erythematosus identifies susceptibility variants in ITGAM, PXK, KIAA1542 and other loci. Nat Genet *40*, 204-210. 10.1038/ng.81.

Irla, M., Hollander, G., and Reith, W. (2010). Control of central self-tolerance induction by autoreactive CD4+ thymocytes. Trends Immunol *31*, 71-79. 10.1016/j.it.2009.11.002.

Jaber, N., Dou, Z., Chen, J.S., Catanzaro, J., Jiang, Y.P., Ballou, L.M., Selinger, E., Ouyang, X., Lin, R.Z., Zhang, J., and Zong, W.X. (2012). Class III PI3K Vps34 plays an essential role in autophagy and in heart and liver function. Proc Natl Acad Sci U S A *109*, 2003-2008. 10.1073/pnas.1112848109.

Jaber, N., Mohd-Naim, N., Wang, Z., DeLeon, J.L., Kim, S., Zhong, H., Sheshadri, N., Dou, Z., Edinger, A.L., Du, G., et al. (2016). Vps34 regulates Rab7 and late endocytic trafficking through recruitment of the GTPase-activating protein Armus. J Cell Sci *129*, 4424-4435. 10.1242/jcs.192260.

Jain, R., Mintern, J.D., Tan, I., Dewson, G., Strasser, A., and Gray, D.H.D. (2018). How do thymic epithelial cells die? Cell Death Differ *25*, 1002-1004. 10.1038/s41418-018-0093-8.

Jain, R., Sheridan, J.M., Policheni, A., Heinlein, M., Gandolfo, L.C., Dewson, G., Smyth, G.K., Sansom, S.N., Fu, N.Y., Visvader, J.E., et al. (2017). A critical epithelial survival axis regulated by MCL-1 maintains thymic function in mice. Blood *130*, 2504-2515. 10.1182/blood-2017-03-771576.

Jenkinson, W.E., Rossi, S.W., Parnell, S.M., Agace, W.W., Takahama, Y., Jenkinson, E.J., and Anderson, G. (2007). Chemokine receptor expression defines heterogeneity in the earliest thymic migrants. Eur J Immunol *37*, 2090-2096. 10.1002/eji.200737212.

Johnson, E.E., Overmeyer, J.H., Gunning, W.T., and Maltese, W.A. (2006). Gene silencing reveals a specific function of hVps34 phosphatidylinositol 3-kinase in late versus early endosomes. J Cell Sci *119*, 1219-1232. 10.1242/jcs.02833.

Joyce, S. (2022). Life In-Between: Bridging Innate and Adaptive Immunity. J Immunol *209*, 193-195. 10.4049/jimmunol.2290012.

Juhasz, G., Hill, J.H., Yan, Y., Sass, M., Baehrecke, E.H., Backer, J.M., and Neufeld, T.P. (2008). The class III PI(3)K Vps34 promotes autophagy and endocytosis but not TOR signaling in Drosophila. J Cell Biol *181*, 655-666. 10.1083/jcb.200712051.

Kadouri, N., Nevo, S., Goldfarb, Y., and Abramson, J. (2020). Thymic epithelial cell heterogeneity: TEC by TEC. Nat Rev Immunol *20*, 239-253. 10.1038/s41577-019-0238-0.

Kasai, M., Tanida, I., Ueno, T., Kominami, E., Seki, S., Ikeda, T., and Mizuochi, T. (2009). Autophagic compartments gain access to the MHC class II compartments in thymic epithelium. J Immunol *183*, 7278-7285. 10.4049/jimmunol.0804087.

Kaushik, S., and Cuervo, A.M. (2018). The coming of age of chaperone-mediated autophagy. Nat Rev Mol Cell Biol *19*, 365-381. 10.1038/s41580-018-0001-6.

Khan, I.S., Mouchess, M.L., Zhu, M.L., Conley, B., Fasano, K.J., Hou, Y., Fong, L., Su, M.A., and Anderson, M.S. (2014). Enhancement of an anti-tumor immune response by transient blockade of central T cell tolerance. J Exp Med *211*, 761-768. 10.1084/jem.20131889.

Khan, W.N. (2009). B cell receptor and BAFF receptor signaling regulation of B cell homeostasis. J Immunol *183*, 3561-3567. 10.4049/jimmunol.0800933.

Kihara, A., Noda, T., Ishihara, N., and Ohsumi, Y. (2001). Two distinct Vps34 phosphatidylinositol 3-kinase complexes function in autophagy and carboxypeptidase Y sorting in Saccharomyces cerevisiae. J Cell Biol *152*, 519-530. 10.1083/jcb.152.3.519.

Kikuchi, K., Lai, A.Y., Hsu, C.L., and Kondo, M. (2005). IL-7 receptor signaling is necessary for stage transition in adult B cell development through up-regulation of EBF. J Exp Med *201*, 1197-1203. 10.1084/jem.20050158.

Klein, L., Kyewski, B., Allen, P.M., and Hogquist, K.A. (2014). Positive and negative selection of the T cell repertoire: what thymocytes see (and don't see). Nat Rev Immunol *14*, 377-391. 10.1038/nri3667.

Klionsky, D.J., Abdelmohsen, K., Abe, A., Abedin, M.J., Abeliovich, H., Acevedo Arozena, A., Adachi, H., Adams, C.M., Adams, P.D., Adeli, K., et al. (2016). Guidelines for the use and interpretaton of assays for monitoring autophagy (3rd Edition). Autophagy *12*, 1-222.

Koch, U., Fiorini, E., Benedito, R., Besseyrias, V., Schuster-Gossler, K., Pierres, M., Manley, N.R., Duarte, A., Macdonald, H.R., and Radtke, F. (2008). Delta-like 4 is the essential, nonredundant ligand for Notch1 during thymic T cell lineage commitment. J Exp Med *205*, 2515-2523. 10.1084/jem.20080829.

Kondo, K., Takada, K., and Takahama, Y. (2017). Antigen processing and presentation in the thymus: implications for T cell repertoire selection. Curr Opin Immunol *46*, 53-57. 10.1016/j.coi.2017.03.014.

Kranich, J., and Krautler, N.J. (2016). How Follicular Dendritic Cells Shape the B-Cell Antigenome. Front Immunol *7*, 225. 10.3389/fimmu.2016.00225.

Kuma, A., Hatano, M., Matsui, M., Yamamoto, A., Nakaya, H., Yoshimori, T., Ohsumi, Y., Tokuhisa, T., and Mizushima, N. (2004). The role of autophagy during the early neonatal starvation period. Nature *432*, 1032-1036. 10.1038/nature03029.

Kuma, A., Komatsu, M., and Mizushima, N. (2017). Autophagy-monitoring and autophagy-deficient mice. Autophagy *13*, 1619-1628. 10.1080/15548627.2017.1343770.

Kwak, K., Akkaya, M., and Pierce, S.K. (2019). B cell signaling in context. Nat Immunol *20*, 963-969. 10.1038/s41590-019-0427-9.

Lantz, O., Grandjean, I., Matzinger, P., and Di Santo, J.P. (2000). Gamma chain required for naive CD4+ T cell survival but not for antigen proliferation. Nat Immunol *1*, 54-58. 10.1038/76917.

Laufer, T.M., DeKoning, J., Markowitz, J.S., Lo, D., and Glimcher, L.H. (1996). Unopposed positive selection and autoreactivity in mice expressing class II MHC only on thymic cortex. Nature *383*, 81-85. 10.1038/383081a0.

Levine, B., and Kroemer, G. (2019). Biological Functions of Autophagy Genes: A Disease Perspective. Cell *176*, 11-42. 10.1016/j.cell.2018.09.048.

Li, L., Wang, Z.V., Hill, J.A., and Lin, F. (2014). New autophagy reporter mice reveal dynamics of proximal tubular autophagy. J Am Soc Nephrol *25*, 305-315. 10.1681/ASN.2013040374.

Li, X., Garrity, A.G., and Xu, H. (2013). Regulation of membrane trafficking by signalling on endosomal and lysosomal membranes. J Physiol *591*, 4389-4401. 10.1113/jphysiol.2013.258301.

Liang, C., Lee, J.S., Inn, K.S., Gack, M.U., Li, Q., Roberts, E.A., Vergne, I., Deretic, V., Feng, P., Akazawa, C., and Jung, J.U. (2008). Beclin1-binding UVRAG targets the class C Vps complex to coordinate autophagosome maturation and endocytic trafficking. Nat Cell Biol *10*, 776-787. 10.1038/ncb1740.

Liu, H., Jain, R., Guan, J., Vuong, V., Ishido, S., La Gruta, N.L., Gray, D.H., Villadangos, J.A., and Mintern, J.D. (2016). Ubiquitin ligase MARCH 8 cooperates with CD83 to control surface MHC II expression in thymic epithelium and CD4 T cell selection. J Exp Med *213*, 1695-1703. 10.1084/jem.20160312.

Ma, T., Li, J., Xu, Y., Yu, C., Xu, T., Wang, H., Liu, K., Cao, N., Nie, B.M., Zhu, S.Y., et al. (2015). Atg5-independent autophagy regulates mitochondrial clearance and is essential for iPSC reprogramming. Nat Cell Biol *17*, 1379-1387. 10.1038/ncb3256.

Madisen, L., Zwingman, T.A., Sunkin, S.M., Oh, S.W., Zariwala, H.A., Gu, H., Ng, L.L., Palmiter, R.D., Hawrylycz, M.J., Jones, A.R., et al. (2010). A robust and high-throughput

Cre reporting and characterization system for the whole mouse brain. Nat Neurosci *13*, 133-140. 10.1038/nn.2467.

Maehr, R., Mintern, J.D., Herman, A.E., Lennon-Dumenil, A.M., Mathis, D., Benoist, C., and Ploegh, H.L. (2005). Cathepsin L is essential for onset of autoimmune diabetes in NOD mice. J Clin Invest *115*, 2934-2943. 10.1172/JCI25485.

Mandl, J.N., Monteiro, J.P., Vrisekoop, N., and Germain, R.N. (2013). T cell-positive selection uses self-ligand binding strength to optimize repertoire recognition of foreign antigens. Immunity *38*, 263-274. 10.1016/j.immuni.2012.09.011.

Manley, N.R., Richie, E.R., Blackburn, C.C., Condie, B.G., and Sage, J. (2011). Structure and function of the thymic microenvironment. Front Biosci (Landmark Ed) *16*, 2461-2477. 10.2741/3866.

Martin, W.D., Hicks, G.G., Mendiratta, S.K., Leva, H.I., Ruley, H.E., and Van Kaer, L. (1996). H2-M mutant mice are defective in the peptide loading of class II molecules, antigen presentation, and T cell repertoire selection. Cell *84*, 543-550. 10.1016/s0092-8674(00)81030-2.

Martinez-Martin, N., Maldonado, P., Gasparrini, F., Frederico, B., Aggarwal, S., Gaya, M., Tsui, C., Burbage, M., Keppler, S.J., Montaner, B., et al. (2017). A switch from canonical to noncanonical autophagy shapes B cell responses. Science *355*, 641-647. 10.1126/science.aal3908.

Martinez-Ruiz, G.U., Morales-Sanchez, A., and Bhandoola, A. (2021). Transcriptional and epigenetic regulation in thymic epithelial cells. Immunol Rev. 10.1111/imr.13034.

Martinez, J., Cunha, L.D., Park, S., Yang, M., Lu, Q., Orchard, R., Li, Q.Z., Yan, M., Janke, L., Guy, C., et al. (2016). Noncanonical autophagy inhibits the autoinflammatory, lupus-like response to dying cells. Nature *533*, 115-119. 10.1038/nature17950.

Martinez, J., Malireddi, R.K., Lu, Q., Cunha, L.D., Pelletier, S., Gingras, S., Orchard, R., Guan, J.L., Tan, H., Peng, J., et al. (2015). Molecular characterization of LC3-associated phagocytosis reveals distinct roles for Rubicon, NOX2 and autophagy proteins. Nat Cell Biol *17*, 893-906. 10.1038/ncb3192.

McAllister, E.J., Apgar, J.R., Leung, C.R., Rickert, R.C., and Jellusova, J. (2017). New Methods To Analyze B Cell Immune Responses to Thymus-Dependent Antigen Sheep Red Blood Cells. J Immunol *199*, 2998-3003. 10.4049/jimmunol.1700454.

McLeod, I.X., Zhou, X., Li, Q.J., Wang, F., and He, Y.W. (2011). The class III kinase Vps34 promotes T lymphocyte survival through regulating IL-7Ralpha surface expression. J Immunol *187*, 5051-5061. 10.4049/jimmunol.1100710.

Melchers, F. (2015). Checkpoints that control B cell development. J Clin Invest *125*, 2203-2210. 10.1172/JCI78083.

Metur, S.P., and Klionsky, D.J. (2021). Adaptive immunity at the crossroads of autophagy and metabolism. Cell Mol Immunol *18*, 1096-1105. 10.1038/s41423-021-00662-3.

Metzger, T.C., Khan, I.S., Gardner, J.M., Mouchess, M.L., Johannes, K.P., Krawisz, A.K., Skrzypczynska, K.M., and Anderson, M.S. (2013). Lineage tracing and cell ablation identify a post-Aire-expressing thymic epithelial cell population. Cell Rep *5*, 166-179. 10.1016/j.celrep.2013.08.038.

Milam, A.V., and Allen, P.M. (2015). Functional Heterogeneity in CD4(+) T Cell Responses Against a Bacterial Pathogen. Front Immunol *6*, 621. 10.3389/fimmu.2015.00621.

Miller, B.C., Zhao, Z., Stephenson, L.M., Cadwell, K., Pua, H.H., Lee, H.K., Mizushima, N.N., Iwasaki, A., He, Y.W., Swat, W., and Virgin, H.W.t. (2008). The autophagy gene ATG5 plays an essential role in B lymphocyte development. Autophagy *4*, 309-314. 10.4161/auto.5474.

Miller, J. (2020). The function of the thymus and its impact on modern medicine. Science *369*. 10.1126/science.aba2429.

Miller, S.D., Karpus, W.J., and Davidson, T.S. (2010). Experimental autoimmune encephalomyelitis in the mouse. Curr Protoc Immunol *Chapter 15*, Unit 15 11. 10.1002/0471142735.im1501s88.

Miqueu, P., Guillet, M., Degauque, N., Dore, J.C., Soulillou, J.P., and Brouard, S. (2007). Statistical analysis of CDR3 length distributions for the assessment of T and B cell repertoire biases. Mol Immunol *44*, 1057-1064. 10.1016/j.molimm.2006.06.026.

Miyazaki, T., Wolf, P., Tourne, S., Waltzinger, C., Dierich, A., Barois, N., Ploegh, H., Benoist, C., and Mathis, D. (1996). Mice lacking H2-M complexes, enigmatic elements of the MHC class II peptide-loading pathway. Cell *84*, 531-541. 10.1016/s0092-8674(00)81029-6.

Mizushima, N. (2018). A brief history of autophagy from cell biology to physiology and disease. Nat Cell Biol *20*, 521-527. 10.1038/s41556-018-0092-5.

Mizushima, N., Yamamoto, A., Matsui, M., Yoshimori, T., and Ohsumi, Y. (2004). In vivo analysis of autophagy in response to nutrient starvation using transgenic mice expressing a fluorescent autophagosome marker. Mol Biol Cell *15*, 1101-1111. 10.1091/mbc.e03-09-0704.

Moran, A.E., and Hogquist, K.A. (2012). T-cell receptor affinity in thymic development. Immunology *135*, 261-267. 10.1111/j.1365-2567.2011.03547.x.

Moses, C.T., Thorstenson, K.M., Jameson, S.C., and Khoruts, A. (2003). Competition for self ligands restrains homeostatic proliferation of naive CD4 T cells. Proc Natl Acad Sci U S A *100*, 1185-1190. 10.1073/pnas.0334572100.

Munz, C. (2018). Non-canonical Functions of Macroautophagy Proteins During Endocytosis by Myeloid Antigen Presenting Cells. Front Immunol *9*, 2765. 10.3389/fimmu.2018.02765.

Munz, C. (2021). The Macroautophagy Machinery in MHC Restricted Antigen Presentation. Front Immunol *12*, 628429. 10.3389/fimmu.2021.628429.

Murata, S., Sasaki, K., Kishimoto, T., Niwa, S., Hayashi, H., Takahama, Y., and Tanaka, K. (2007). Regulation of CD8+ T cell development by thymus-specific proteasomes. Science *316*, 1349-1353. 10.1126/science.1141915.

Murphy, K., and Weaver, C. (2016). Janeway's immunobiology, 9th edition. Edition (Garland Science/Taylor & Francis Group, LLC).

Nakagawa, T., Roth, W., Wong, P., Nelson, A., Farr, A., Deussing, J., Villadangos, J.A., Ploegh, H., Peters, C., and Rudensky, A.Y. (1998). Cathepsin L: critical role in Ii degradation and CD4 T cell selection in the thymus. Science *280*, 450-453. 10.1126/science.280.5362.450.

Nakagawa, T.Y., Brissette, W.H., Lira, P.D., Griffiths, R.J., Petrushova, N., Stock, J., McNeish, J.D., Eastman, S.E., Howard, E.D., Clarke, S.R., et al. (1999). Impaired invariant chain degradation and antigen presentation and diminished collagen-induced arthritis in cathepsin S null mice. Immunity *10*, 207-217. 10.1016/s1074-7613(00)80021-7.

Nedjic, J., Aichinger, M., Emmerich, J., Mizushima, N., and Klein, L. (2008). Autophagy in thymic epithelium shapes the T-cell repertoire and is essential for tolerance. Nature *455*, 396-400. 10.1038/nature07208.

Nemazee, D. (2017). Mechanisms of central tolerance for B cells. Nat Rev Immunol *17*, 281-294. 10.1038/nri.2017.19.

Netea, M.G., Dominguez-Andres, J., Barreiro, L.B., Chavakis, T., Divangahi, M., Fuchs, E., Joosten, L.A.B., van der Meer, J.W.M., Mhlanga, M.M., Mulder, W.J.M., et al. (2020). Defining trained immunity and its role in health and disease. Nat Rev Immunol *20*, 375-388. 10.1038/s41577-020-0285-6.

Nikolic-Zugic, J., and Bevan, M.J. (1990). Functional and phenotypic delineation of two subsets of CD4 single positive cells in the thymus. Int Immunol *2*, 135-141. 10.1093/intimm/2.2.135.

Nishida, Y., Arakawa, S., Fujitani, K., Yamaguchi, H., Mizuta, T., Kanaseki, T., Komatsu, M., Otsu, K., Tsujimoto, Y., and Shimizu, S. (2009). Discovery of Atg5/Atg7-independent alternative macroautophagy. Nature *461*, 654-658. 10.1038/nature08455.

Nitta, T., Murata, S., Sasaki, K., Fujii, H., Ripen, A.M., Ishimaru, N., Koyasu, S., Tanaka, K., and Takahama, Y. (2010). Thymoproteasome shapes immunocompetent repertoire of CD8+ T cells. Immunity *32*, 29-40. 10.1016/j.immuni.2009.10.009.

Nitta, T., Nitta, S., Lei, Y., Lipp, M., and Takahama, Y. (2009). CCR7-mediated migration of developing thymocytes to the medulla is essential for negative selection to tissue-restricted antigens. Proc Natl Acad Sci U S A *106*, 17129-17133. 10.1073/pnas.0906956106.

Nobukuni, T., Joaquin, M., Roccio, M., Dann, S.G., Kim, S.Y., Gulati, P., Byfield, M.P., Backer, J.M., Natt, F., Bos, J.L., et al. (2005). Amino acids mediate mTOR/raptor signaling through activation of class 3 phosphatidylinositol 3OH-kinase. Proc Natl Acad Sci U S A *102*, 14238-14243. 10.1073/pnas.0506925102.

Oh, J., and Shin, J.S. (2015). The Role of Dendritic Cells in Central Tolerance. Immune Netw *15*, 111-120. 10.4110/in.2015.15.3.111.

Pacholczyk, R., Ignatowicz, H., Kraj, P., and Ignatowicz, L. (2006). Origin and T cell receptor diversity of Foxp3+CD4+CD25+ T cells. Immunity *25*, 249-259. 10.1016/j.immuni.2006.05.016.

Pannetier, C., Cochet, M., Darche, S., Casrouge, A., Zoller, M., and Kourilsky, P. (1993). The sizes of the CDR3 hypervariable regions of the murine T-cell receptor beta chains vary as a function of the recombined germ-line segments. Proc Natl Acad Sci U S A *90*, 4319-4323. 10.1073/pnas.90.9.4319.

Parekh, V.V., Pabbisetty, S.K., Wu, L., Sebzda, E., Martinez, J., Zhang, J., and Van Kaer, L. (2017). Autophagy-related protein Vps34 controls the homeostasis and function of antigen cross-presenting CD8alpha(+) dendritic cells. Proc Natl Acad Sci U S A *114*, E6371-E6380. 10.1073/pnas.1706504114.

Parekh, V.V., Wu, L., Boyd, K.L., Williams, J.A., Gaddy, J.A., Olivares-Villagomez, D., Cover, T.L., Zong, W.X., Zhang, J., and Van Kaer, L. (2013). Impaired autophagy, defective T cell homeostasis, and a wasting syndrome in mice with a T cell-specific deletion of Vps34. J Immunol *190*, 5086-5101. 10.4049/jimmunol.1202071.

Pengo, N., Scolari, M., Oliva, L., Milan, E., Mainoldi, F., Raimondi, A., Fagioli, C., Merlini, A., Mariani, E., Pasqualetto, E., et al. (2013). Plasma cells require autophagy for sustainable immunoglobulin production. Nat Immunol *14*, 298-305. 10.1038/ni.2524.

Persaud, S.P., Parker, C.R., Lo, W.L., Weber, K.S., and Allen, P.M. (2014). Intrinsic CD4+ T cell sensitivity and response to a pathogen are set and sustained by avidity for thymic and peripheral complexes of self peptide and MHC. Nat Immunol *15*, 266-274. 10.1038/ni.2822.

Phan, T.G., Gray, E.E., and Cyster, J.G. (2009). The microanatomy of B cell activation. Curr Opin Immunol *21*, 258-265. 10.1016/j.coi.2009.05.006.

Pishesha, N., Harmand, T.J., and Ploegh, H.L. (2022). A guide to antigen processing and presentation. Nat Rev Immunol. 10.1038/s41577-022-00707-2.

Plotkin, J., Prockop, S.E., Lepique, A., and Petrie, H.T. (2003). Critical role for CXCR4 signaling in progenitor localization and T cell differentiation in the postnatal thymus. J Immunol *171*, 4521-4527. 10.4049/jimmunol.171.9.4521.

Postoak, J.L., Song, W., Yang, G., Guo, X., Xiao, S., Saffold, C.E., Zhang, J., Joyce, S., Manley, N.R., Wu, L., and Van Kaer, L. (2022). Thymic epithelial cells require lipid kinase Vps34 for CD4 but not CD8 T cell selection. J Exp Med *219*. 10.1084/jem.20212554.

Ramsdell, F., Jenkins, M., Dinh, Q., and Fowlkes, B.J. (1991). The majority of CD4+8- thymocytes are functionally immature. J Immunol *147*, 1779-1785.

Raza, I.G.A., and Clarke, A.J. (2021). B Cell Metabolism and Autophagy in Autoimmunity. Front Immunol *12*, 681105. 10.3389/fimmu.2021.681105.

Reifler, A., Li, X., Archambeau, A.J., McDade, J.R., Sabha, N., Michele, D.E., and Dowling, J.J. (2014). Conditional knockout of pik3c3 causes a murine muscular dystrophy. Am J Pathol *184*, 1819-1830. 10.1016/j.ajpath.2014.02.012.

Rickert, R.C., Roes, J., and Rajewsky, K. (1997). B lymphocyte-specific, Cre-mediated mutagenesis in mice. Nucleic Acids Res *25*, 1317-1318. 10.1093/nar/25.6.1317.

Riese, R.J., Mitchell, R.N., Villadangos, J.A., Shi, G.P., Palmer, J.T., Karp, E.R., De Sanctis, G.T., Ploegh, H.L., and Chapman, H.A. (1998). Cathepsin S activity regulates antigen presentation and immunity. J Clin Invest *101*, 2351-2363. 10.1172/JCI1158.

Robinson, J.S., Klionsky, D.J., Banta, L.M., and Emr, S.D. (1988). Protein sorting in Saccharomyces cerevisiae: isolation of mutants defective in the delivery and processing of multiple vacuolar hydrolases. Mol Cell Biol *8*, 4936-4948. 10.1128/mcb.8.11.4936-4948.1988.

Roche, P.A., and Furuta, K. (2015). The ins and outs of MHC class II-mediated antigen processing and presentation. Nat Rev Immunol *15*, 203-216. 10.1038/nri3818.

Rodrigues, P.M., Sousa, L.G., Perrod, C., Maceiras, A.R., Ferreirinha, P., Pombinho, R., Romera-Cardenas, G., Gomez-Lazaro, M., Senkara, M., Pistolic, J., et al. (2022). LAMP2 regulates autophagy in the thymic epithelium and thymic stroma-dependent CD4 T cell development. Autophagy, 1-14. 10.1080/15548627.2022.2074105.

Roggo, L., Bernard, V., Kovacs, A.L., Rose, A.M., Savoy, F., Zetka, M., Wymann, M.P., and Muller, F. (2002). Membrane transport in Caenorhabditis elegans: an essential role for VPS34 at the nuclear membrane. EMBO J *21*, 1673-1683. 10.1093/emboj/21.7.1673.

Ronan, B., Flamand, O., Vescovi, L., Dureuil, C., Durand, L., Fassy, F., Bachelot, M.F., Lamberton, A., Mathieu, M., Bertrand, T., et al. (2014). A highly potent and selective Vps34 inhibitor alters vesicle trafficking and autophagy. Nat Chem Biol *10*, 1013-1019. 10.1038/nchembio.1681.

Rossjohn, J., Gras, S., Miles, J.J., Turner, S.J., Godfrey, D.I., and McCluskey, J. (2015). T cell antigen receptor recognition of antigen-presenting molecules. Annu Rev Immunol *33*, 169-200. 10.1146/annurev-immunol-032414-112334.

Row, P.E., Reaves, B.J., Domin, J., Luzio, J.P., and Davidson, H.W. (2001). Overexpression of a rat kinase-deficient phosphoinositide 3-kinase, Vps34p, inhibits cathepsin D maturation. Biochem J *353*, 655-661. 10.1042/0264-6021:3530655.

Russell, R.C., Tian, Y., Yuan, H., Park, H.W., Chang, Y.Y., Kim, J., Kim, H., Neufeld, T.P., Dillin, A., and Guan, K.L. (2013). ULK1 induces autophagy by phosphorylating Beclin-1 and activating VPS34 lipid kinase. Nat Cell Biol *15*, 741-750. 10.1038/ncb2757.

Sagona, A.P., Nezis, I.P., Pedersen, N.M., Liestol, K., Poulton, J., Rusten, T.E., Skotheim, R.I., Raiborg, C., and Stenmark, H. (2010). PtdIns(3)P controls cytokinesis through KIF13A-mediated recruitment of FYVE-CENT to the midbody. Nat Cell Biol *12*, 362-371. 10.1038/ncb2036.

Sandoval, H., Kodali, S., and Wang, J. (2018). Regulation of B cell fate, survival, and function by mitochondria and autophagy. Mitochondrion *41*, 58-65. 10.1016/j.mito.2017.11.005.

Sansom, S.N., Shikama-Dorn, N., Zhanybekova, S., Nusspaumer, G., Macaulay, I.C., Deadman, M.E., Heger, A., Ponting, C.P., and Hollander, G.A. (2014). Population and single-cell genomics reveal the Aire dependency, relief from Polycomb silencing, and distribution of self-antigen expression in thymic epithelia. Genome Res *24*, 1918-1931. 10.1101/gr.171645.113.

Savage, P.A., Klawon, D.E.J., and Miller, C.H. (2020). Regulatory T Cell Development. Annu Rev Immunol *38*, 421-453. 10.1146/annurev-immunol-100219-020937.

Schmid, D., Pypaert, M., and Munz, C. (2007). Antigen-loading compartments for major histocompatibility complex class II molecules continuously receive input from autophagosomes. Immunity *26*, 79-92. 10.1016/j.immuni.2006.10.018.

Schu, P.V., Takegawa, K., Fry, M.J., Stack, J.H., Waterfield, M.D., and Emr, S.D. (1993). Phosphatidylinositol 3-kinase encoded by yeast VPS34 gene essential for protein sorting. Science *260*, 88-91. 10.1126/science.8385367.

Schurigt, U., Eilenstein, R., Gajda, M., Leipner, C., Sevenich, L., Reinheckel, T., Peters, C., Wiederanders, B., and Brauer, R. (2012). Decreased arthritis severity in cathepsin L-deficient mice is attributed to an impaired T helper cell compartment. Inflamm Res *61*, 1021-1029. 10.1007/s00011-012-0495-x.

Schuster, C., Gerold, K.D., Schober, K., Probst, L., Boerner, K., Kim, M.J., Ruckdeschel, A., Serwold, T., and Kissler, S. (2015). The Autoimmunity-Associated Gene CLEC16A Modulates Thymic Epithelial Cell Autophagy and Alters T Cell Selection. Immunity *42*, 942-952. 10.1016/j.immuni.2015.04.011.

Semwal, M.K., Jones, N.E., and Griffith, A.V. (2021). Metabolic Regulation of Thymic Epithelial Cell Function. Front Immunol *12*, 636072. 10.3389/fimmu.2021.636072.

Serre, L., Fazilleau, N., and Guerder, S. (2015). Central tolerance spares the private high-avidity CD4(+) T-cell repertoire specific for an islet antigen in NOD mice. Eur J Immunol *45*, 1946-1956. 10.1002/eji.201445290.

Shi, G.P., Villadangos, J.A., Dranoff, G., Small, C., Gu, L., Haley, K.J., Riese, R., Ploegh, H.L., and Chapman, H.A. (1999). Cathepsin S required for normal MHC class II peptide loading and germinal center development. Immunity *10*, 197-206. 10.1016/s1074-7613(00)80020-5.

Singer, A., Adoro, S., and Park, J.H. (2008). Lineage fate and intense debate: myths, models and mechanisms of CD4- versus CD8-lineage choice. Nat Rev Immunol *8*, 788-801. 10.1038/nri2416.

Smith, N.L., Patel, R.K., Reynaldi, A., Grenier, J.K., Wang, J., Watson, N.B., Nzingha, K., Yee Mon, K.J., Peng, S.A., Grimson, A., et al. (2018). Developmental Origin Governs CD8(+) T Cell Fate Decisions during Infection. Cell *174*, 117-130 e114. 10.1016/j.cell.2018.05.029.

Smulski, C.R., and Eibel, H. (2018). BAFF and BAFF-Receptor in B Cell Selection and Survival. Front Immunol *9*, 2285. 10.3389/fimmu.2018.02285.

Song, W., Ma, Y., Wang, J., Brantley-Sieders, D., and Chen, J. (2014). JNK signaling mediates EPHA2-dependent tumor cell proliferation, motility, and cancer stem cell-like properties in non-small cell lung cancer. Cancer Res *74*, 2444-2454. 10.1158/0008-5472.CAN-13-2136.

Stein, M.P., Feng, Y., Cooper, K.L., Welford, A.M., and Wandinger-Ness, A. (2003). Human VPS34 and p150 are Rab7 interacting partners. Traffic *4*, 754-771. 10.1034/j.1600-0854.2003.00133.x.

Stjepanovic, G., Baskaran, S., Lin, M.G., and Hurley, J.H. (2017). Unveiling the role of VPS34 kinase domain dynamics in regulation of the autophagic PI3K complex. Mol Cell Oncol *4*, e1367873. 10.1080/23723556.2017.1367873.

Sudhakar, J.N., Lu, H.H., Chiang, H.Y., Suen, C.S., Hwang, M.J., Wu, S.Y., Shen, C.N., Chang, Y.M., Li, F.A., Liu, F.T., and Shui, J.W. (2020). Lumenal Galectin-9-Lamp2 interaction regulates lysosome and autophagy to prevent pathogenesis in the intestine and pancreas. Nat Commun *11*, 4286. 10.1038/s41467-020-18102-7.

Sukseree, S., Mildner, M., Rossiter, H., Pammer, J., Zhang, C.F., Watanapokasin, R., Tschachler, E., and Eckhart, L. (2012). Autophagy in the thymic epithelium is dispensable for the development of self-tolerance in a novel mouse model. PLoS One *7*, e38933. 10.1371/journal.pone.0038933.

Sukseree, S., Rossiter, H., Mildner, M., Pammer, J., Buchberger, M., Gruber, F., Watanapokasin, R., Tschachler, E., and Eckhart, L. (2013). Targeted deletion of Atg5 reveals differential roles of autophagy in keratin K5-expressing epithelia. Biochem Biophys Res Commun *430*, 689-694. 10.1016/j.bbrc.2012.11.090.

Takaba, H., Morishita, Y., Tomofuji, Y., Danks, L., Nitta, T., Komatsu, N., Kodama, T., and Takayanagi, H. (2015). Fezf2 Orchestrates a Thymic Program of Self-Antigen Expression for Immune Tolerance. Cell *163*, 975-987. 10.1016/j.cell.2015.10.013.

Takaba, H., and Takayanagi, H. (2017). The Mechanisms of T Cell Selection in the Thymus. Trends Immunol *38*, 805-816. 10.1016/j.it.2017.07.010.

Takada, K., Kondo, K., and Takahama, Y. (2017). Generation of Peptides That Promote Positive Selection in the Thymus. J Immunol *198*, 2215-2222. 10.4049/jimmunol.1601862.

Takada, K., Van Laethem, F., Xing, Y., Akane, K., Suzuki, H., Murata, S., Tanaka, K., Jameson, S.C., Singer, A., and Takahama, Y. (2015). TCR affinity for thymoproteasome-dependent positively selecting peptides conditions antigen responsiveness in CD8(+) T cells. Nat Immunol *16*, 1069-1076. 10.1038/ni.3237.

Takahama, Y. (2006). Journey through the thymus: stromal guides for T-cell development and selection. Nat Rev Immunol *6*, 127-135. 10.1038/nri1781.

Takahama, Y., Ohigashi, I., Baik, S., and Anderson, G. (2017). Generation of diversity in thymic epithelial cells. Nat Rev Immunol *17*, 295-305. 10.1038/nri.2017.12.

Takahama, Y., Ohigashi, I., Murata, S., and Tanaka, K. (2019). Thymoproteasome and peptidic self. Immunogenetics *71*, 217-221. 10.1007/s00251-018-1081-3.

Thoresen, S.B., Pedersen, N.M., Liestol, K., and Stenmark, H. (2010). A phosphatidylinositol 3-kinase class III sub-complex containing VPS15, VPS34, Beclin 1, UVRAG and BIF-1 regulates cytokinesis and degradative endocytic traffic. Exp Cell Res *316*, 3368-3378. 10.1016/j.yexcr.2010.07.008.

Uddin, M.N., Nishio, N., Ito, S., Suzuki, H., and Isobe, K. (2012). Autophagic activity in thymus and liver during aging. Age (Dordr) *34*, 75-85. 10.1007/s11357-011-9221-9.

Ueno, T., Saito, F., Gray, D.H., Kuse, S., Hieshima, K., Nakano, H., Kakiuchi, T., Lipp, M., Boyd, R.L., and Takahama, Y. (2004). CCR7 signals are essential for cortex-medulla migration of developing thymocytes. J Exp Med *200*, 493-505. 10.1084/jem.20040643.

Unno, M., Mizushima, T., Morimoto, Y., Tomisugi, Y., Tanaka, K., Yasuoka, N., and Tsukihara, T. (2002). The structure of the mammalian 20S proteasome at 2.75 A resolution. Structure *10*, 609-618. 10.1016/s0969-2126(02)00748-7.

Van Kaer, L. (2002). Major histocompatibility complex class I-restricted antigen processing and presentation. Tissue Antigens *60*, 1-9.

Van Kaer, L., Parekh, V.V., Postoak, J.L., and Wu, L. (2019). Role of autophagy in MHC class I-restricted antigen presentation. Mol Immunol *113*, 2-5. 10.1016/j.molimm.2017.10.021.

Van Kaer, L., Postoak, J.L., Song, W., and Wu, L. (2022). Innate and Innate-like Effector Lymphocytes in Health and Disease. J Immunol *209*, 199-207. 10.4049/jimmunol.2200074.

Van Keymeulen, A., Rocha, A.S., Ousset, M., Beck, B., Bouvencourt, G., Rock, J., Sharma, N., Dekoninck, S., and Blanpain, C. (2011). Distinct stem cells contribute to mammary gland development and maintenance. Nature *479*, 189-193. 10.1038/nature10573.

Ventura, A., Kirsch, D.G., McLaughlin, M.E., Tuveson, D.A., Grimm, J., Lintault, L., Newman, J., Reczek, E.E., Weissleder, R., and Jacks, T. (2007). Restoration of p53 function leads to tumour regression in vivo. Nature *445*, 661-665. 10.1038/nature05541.

Victora, G.D., and Nussenzweig, M.C. (2022). Germinal Centers. Annu Rev Immunol *40*, 413-442. 10.1146/annurev-immunol-120419-022408.

Vieira, O.V., Bucci, C., Harrison, R.E., Trimble, W.S., Lanzetti, L., Gruenberg, J., Schreiber, A.D., Stahl, P.D., and Grinstein, S. (2003). Modulation of Rab5 and Rab7 recruitment to phagosomes by phosphatidylinositol 3-kinase. Mol Cell Biol *23*, 2501-2514. 10.1128/MCB.23.7.2501-2514.2003.

Viret, C., Lamare, C., Guiraud, M., Fazilleau, N., Bour, A., Malissen, B., Carrier, A., and Guerder, S. (2011a). Thymus-specific serine protease contributes to the diversification of the functional endogenous CD4 T cell receptor repertoire. J Exp Med *208*, 3-11. 10.1084/jem.20100027.

Viret, C., Leung-Theung-Long, S., Serre, L., Lamare, C., Vignali, D.A., Malissen, B., Carrier, A., and Guerder, S. (2011b). Thymus-specific serine protease controls autoreactive CD4 T cell development and autoimmune diabetes in mice. J Clin Invest *121*, 1810-1821. 10.1172/JCI43314.

Viret, C., Mahiddine, K., Baker, R.L., Haskins, K., and Guerder, S. (2015). The T Cell Repertoire-Diversifying Enzyme TSSP Contributes to Thymic Selection of Diabetogenic CD4 T Cell Specificities Reactive to ChgA and IAPP Autoantigens. J Immunol *195*, 1964-1973. 10.4049/jimmunol.1401683.

Viville, S., Neefjes, J., Lotteau, V., Dierich, A., Lemeur, M., Ploegh, H., Benoist, C., and Mathis, D. (1993). Mice lacking the MHC class II-associated invariant chain. Cell *72*, 635-648. 10.1016/0092-8674(93)90081-z.

von Rohrscheidt, J., Petrozziello, E., Nedjic, J., Federle, C., Krzyzak, L., Ploegh, H.L., Ishido, S., Steinkasserer, A., and Klein, L. (2016). Thymic CD4 T cell selection requires attenuation of March8-mediated MHCII turnover in cortical epithelial cells through CD83. J Exp Med *213*, 1685-1694. 10.1084/jem.20160316.

Waisman, A., Lukas, D., Clausen, B.E., and Yogev, N. (2017). Dendritic cells as gatekeepers of tolerance. Semin Immunopathol *39*, 153-163. 10.1007/s00281-016-0583-z.

Wallroth, A., and Haucke, V. (2018). Phosphoinositide conversion in endocytosis and the endolysosomal system. J Biol Chem *293*, 1526-1535. 10.1074/jbc.R117.000629.

Wang, R.C., and Levine, B. (2010). Autophagy in cellular growth control. FEBS Lett *584*, 1417-1426. 10.1016/j.febslet.2010.01.009.

Watts, C. (2004). The exogenous pathway for antigen presentation on major histocompatibility complex class II and CD1 molecules. Nat Immunol *5*, 685-692. 10.1038/ni1088.

Wearsch, P.A., and Cresswell, P. (2008). The quality control of MHC class I peptide loading. Curr Opin Cell Biol *20*, 624-631. 10.1016/j.ceb.2008.09.005.

Welsh, R.A., Song, N., Foss, C.A., Boronina, T., Cole, R.N., and Sadegh-Nasseri, S. (2020). Lack of the MHC class II chaperone H2-O causes susceptibility to autoimmune diseases. PLoS Biol *18*, e3000590. 10.1371/journal.pbio.3000590.

Wertheimer, T., Velardi, E., Tsai, J., Cooper, K., Xiao, S., Kloss, C.C., Ottmuller, K.J., Mokhtari, Z., Brede, C., deRoos, P., et al. (2018). Production of BMP4 by endothelial cells is crucial for endogenous thymic regeneration. Sci Immunol *3*. 10.1126/sciimmunol.aal2736.

Willinger, T., and Flavell, R.A. (2012). Canonical autophagy dependent on the class III phosphoinositide-3 kinase Vps34 is required for naive T-cell homeostasis. Proc Natl Acad Sci U S A *109*, 8670-8675. 10.1073/pnas.1205305109.

Wong, J., Obst, R., Correia-Neves, M., Losyev, G., Mathis, D., and Benoist, C. (2007). Adaptation of TCR repertoires to self-peptides in regulatory and nonregulatory CD4+ T cells. J Immunol *178*, 7032-7041. 10.4049/jimmunol.178.11.7032.

Xing, Y., Jameson, S.C., and Hogquist, K.A. (2013). Thymoproteasome subunit-beta5T generates peptide-MHC complexes specialized for positive selection. Proc Natl Acad Sci U S A *110*, 6979-6984. 10.1073/pnas.1222244110.

Yamano, T., Nedjic, J., Hinterberger, M., Steinert, M., Koser, S., Pinto, S., Gerdes, N., Lutgens, E., Ishimaru, N., Busslinger, M., et al. (2015). Thymic B Cells Are Licensed to Present Self Antigens for Central T Cell Tolerance Induction. Immunity *42*, 1048-1061. 10.1016/j.immuni.2015.05.013.

Yang, G., Postoak, J.L., Song, W., Martinez, J., Zhang, J., Wu, L., and Van Kaer, L. (2021). Dendritic cell PIK3C3/VPS34 controls the pathogenicity of CNS autoimmunity independently of LC3-associated phagocytosis. Autophagy, 1-10. 10.1080/15548627.2021.1922051.

Yewdell, J.W. (2011). DRiPs solidify: progress in understanding endogenous MHC class I antigen processing. Trends Immunol *32*, 548-558. 10.1016/j.it.2011.08.001.

Yoon, M.S., Du, G., Backer, J.M., Frohman, M.A., and Chen, J. (2011). Class III PI-3-kinase activates phospholipase D in an amino acid-sensing mTORC1 pathway. J Cell Biol *195*, 435-447. 10.1083/jcb.201107033.

Yoshii, S.R., and Mizushima, N. (2017). Monitoring and Measuring Autophagy. Int J Mol Sci *18*. 10.3390/ijms18091865.

Yu, L., Chen, Y., and Tooze, S.A. (2018). Autophagy pathway: Cellular and molecular mechanisms. Autophagy *14*, 207-215. 10.1080/15548627.2017.1378838.

Zhou, X., Takatoh, J., and Wang, F. (2011). The mammalian class 3 PI3K (PIK3C3) is required for early embryogenesis and cell proliferation. PLoS One *6*, e16358. 10.1371/journal.pone.0016358.

Zhou, X., Wang, L., Hasegawa, H., Amin, P., Han, B.X., Kaneko, S., He, Y., and Wang, F. (2010). Deletion of PIK3C3/Vps34 in sensory neurons causes rapid neurodegeneration by disrupting the endosomal but not the autophagic pathway. Proc Natl Acad Sci U S A *107*, 9424-9429. 10.1073/pnas.0914725107.